The Pennsylvania State University

The Graduate School

Intercollege Graduate Program in Physiology

THE INTERPLAY OF EXERCISE AND GENETICS IN THE TIBIAE OF FEMALE C57BL/6J AND DBA/2J MOUSE STRAINS

A Thesis in

Physiology

by

Eleanore Hernandez

Submitted in Partial Fulfillment
of the Requirements
for the Degree of

Master of Science

August 2008

The thesis of Eleanore Hernandez was reviewed and approved* by the following:

Neil A. Sharkey
Professor of Kinesiology, Orthopaedics and Rehabilitation
Associate Dean of Research and Graduate Education
Thesis Adviser

Henry J. Donahue
Professor, Department of Orthopaedics and Rehabilitation

Teresa Caroldean Lang
Research Associate Faculty, Kinesiology

Leonard S. Jefferson, Jr.
Evan Pugh Professor
Chair of Cellular and Molecular Physiology
Chair of Intercollege Graduate Program in Physiology

*Signatures are on file in the Graduate School

ABSTRACT

Osteoporosis is a skeletal disease characterized by a progressive reduction in bone mineral density (BMD) that results in susceptibility to fractures and increased morbidity. Exercise is commonly advocated as a preventative strategy against the development of osteoporosis and as a treatment for individuals already affected. However, considerable variance in the utility of exercise or physical activity as an intervention has been observed, suggesting an intrinsic component. Defining interactions between environmental loading and genes will facilitate design of new interventions for the prevention and treatment of osteoporosis. The objective of this study was to examine the effects of exercise on skeletal strength and architecture in female C57BL/6J (B6) and DBA/2J (D2) inbred mouse strains.

Each strain was divided into the following exercise treatment groups: treadmill running, tower climbing, and non-exercised control. The treadmill regimen was performed 5 consecutive days per week for a total of 5 weeks with a gradual increase to a 25 degree incline at 15 m/min for 30 minutes/day. The tower climbing mice were continually housed in a cage equipped with a cylindrical tower 17 cm in diameter and 100 cm tall for a total of 5 weeks. For the first week, water bottles were adjusted from 20 to 100 cm from the bottom of the cage to train the animal to climb the tower. Upon completion of the five week exercise intervention, the tibiae were extracted and then analyzed using a Scanco Medical micro-computed tomography (μCT-40) instrument to obtain quantitative data of cortical and trabecular bone architecture. Following scanning, the tibial midshafts were tested to failure in three-point bending using a semi-hydraulic Materials Testing System (MTS) 858 MiniBionix apparatus. The proximal end was

embedded and sectioned to qualitatively assess bone apposition using dynamic histomorphometry based upon fluorescent dyes that were administered during the 5 week exercise regimen. The distal segment of the tibia was dried and ashed to determine bone composition.

Genetic strain and the type of exercise intervention significantly affected the outcome. Significant exercise treatment effects were identified for several measures including cortical thickness, trabecular bone volume fraction as well as trabecular number and thickness in B6 mice with the magnitude of effect dependent upon the intervention type, whereas no exercise treatment effect was observed in the D2 animals.

Taken as a whole, these results demonstrate the impact of different types of exercise on skeletal architecture, strength, and composition as a function of genetic predisposition. A more complete understanding of the underlying factors of bone regulation may lead to improvements in recognizing individuals most at risk for developing osteoporosis as well as constructing effective patient-specific interventions.

TABLE OF CONTENTS

LIST OF FIGURES

LIST OF TABLES

ACKNOWLEDGEMENTS

I would like to thank my advisor, Dr. Neil Sharkey, for his advice and support in pursuing my Master's degree. I would like to express gratitude to Dr. Sharkey for providing the opportunity to become involved in his research group as well as the chance to learn a great deal from him and members of the Sharkey lab group. This experience has encouraged and reinforced my interest in scientific research and I am greatly appreciative of my time in the Biomechanics Laboratory.

I would also like to thank Dr. Dena Lang for giving me the chance to take part in this collaborative project. I greatly appreciate her guidance, patience, and encouragement in helping me through this process. Dr. Lang's feedback and support were greatly valued in pursuing my degree. In addition, I would like to thank Dr. Lang and Dr. Henry Donahue for their suggestions and agreeing to be members on my thesis committee.

I would like to thank the support staff as well as the graduate and undergraduate students involved in this research project, including Holly Preston, Alana Henry, Ryan Burton, Michelle Scanze, and Victoria Lanzara. I also appreciate the microscopy work completed by Dr. David Erikson, Dr. Katherine Dunlap, and Dr. Bob Burghardt at Texas A&M University.

I would like to thank the graduate students in the Kinesiology Department and the Intercollege Graduate Degree Program in Physiology for their friendship and support. I would also like to give special notice to Dr. Erikson in lending his experiences as a former Physiology student as well as his guidance through the completion of my thesis. Lastly, I would like to thank my parents, Bert and Nora Hernandez and my sister, Laureen for all their love and endless amounts of encouragement.

CHAPTER 1

INTRODUCTION

Osteoporosis

Osteoporosis is a debilitating skeletal disease that affects 10 million Americans with an additional 34 million American individuals at high risk for the disease (NOF, 2008). Osteoporosis is characterized by a reduction in bone mineral density (BMD) that results in increased bone fragility as well as susceptibility to fractures. Osteoporotic-related fractures lower a patient's quality of life and lead to increased morbidity and mortality. Osteoporosis can occur at any age, in men as well as in women, but certain populations are at significantly greater risk for the disease. Although men are susceptible to osteoporosis, eighty percent of those who suffer from this disease are women, and nearly one out of every two women over the age of 50 will suffer an osteoporosis-related fracture (NOF, 2008). Furthermore, women with certain types of fractures are at a four-fold greater risk of a second fracture (NOF, 2008). Osteoporosis-related fractures account for hospital, long term facility, and other treatment costs in excess of 19 billion dollars annually (NOF, 2008). Bone quality is dictated by a complex blend of hormone regulation, nutrition, physical activity, and genetics. It is important to understand these factors, the interplay, and the mechanisms responsible for the regulation and maintenance of bone.

Osteoporosis is most often diagnosed by measuring BMD using dual energy X-ray absorptiometry (DEXA). When BMD is less than or equal to 2.5 standard deviations below that of a young adult reference population, the bone is considered diseased.

Osteoporosis does not have specific symptoms, but its main consequence is the increased risk of bone fractures in situations where healthy people would not normally break a bone. Fracture risk due to fragility increases two to three times for every 10 percent drop in bone density (NOF, 2008). Commonly involved sites of such fractures are the lumbar vertebrae, pelvis, and distal forearm. The lifetime risk of sustaining an osteoporotic fracture has been estimated at 50 percent and the cost of managing osteoporotic fractures is quite high (NOF, 2008).

Several factors are important in regulating bone mineral density. One of the most important risk factors for osteoporosis is advanced age associated with a decrease in sex hormones. Estrogen deficiency following menopause is correlated with a rapid reduction in BMD (Frost, 1999). People who are bedridden are at a significantly increasing risk for osteoporosis because mechanical stimulation is important in promoting optimal skeletal health. However, excessive mechanical demand can damage bones by overwhelming bones adaptive capacity. In particular, high volumes of exercise have been associated with low bone density and high occurrence of stress fractures (Pouilles et al., 1989; Gutin and Kasper, 1992). Therefore, people who remain physically active within normal reasonable limits throughout life have a lower risk of osteoporosis (Gutin and Kasper, 1992). Heritability and family history of osteoporosis are also associated with increased risk. Family and twin studies have revealed that 70% of the variance in BMD is explained by gene inheritance (Dequeker et al., 1987; Slemenda et al., 1999). The genetic regulation of skeletal integrity and other related phenotypes that dictate overall bone health have been extensively studied in both humans and mouse models. Specific genes have been identified in the determination of intrinsic bone material properties, thus predisposing a

group of the population to a specific phenotype. Further understanding of the genes and signaling pathways regulating bone density holds great potential in the design of effective interventions to reduce the incidence of osteoporosis-related fracture.

Experimental animals, particularly inbred strains of mice, are important models for use in exploring bone regulation in controlled environments. Inbred strains of mice provide identical genetic backgrounds allowing efficient exploration of environmental influence as well as the manipulation of one or more genes to study their effects. In particular, these animals provide the opportunity to gain insight into gene by environment interactions. Each inbred strain is genetically different from other inbred strains, allowing the segregation of genetic alleles that influence bone density as a function of other variants such as diet and exercise. The C57BL/6J (B6) mouse strain exhibits low BMD while the DBA/2J (D2) mouse strain possesses moderately high BMD, despite similar body weights in the two strains (Beamer et al., 1996; Akhter et al., 2000). Utilizing these strains of mice enables effective comparisons of different bone architectures; however, studies focusing on the interaction between genes and environment in inbred mice are limited.

The factors that regulate bone quality are still being delineated, and the relationship between environment and genetics in determining bone architecture is unclear. Osteoporosis continues to be under diagnosed and under treated as well as associated with significant costs to society in direct and indirect medical expenses and lost productivity. A more complete understanding of the underlying factors of the regulation of bone strength and architecture as a function of genetic regulation and

mechanical loading may lead to improvements in recognizing individuals most at risk for developing osteoporosis and in the design of new therapeutic interventions.

Objective of the Study

The overall objective of this work was to expose young B6 and D2 female mice to treadmill exercise and tower climbing in order to examine differential changes in skeletal strength and architecture as a function of genetic strain and exercise intervention.

1. **Conduct two exercise interventions designed to compare aerobic versus resistance exercise.**

   At 180 days of age, B6 and D2 young female mice were randomized into three groups: treadmill exercise, tower climbing, and sedentary controls. The intervention program spanned the course of five weeks.

2. **Determine gross anatomical morphology, cortical and trabecular architecture, composition, and mechanical performance of the tibia in mice specific to the three treatment regimens.**

   Upon completion of the exercise intervention, the tibia was extracted and measured to obtain gross dimensional measurements. The bones were scanned and analyzed using a Scanco Medical micro-computed tomography (μCT-40) instrument to obtain quantitative data of the cortical and trabecular bone architecture. Using a Material Testing System (MTS) Minibionix apparatus, the midshaft of the tibia was tested to failure in a three-point-bending test to determine the structural performance of the bone in response to mechanical loading. Together with the cross-sectional images obtained from the μCT data,

this information was used to estimate the material properties of the cortical mid-shaft bone. Following mechanical testing, the distal fragment was analyzed to determine hydrated, dry, and ash weight and derive the percentage of water, organic, and mineral components of the bone.

3. **Qualitatively assess the anabolic responses to exercise with the use of fluorochrome labels.**

   During the exercise program, all animals received sequential IP injections of alizarin and calcein dyes, which integrated into new bone as it mineralized. After mechanical testing, the proximal fragment of the tibia was dehydrated, embedded, and sectioned for dynamic histomorphometry. The cross sections of representative bones were examined to assess the uptake of the dyes on the labeled surface.

Central Hypothesis:

Aerobic versus resistance exercise will induce different changes in bone strength and architecture. Furthermore, changes as a consequence of exercise will be dependent upon genetic strain.

Assumptions of the Study

1. Animals of the same strain are genetically identical irrespective of litter or batch.
2. Phenotypes of individuals do not differ because of genotype being passed through either the sire or the dam.
3. The threshold value selected for the identification of bone tissue in the μCT scans

appropriately differentiates bone from the background.

4. The model used to calculate structure of the trabeculae is appropriate and accurate.
5. The boundaries between cortical and trabecular bone are accurately defined and consistent for each specimen.
6. Food intake relative to body size is consistent for all animals.

Limitations of the Study

1. The sample size of 90 females (15 per group) in this study limits statistical power.
2. Some animals were more willing to participate in the tower climbing exercise intervention program than others, leading to slight variations in the amount of physical activity experienced by each animal.
3. Regardless of the animals being housed in identical conditions, there will be environmental differences. This may be due to differences in food consumption and other factors.
4. There are scaling effects as a result of bone size. Larger animals may have larger metaphyses, which may lead to more trabecular bone in comparison to smaller animals.

Definition of Pertinent Terms

Aerobic exercise: Endurance activities that involve the use of oxygen to provide energy for muscle contraction during moderate levels of intensity for long periods of time. Examples of aerobic activities are long-distance running, walking, swimming, and cycling.

Bone Surface (BS): A parameter based on the virtual triangularization of the bone surface to obtain a two-dimensional measurement of bone/soft tissue interface. BS is expressed as mm^2.

Bone Surface Fraction (BS/BV): A parameter based on the virtual triangularization of the bone surface to calculate the ratio of bone surface area to bone volume. BS/BV is expressed as 1/mm.

Bone Volume/Tissue Volume (BV/TV): A parameter that calculates the number of bone voxels in the scanned area divided by the total number of voxels in the scanned area. BV/TV is expressed as a percentage (%).

Connectivity Density (Conn.D): An estimate of the number of trabecular connections/mm^3 based on the Euler number (χ) (Feldkamp et al., 1989; Odgaard and Gunderson, 1993). This variable is defined as

$$\chi = \beta_0 - \beta_1 - \beta_2$$

Equation 1.1

where β_0 is the number of disconnected struts, β_1 is the connectivity, and β_2 is the number of isolated marrow cavities. Conn.D is expressed as $1/mm^3$.

Cortical bone: (also known as compact or haversian bone) Composed of dense tissue that includes Haversian canals, which contain capillaries and nerves that run longitudinally along the long axis of the bone. These ducts are connected to Volkmann's canals, structures that contain blood vessels and nerves. Dense bone is located in the shafts of long bones as well as the outer layer around spongy bone.

Degree of Anisotropy (DA): A parameter that describes bone orientation. A DA value of 1 indicates that the structure is isotropic, meaning that the object possesses the same properties in all directions of testing. As the number increases from 1, the object becomes increasingly anisotropic.

Distance Transformation (DT) Model: A model used with the micro-computed tomography software that calculates trabecular characteristics based on an algorithm that superimposes virtual spheres onto the volume of interest in order to calculate the area of the spheres.

Heritability: The ratio of additive genetic variance (V_A) to phenotypic variance (V_P). in a population.

$$h^2 = \frac{V_A}{V_P}$$

Micro-computed tomography (μCT): High resolution computed tomography that utilizes x-rays to create cross-sections of a three dimensional object that can be used to recreate a virtual model in order to obtain quantitative measurements of structural properties.

Quantitative Trait Loci (QTL): Refers to the inheritance of phenotypic characteristics that vary in degree and can possibly be attributed to the interactions between two or more genes and their environment. QTL analyses has been used in both human and experimental animal models to study genetic regulation of bone density, strength, quality, and other traits (Koller et al., 2003; Beamer et al., 2001; Li et al., 2002).

Recombinant Inbred Mice (RI): Strains of mice that are derived by systematic inbreeding following a cross between mice of two genetically distinct progenitor inbred strains.

Resistance exercise: Form of strength training in which each effort is performed against a specific opposing forced generated by resistance. Activities such as weight training and climbing are considered examples of resistance exercise.

Structural Model Index (SMI): A descriptive parameter that indicates the extent to which bone trabeculae are more plate-like or more rod-like (Hildebrand and Rüegsegger, 1997). SMI is defined as a value between zero and three. Zero indicates a completely plate-like arrangement and three indicates a completely rod-like arrangement.

Threshold: Refers to the process of distinguishing bone from background such as tissue or water. One gray-scale value is used as a threshold for each volume of interest. Values above this threshold value are considered bone and values below it are considered background.

Trabecular Bone: (also known as cancellous or spongy bone) Composed of highly porous meshwork that contains marrow, the site of hematopoesis (Martin et al, 1998). The microarchitecture consists of struts or plates, depending on the skeletal site. Trabecular bone is found in cuboidal bones, flat bones, and the ends of long bones.

Trabecular Number (Tb.N): The number of trabeculae per millimeter. Tb.N is expressed as 1/mm.

Trabecular Separation (Tb.Sp): The distance between trabeculae. Tb.Sp is expressed as mm.

Trabecular Thickness (Tb.Th): An estimate of trabecular thinning calculated from bone surface and bone volume. Tb.Th is expressed as mm.

Triangulation (TRI) Model: A model used with the micro-computed tomography software that calculates structural parameters based on the virtual triangularization of the bone surface.

Voxel (VOX) Model: A model used with the micro-computed tomography software that calculates structural parameters based on counting the numbers of voxels above and below the threshold value,

CHAPTER 2

REVIEW OF THE LITERATURE

Bone as a Dynamic Tissue

Bone is a self-repairing, dynamic tissue that continually alters its properties and structure in response to its physiological and mechanical demands. The ability of the skeleton to adapt to its environment was formally proposed by Julius Wolff and is known as Wolff's Law. This theory states that bones are able to sense mechanical loads and can modify their structure to accommodate changes in these loads (Wolff, 1892). Therefore, increased loading will cause arrangement of the internal structure in order to optimize bone strength with respect to its weight while the absence of a stimulus will result in the removal of bone because of the metabolic costs in maintaining bone.

Bone is composed of various substances that support its structural functions. It primarily consists of organic matrix, mineral, and water. These three substances have distinctive physical properties that influence the mechanical properties of bone. The organic matrix component is composed largely of collagen, which provides flexibility and tensile strength. In contrast, the mineral component mainly consists of hydroxyapatite crystals, which imposes rigidity and resists compression. The calcified bone matrix contains free and bound molecules of water. Because water is displaced during mineralization, the water content of new bone tissue changes as it mineralizes (Martin et al., 1998).

There are two types of bone tissue, trabecular and cortical. The main difference between trabecular and cortical bone is the degree of porosity. This distinguishing feature

reflects the different adaptations to various types of loading. The level of porosity is capable of changing as the result of metabolic pathologies or mechanical stimulus (Martin et al., 1998). Trabecular bone (also known as cancellous or spongy bone) is a highly porous meshwork containing marrow, the site of hematopoesis (Martin et al., 1998). The microarchitecture consists of struts or plates, depending on the skeletal site. Trabecular bone is found in cuboidal bones, flat bones, and the epiphyses of long bones. In contrast, cortical bone (also known as compact or haversian bone) is composed of dense, low porous tissue. It contains Haversian canals, which contain capillaries and nerves that run longitudinally along the long axis of the bone. These ducts are connected to transversely oriented Volkmann's canals, structures that contain blood vessels and nerves. Dense cortical bone is located in the shafts of long bones as well as the outer layer around spongy bone.

Within each type of bone, there are two major subgroups of bone tissue: woven and lamellar bone. These two types of tissue differ in rate of formation, organization, and strength. Woven bone (also known as primary bone tissue) is initially deposited and also formed during fracture healing. This type of tissue is rapidly formed and poorly organized. The collagen fibers are randomly arranged, resulting in a weak structure. Woven bone is usually replaced by lamellar bone (also known as secondary bone tissue). This type of tissue is slowly formed and consists of highly organized, parallel layers. The fibers run in opposite directions that impart strength and stability.

Within all bone, there are four distinct types of bone cells: osteoblasts, bone-lining cells, osteocytes, and osteoclasts. Osteoblasts are mononuclear bone cells that are responsible for bone formation. These cells originate from the mesenchymal lineage and

synthesize the enzyme alkaline phosphatase (AP), which is needed locally for the mineralization of osteoid. Osteoblasts produce osteoid at a rate of approximately 1 μm/day, resulting in bone deposition (Martin et al., 1998). Eventually, osteoblasts become quiescent on the bone surface to become bone-lining cells, or encased within calcified matrix to become osteocytes. These cells possess cellular extensions for exchange and communication among neighboring osteocytes. Osteoclasts are multinuclear bone cells that are responsible for bone resorption. These cells develop from the monocyte lineage and are rich in lysosomes that contain tartrate-resistant acid phosphatase (TRAP). When activated, osteoclasts adhere to the bone surface and secrete hydrogen ions to dissolve the inorganic and organic components of the bone mineral. This cell type is capable of resorbing bone at 40 μm/day (Martin et al., 1998). Together, these four cell types work together to maintain the integrity of bone.

Bone Remodeling

Bone is able to maintain its structural integrity through the process of remodeling. Bone remodeling is a local process that involves populations of osteoclasts and osteoblasts called basic multicellular units (BMU). Each unit is organized into a cutting cone of osteoclasts that reabsorb bone followed by osteoblasts that are responsible for filling the defect left by the osteoclasts (Martin et al., 1998). BMUs operate on the periosteal, endosteal, and trabecular surfaces as well as within cortical bone, replacing old bone with new bone in discrete packets (Martin et al., 1998). The removal and formation of bone are normally in balance to maintain structural integrity. Pathologic conditions in bone may result due to an imbalance in the total number of BMUs, causing

irreversible bone loss in cortical and trabecular bone. An increase in bone loss per BMU can result from overactivity of osteoclasts so that more bone is resorbed than normal osteoblasts can replace. This disruption in the equilibrium resulting in greater resorption relative to formation can severely weaken bones, and could eventually lead to the fractures that characterize osteoporosis.

The entire bone remodeling process is primarily under endocrine control. Parathyroid hormone (PTH) is a peptide hormone synthesized and secreted by chief cells of the parathyroid gland. Synthesis and secretion are controlled by ionic calcium (Ca^{2+}) concentration. PTH mobilizes Ca^{2+} from bone and increases urinary phosphate excretion, resulting in increased bone resorption. Another hormone responsible for bone remodeling is calcitonin, which is secreted from the thyroid gland, specifically the parafollicular cells. Unlike PTH, calcitonin deposits Ca^{2+} in bone and inhibits bone resorption. The sex steroid hormone, estrogen, is another important component in bone resorption. It is synthesized from androgens in the ovaries, testes, and adrenal glands. Estrogen is required for maximum bone mass in both sexes and has demonstrated positive effects on bone density. The action of estrogen is mediated by estrogen receptors in both osteoblasts and osteoclasts. Specifically, androgens suppress osteoclastogenesis and promote bone formation. Estrogen deficiency is the major determinant of age-related bone loss in both sexes (Frost, 1999).

Remodeling occurs in both trabecular and cortical bone. Trabecular bone, in comparison with cortical tissue, has a high turnover rate, and is more susceptible to structural changes as a consequence of imbalances in bone remodeling. This remodeling process is partly due to more metabolite concentrations available to the trabecular bone.

The transport of waste and nutrients are maintained through diffusion from the marrow to the mineralized tissue. As the concentration of nutrients increases, less bone surface is required to supply the same amount of bone tissue. It is theorized that loading of the tissue assists the ability of molecules to diffuse from the marrow into the hard tissue (Fyhrie and Kimura, 1999). Therefore, a reduction in loading produces a decline in the nutrients available to the trabeculae, resulting in a decrease in bone tissue and a reduction in bone volume fraction. These changes often lead to fractures and bone weakness in the trabeculae.

Mechanical Loading

Bone possesses the ability to continually alter its properties and structure in response to mechanical demand. Substantial experimental and clinical evidence has supported the importance of mechanical stimulation in promoting optimal skeletal health. Functional material strains provide an input to the skeletal cells responsible for the maintenance of bone density and morphology in order to accommodate changes in these loads (Lanyon, 1987; Mosley et al., 1997; Zernicke et al., 2006). Besides cell-to-cell communication, fluid surrounding the bone cells and adjacent bone matrix serves as a potential link between mechanical stimuli and cellular perception (Zernicke et al., 2006). Therefore, greater loading increases bone mass to alter architecture in order to optimize bone strength, while the absence of a stimulus results in the removal of bone to reduce metabolic costs as evidence by bed rest or space flight studies (Bikle and Halloran, 1999; Lang et al., 2006). Immobilization studies further suggest that skeletal unloading leads to

increased bone resorption and rapid bone loss, ultimately resulting in decreased bone mass and increasing risk of fracture.

Bed rest studies in humans have demonstrated the catabolic effects of reduced weight bearing on the skeleton. A study conducted by Zerwekh et al. (1998) examined the consequences of 12 weeks of skeletal unloading based on parameters of calcium homeostasis and bone histology in 11 normal subjects. The results suggested that bed rest prompted a rapid, sustained increase in urinary calcium and phosphorus, suggesting increased bone resorption. Significant changes in bone histology included a suppression of osteoblastic surface for trabecular bone and increased bone resorption for both trabecular and cortical bone. Taken together, the biochemical data and histologic parameters provide strong support that the human skeleton responds to unloading by an immediate increase in bone resorption and a more subtle decrease in bone formation. However, clinical studies are limited because of the small sample sizes and invasiveness of the procedures. Also, studies in humans cannot definitively investigate mechanical strength, one of the main predictors of fracture risk.

Similar to bed rest studies, a hind limb suspension model was developed to study the effects of skeletal unloading and reloading on the long bones of rodents (Morey, 1979). In this model, the hind limbs are unloaded while the forelimbs are loaded similarly to a normal weight-bearing rat, providing internal control bones to distinguish between local and systemic effects of hind limb unloading. This condition leads to profound changes in the mass, maturity, and structural integrity of unloaded bones. The mass of unloaded bones declines relative to controls due to a transient decrease in trabecular osteoblast number and cortical periosteal mineralization rate (Morey-Holton and Globus,

1998). Unlike humans, parameters related to bone resorption did not change in rodents. Ultimately, unloading appears to compromise the mechanical strength of affected bones, posing an increase risk for fracture.

Significance of Exercise

The implications from the mechanical loading studies support the importance of physical exercise as an important therapeutic strategy to maintain bone mass in both humans and animals. Several studies have supported the notion that exercise has a positive effect on bone mineral density (BMD) in young, postmenopausal, and elderly women (Bassey and Ramsdale, 1994; Friedlander et al., 1993; Kohrt et al., 1997; Ryan et al., 1998). Similarly, several studies have demonstrated positive effects of exercise on BMD, bone mineral content, trabecular bone structure, and bone strength in young, aged, and ovariectomized rats (Barengolts et al., 1993; Yeh et al., 1993a; Yeh et al., 1993b). Furthermore, it has been suggested that the osteogenic response to training may be a function of intensity of exercise. The impact of physical activity on bone turnover depends on the type of exercise performed by the individual. In particular, aerobic and resistance exercises produce distinct effects on bone development. The various modes of exercise may benefit bone mechanical properties in different ways. Little is known about the specific changes in bone response induced by various forms of systematic exercise in inbred mice.

Aerobic Exercise

Aerobic exercise involves the use of oxygen to provide energy for muscle contraction. Many types of activities are considered aerobic such as long distance running, walking, swimming, and cycling. These activities are distinguished by moderate levels of intensity for long periods of time. The benefits of endurance exercise are commonly associated with the cardiorespiratory system such as strengthening the heart muscle to improve its pumping efficiency as well as increasing the maximum volume of oxygen (VO_2) that can be consumed by muscles during exercise. Aerobic exercise has also been considered to have beneficial effects on bone health. In particular, it is associated with positive effects in the maintenance of bone mass and strength. A variety of endurance exercises have been studied in mice and rats such as treadmill running (weight-bearing) and swimming (non-weight-bearing). A study by Warner et al. (2006) compared treadmill activity and swimming in rats to understand the differential effects of each mode of exercise. Treadmill speed was adjusted to correspond to the average limb loading frequency used during swimming. The differences in limb load magnitude, rate, and direction are assumed to account for disparities in skeletal response to the varying exercise modes. All exercise sessions were performed 1 hour/day for 5 days per week for a total of 12 weeks. Both types of activity produce positive osteogenic effects, but swimming appears to produce novel bone strains and distinct adaptations in the humerus and femur, which are different from those generated by treadmill activity. Because bones cannot sense the cause of deformation in swimming, it is possible that bone strains induced by atypical muscle contractions are as effective as those induced by ground reaction forces in the maintenance of bone homeostasis during treadmill exercise (Warner

et al., 2006). Further research is needed to define the bone strains and loading characteristics involved with swimming.

Treadmill Exercise

Treadmill exercise is capable of increasing bone mass and strength in both animals and humans. The skeleton is sensitive to mechanical stimuli at all ages, but the adaptability of bone is greater before skeletal maturity. Specifically, responsiveness peaks and, therefore, exercise regimes would be most efficacious during peripuberty. As a result, the effects of treadmill exercise have been closely studied in prepubescent rats. Exercise regimens in rodents employed during adolescence result in increases in BMD, bone mineral content, and cortical thickness at skeletal maturity, whereas regimens employed during mid to late adulthood lead to an attenuation of bone mineral loss and are designed essentially to increase coordination and prevent falls in humans. Exposure to treadmill exercise in 6-week-old Wistar rats stimulated longitudinal bone growth and increased bone mineral content at weight-bearing sites, but did not alter BMD (Iwamoto et al., 2004). The exercise regimen was performed for 25 m/min for 1 hour per day for 5 days per week for a total of 11 weeks. The findings suggest that treadmill exercise during the growth period increases the size of long bones in the longitudinal and/or radial direction, maintaining bone density. In addition, weight-bearing activity is important to increase the bone mineral content of long bones, as demonstrated by short-term treadmill exercise in young rats.

Treadmill exercise exerts distinct effects on different types of bone tissue. Yeh et al. (1993b) examined the influence of physical activity on bone formation and resorption

in the tibias of 6-week old Sprague Dawley rats exposed to treadmill running for three weeks. The exercise running speed was gradually increased to a target speed of 20 m/min for 60 minutes during the third week and was maintained for the duration of the exercise regimen. The treadmill exercised rats initially exhibited increased and then decreased bone resorption, resulting in an increase in periosteal bone formation and cortical bone area of the tibia. The trabecular bone microarchitecture also exhibits positive osteogenic effects. A study examined the effect of exercise on the trabecular bone microarchitecture in three-dimensions by micro-computed tomography (μ-CT) (Joo et al., 2003). Wistar rats were trained on a treadmill for 10 weeks. The speed and duration of each running session were gradually increased to the final level of 30m/min for 60 minutes within the following week (Joo et al., 2003). The results suggested that endurance exercise increases trabecular bone mass as a result of the creation of new trabeculae, as well as by increasing trabecular thickness and decreasing trabecular separation in the distal femoral metaphysis.

Different exercise modes exert distinct effects on the bone of interest since bone adaptation is a site-specific phenomenon. It has been documented that weight-bearing bones like the tibia and femur have higher sensitivity to treadmill exercise than less weight-bearing bones like the lumbar spine. Iwamoto et al. (1999) examined trabecular bone changes induced by treadmill exercise on three different skeletal sites, the lumbar vertebra, the proximal, and the distal tibia in young growing rats. The exercise regimen consisted of treadmill running at 24 m/min, 1 hr per day for 5 days per week. This study demonstrated increased trabecular bone volume/tissue volume (BV/TV) in the proximal and distal tibia, but not in the lumbar vertebrae. The response of trabecular bone to

treadmill exercise was greater in the distal tibia than in the proximal tibia. The reason for this is uncertain, however, it may be somewhat attributable to the location and diameter of the bone tissue. The distal tibia is likely to experience more mechanical loading than the proximal tibia during treadmill exercise because the distal tibia is situated further from the body of the rat, thus increasing the total load on the distal tibia (Iwamoto, 2005). Additionally, the diameter of the distal tibia is smaller, and therefore, the distal tibia supports greater weight per surface area during treadmill exercise than the proximal tibia.

Continued exercise is needed to maintain bone mass gained through exercise. Iwamoto et al. (2000) subjected young, female Sprague-Dawley rats to 4 weeks of deconditioning after 8 weeks of treadmill exercise to determine the extent of the lost benefits obtained through exercise. The exercise program consisted of treadmill running with a 5° slope at 24 m/minute for 1 h/day and 5 days/week. The results demonstrated that deconditioning for 4 weeks resulted in decreases in cortical bone area and cancellous BV/TV of the tibia and bone formation parameters to levels not significantly different from those rats without treadmill exercise. Thus, continued exercise is required to maintain bone mass gained through exercise. A study by Yeh and Aloia (1990) provided similar results that rats trained with treadmill exercise, when deconditioned for 4 weeks lose the benefits gained through exercise. Using bone turnover markers, bone mass gained through exercise was lost during deconditioning as a result of a decline in bone formation and an increase in bone resorption. Therefore, both studies conclude that exercise must be continued to sustain any gain it produces in bone mineral.

Resistance Exercise

Resistance exercise is a form of strength training in which each effort is performed against a specific opposing force generated by resistance. Activities such as weight training, climbing, and sprinting are considered examples of resistance exercise. The effects of resistance training are increased strength due to increased bone mass and muscle mass. Training studies involving men and women of various ages have demonstrated the osteogenic effects of resistance exercise, including increased BMD of the spine, hip, and lower limbs (Gleeson et al., 1990; Menkes et al., 1993). Furthermore, a study of hindlimb-suspended rats showed that resistance exercise could possibly attenuate bone loss during periods of unloading (Fluckey et al., 2002; Shackelford et al., 2004). Several studies in rodents have examined the specific effects of resistance training such as jumping exercise (involuntary activity) and tower climbing (voluntary activity). In the jumping model, each rat was placed with its hind legs on the floor and jumped when the tail was electrically stimulated at 2-s intervals (Notomi et al., 2000a). This type of exercise increased mass and strength of the lumbar vertebrae and mid-femur by stimulating bone formation in the periosteal surface and reducing the endocortical mineral apposition rate (MAR). However, the direction or the amount of mechanical stress on the skeleton induced by electrical stimulation is not controllable during jumping exercise (Umemura et al., 1997; Westerlind et al., 1998). Most importantly, the jumping rat training models do not seem to exclude the effects from electrical stimulus and/or non-voluntary training regimen. Therefore, voluntary tower climbing exercise is a more appropriate method in understanding the effects of resistance exercise.

Tower Climbing

Tower climbing is a newly studied mode of resistance exercise and has been utilized in both mice and rats (Notomi et al., 2001; Notomi et al., 2002; Mori et al., 2003; Notomi et al., 2003). Each animal is housed in a cage with a meshed-wire tower, which the animal voluntarily climbs to drink from two water bottles placed at the top of the tower. The set point of the bottles is gradually elevated over the first week. This setup is similar in both mouse and rat studies, except that the height of the tower is 100-cm for the mouse model and 200-cm for the rat model. Tower climbing demonstrates positive osteogenic effects in both rats and mice; however, there are limited studies examining differences between strains of mice.

The effects of voluntary tower climbing exercise have been analzyed in growing rats to examine bone mass strength and local turnover of bone (Notomi et al., 2001). In 4 weeks, the tibia exhibited increased trabecular bone formation rate, bone volume/tissue volume (BV/TV), trabecular thickness (Tb.Th), and bone mineral density (BMD) while the osteoclast surface (Oc.S) decreased. The increase in trabecular bone mass of the tibia was caused by both increased bone formation and reduced bone resorption. In the midfemur, the periosteal properties, total cross-sectional area, moment of inertia, mineralizing surface, mineral apposition rate, trabecular bone formation rate, and bending load increased while the mineral apposition rate of the endosteal surface decreased. Voluntary climbing exercise accelerated the radial cortical growth of the midfemur by stimulating periosteal bone formation. The cortical bone formation is suggested to strengthen the structure of the midfemur. In 8 weeks, the increase in the BMC and BMD

of the femur and tibia were significant. The results show that climbing exercise has a beneficial effect on the cortex of the femur and trabecular bone in the tibia.

A similar study was performed in C57BL/6J (B6) mice exposed to voluntary climbing exercise to study the relationship between the effects of bone turnover and bone marrow cell development in bone cells (Mori et al., 2003). The results supported previous rat studies; however, there was no change in the properties of the endosteal surface. The mice subjected to climbing exercise showed an increase in the following periosteal properties: bone formation rate, cross-sectional area, and moment of inertia, but the bone formation rate of the endosteal surface did not differ. In the proximal tibia of the climbing mice, the trabecular bone volume increased while the osteoclast surface (Oc.S) and osteoclast number (Oc.N) decreased. In marrow cell cultures from the tibia, the number of osteoclast-like tartrate-resistant acid phosphatase (TRACP) multinucleated cells was lower at 2 weeks, but recovered to levels of the ground controls at 4 weeks. The results indicate that climbing increased trabecular bone volume and reduced resorption with a subsequent increase in bone formation. Intermittent climbing downregulated marrow osteoclastogenic cells and upregulates osteogenic cells initially, but further exercise seemed to desensitive them.

The effects of tower climbing have also been studied in aged female ovariectomized (OVX) rats to predict the preventative and recovery effect on bone strength. The rats were separated into baseline, sham-operated sedentary, OVX-sedentary, and OVX-exercise (Notomi et al., 2003). The climbing exercise started 3 days after the OVX operation. At 3 months, OVX-sedentary exhibited an increase in femoral cortex and lumbar trabecular turnover, leading to a reduction in bone mass and strength.

In contrast, the OVX-exercise rats maintained values as the same level as the sham-sedentary. The climbing exercise prevented OVX-induced cortical and trabecular bone loss by depressing turnover rate. The second part of the study examined the recovery effect of tower climbing exercise after ovariectomy. The exercise started 3 months after the OVX operation. At 3 months, both groups of OVX-rats exhibited an increase in trabecular formation and osteoclast surface, leading to a decrease in compressive strength and the mid-femur exhibited a decrease in cross-sectional area, moment of inertia, and bending load values. At 6 months, the OVX-exercise recovered to values similar to those in the sham-sedentary rats, but the cortical bone area did not recover to previous values. These results showed that the climbing exercise had both a preventative and recovery effect on bone strength in OVX-rats.

A study using a similar setup examined the effects of tower climbing in young male orchidectomized (ORX) rats (Notomi et al., 2002). At 4 weeks, the periosteal bone formation rate, moment of inertia, bone mineral content, and bending load at the midfemur were maintained in ORX-exercise rats, whereas these parameters were reduced in ORX-sedentary rats. These results show that, in the midfemur, the voluntary climbing exercise maintained cortical bone mass and strength by stimulating periosteal bone formation and partially prevented ORX induced trabecular bone loss by depressing the turnover rate. Interestingly, in ORX-rats, the climbing exercise had the opposite effect on bone formation at the periosteal femoral cortical bone, unlike the vertebral trabecular bone, where the exercise decreased it. This result suggests that the effects of bone formation are site-specific. The above studies have not been performed in inbred strains of mice to compare strain specific differences in bone.

Comparison between Resistance and Endurance Exercise

As shown from the above studies, different modes of exercise have distinct effects on bone formation. However, there are few studies that directly compare endurance and resistance exercise. A clinical study examined changes in bone turnover induced by aerobic and resistance exercise in young males. An aerobic exercise program focused on long distance running while a resistance program consisted of a combination of weight-lifting and sprints. Twenty young healthy males were divided to follow through an 8-week program of either aerobic or resistance exercise. Using different biochemical markers, it was concluded that aerobic and resistance training exert different effects on bone metabolism. Aerobic training leads to changes compatible with reduced bone resorption while resistance training results in an overall accelerated bone turnover (Woitge et al., 1998).

The results from a rodent study disagreed with those of the clinical study. A study was performed to compare the effects of resistance and aerobic exercise on the mass, strength, and turnover of bone (Notomi et al., 2000b). Thirty Sprague Dawley rats were assigned to one of three experimental groups: sedentary, treadmill running, or jumping. The treadmill rats ran at speeds of 24 m/min for an hour every other day. The duration of the running exercise was equalized to that of the jumping activity. The jumping rats wore leather jackets attached to a bar with a load to keep their trunk upright. The tail was electrically stimulated, causing each rat to perform the jumping exercise for 1 h every other day. The jumping rats exhibited increases in the mass and strength of the lumbar-vertebrae and of the mid-diaphysis of the femur. In addition, there were increases in the cross-sectional morphology: trabecular bone volume per bone surface, the trabecular

thickness, the trabecular bone formation rate per bone surface (BFR/BS). The jumping rats also exhibited reduced trabecular separation and the area of osteoclast surface per bone surface. The running and sedentary rats showed no such changes. Both jumping and running rats exhibited an increase in the periosteal BFR/BS. However, the jumping rats exclusively showed a reduction in the BFR/BS at the endocortical surface. These results suggest that resistance exercise increases the bone mass and strength by stimulating bone formation more efficiently than does aerobic exercise. These results further support the notion that mechanical loading affects bone development and that different types of exercise exert distinct effects. However, there are limited studies comparing treadmill exercise and tower climbing in mice.

Genetic Regulation of Bone

Genetics is known to contribute to the regulation and maintenance of bone. Although mechanical loading influences bone formation, exercise intervention studies in humans and rodents have demonstrated that anabolic responses in bone vary widely among individuals when subjected to the same degree of mechanical load, suggesting an intrinsic component to bone adaptation. These variations in skeletal response are largely determined by genetic factors. Family and twin studies have revealed that 70% of the variance in BMD is explained by heredity (Dequeker et al., 1987; Slemenda et al., 1991). BMD is one of the main determinants of osteoporotic fractures in both men and women. However, it is a complex trait whose expression is complicated by environmental influences and polygenic inheritance (Klein, 2002). Studies have begun to identify the genes that may be responsible for acquisition of peak bone density in both humans and

mouse models (Klein et al., 1998; Lang et al., 2005). Further evidence has supported the existence of several prominent locus affecting variation in BMD measures. Therefore, understanding the interaction of several genes and the signaling pathways regulating bone density holds the greatest potential in affecting bone mass accumulation, and ultimately, fracture incidence.

Clinical Research

Recent studies in humans have demonstrated that the adaptive responses to functional loading are variable, with some individuals exhibiting robust osteogenic responses while others respond modestly (Snow-Harter et al., 1992; Dalsky, 1998). Comparison within twin pairs or among siblings provides a reasonable method to investigate the importance of genetic and environmental factors in determining bone quality. In particular, twin pairs are the most reliable way to assess genetic regulation while maintaining a reasonably constant environment. Human-twin studies, specifically monozygotic and dizygotic twins demonstrate the importance of bone mass inheritance. A study was performed to assess genetic variability using a comparison of intrapair differences between monozygotic and dizygotic twin pairs in order to assess genetic variability (Pocock et al., 1987). Since monozygotic twins are genetically identical, their intrapair differences are assumed to arise exclusively from environmental factors while intrapair differences in dizygotic twins arise due to both genetic and environmental factors (Smith et al., 1973). Lumbar spine and proximal femur were measured in 38 monozygotic and 27 dizygotic twin pairs (Pocock et al., 1987). BMD was more highly correlated in monozygotic than in dizygotic twins for the spine and proximal femur. The

large variation of intrapair differences in dizygotic twins infers that genetic factors largely contribute to the observed variation. The results emphasized the importance of family history and further suggested the potential for the use of twin pairs at isolating the genetic determinants of phenotypic traits.

Despite the benefits of human twin studies, this approach requires large numbers of both dizygotic and monozygotic twin pairs, which are infrequent in the population. The genetic variability between pairs of dizyogtic twins has also been suggested to be as large as in the general population (Beamer et al., 1996). Furthermore, the phenotypes most closely related to bone density require invasive measurements as well as destructive testing.

Mouse Research

Animal models are critical for experimentally defining the genetic regulation of bone density. In particular, inbred mouse strains provide the opportunity to gain insight into the genetic basis of variation in bone density. Inbred strains of animals are defined as the product of at least 20 generations of brother-sister mating, resulting in ~97.5% homozygosity at any given locus (Festing, 1979). This type of breeding provides subjects that are genetically identical under strictly controlled environment (Lightfoot et al., 2001). The comparison of various inbred strains can further provide heritability estimates for specific observed phenotypes. In addition, since each inbred strain is genetically different from every other inbred strain, planned matings can be arranged to study segregation of genes essential to bone density as well as provide a foundation for future human studies.

Similar to human studies, inbred strains of mice have also exhibited genetic differences and variable responses to mechanical loading (Kodama et al., 2000; Lerman et al., 2002; Kesavan et al., 2005; Masset and Berk, 2005). A study by Beamer et al. compared the bone density of femoral, vertebral and phalangeal bones from the following 11 inbred strains of mice: AKR/J, BALB/cByJ, C3H/HeJ, C57BL/6J, C57L/J, DBA/2J, NZB/B1NJ, SM/J, SJL/BmJ, SWR/BmJ, and 129/J (1996). Comparison of bone parameters among inbred strains revealed significant strain-related differences at each of the investigated sites. Since these genetically distinct strains of mice were raised in a controlled environment, the differences observed in bone parameters are primarily the result of genetic variation. Total and cortical density, mineral, volume, and length differed among the strains at the femur, vertebrae, and proximal phalanges. In particular, femoral and phalangeal bones differed among strains with respect to total and cortical density, mineral, and volume while the vertebral site only exhibited differences in cortical bone parameters. The study demonstrated that specific bones exhibit strain-related differences as well as provided a basis for further analyses for each particular strain. Similarly, a study by Akhter et al. (2000) has also supported the breed-related differences in the femurs and tibiae of C3H/HeJ, C57BL/6J, and DBA/2J. In particular, the bone mineral content (BMC) and bone mineral density (BMD) were highest in C3H/HeJ and lowest in C57BL/6J. The higher BMD in the C3H/HeJ was associated with greater trabecular bone volume, cortical bone area, and periosteal bone formation. The differences in structure suggest the need for further investigation in examining genetically regulated mechanisms of bone adaptation to similar mechanical loads.

Skeletal Differences between C57BL/6 and DBA/2J Inbred Strains

The phenotypes of C57BL/6 (B6) and DBA/2J (D2) inbred mouse strains have been extensively studied in skeletal genetics. These mouse strains have previously shown to exhibit differences in BMD (Beamer et al., 1996; Akhter et al., 2000). B6 mice exhibit low BMD while D2 mice possess moderately high BMD, despite the fact that the two strains exhibit similar body weights. In addition, these two strains exhibit different mechanical properties. B6 mice have thinner cortical thickness, large total cross-sectional area (CSA), and greater moment of inertia in the midshaft femur and tibia in comparison to D2 mice (Beamer et al., 1996; Akhter et al., 2000; Robling and Turner, 2002). The specific distribution of cortical bone is suggested to represent a difference in adaptive response to similar mechanical loads. As a result, studies have further examined these skeletal differences and its interaction in adaptive bone response due to genetic strain.

Clinical studies have examined the response of macrolevel strength properties of bone tissue to mechanical loading. The results indicate that mechanical loading of the skeleton during growth can substantially enhance periosteal bone apposition, producing a diaphyseal cross section with an enlarged area (Kannus et al., 1996; Haapasalo et al., 2000). It has been suggested that bones with greater CSA become this way because they are more sensitive to routine mechanical loading signals. A similar study by Robling and Turner (2002) had been performed in mice, investigating the effects of controlled mechanical loading in the ulnae of 20-week old adult female mice of different inbred strains, including D2 and B6. As shown from previous studies, B6 mice exhibit a larger femoral CSA than D2 mouse strain. Thus, B6 mice are thought to be more mechanosensitive than D2 mice (Beamer et al., 1996; Akhter et al., 2000; Robling and

Turner, 2002). However, D2 mice with the smallest ulnar cross sections were among the most sensitive to mechanical strain while B6 mice with significantly larger ulnar cross sections were the least responsive to mechanical loading. Though the magnitudes of the responses were different, these two biological strains exhibited almost exactly the same type of osteogenic response to loading. The main effect of loading in both strains appears to have been on the rate of new bone apposition (MAR), mineralizing surface/bone surface (MS/BS), and bone formation rate/bone surface (BFR/BS) of periosteal cell populations. Strain-related differences in mechanosensitivity and cortical bone material properties and structural properties at the ulnar midshaft were detected among strains. The data suggest that the propensity for bone to respond to mechanical loading is at least partially influenced by genes. Identifying the set of genes that exert their influence on mechanosensitivity has the potential to reveal target molecules and signaling pathways for pharmacological intervention.

The previous study supports the notion that mouse mechanical strain-related bone structural and strength properties are under genetic control, but microlevel intrinsic cortical and trabecular bone properties were not examined. A study by Akhter et al. (2004) examined breed differences in the intrinsic material properties of both cortical and trabecular in adult female D2 and B6 mice. The intrinsic material properties tested were modulus (E_b) and hardness (H) of the midshaft femoral and tibial cortical bone cross sections and of trabecular bone in the distal femur. The technique of nanoindentation provides precise measurement of intrinsic material properties to study local bone tissue properties. Femoral modulus and tibial hardness in cortical bone and hardness in trabecular bone were greater in D2 than in B6. The whole-bone structural and apparent

material strength properties were greater in D2 in comparison to B6. The study suggests that B6 mice exhibit greater femoral cross-sectional area to compensate for the poor intrinsic properties through bone distribution over a larger cross-sectional area.

Quantitative Trait Loci Analyses

Strain-related phenotypes can be utilized to search entire genomes for chromosomal locations called quantitative trait loci (QTL) analyses that contain genes that contribute to phenotypic variation. Mapping the loci that specify quantitative traits poses a challenge because the effect of each QTL may account for only a fraction of the trait variance (Klein, 2002). However, the development of high-density genetic maps allows precise QTL mapping as well as the positional cloning of underlying genes. This approach has been used in both human and experimental animal models to study genetic regulation of bone density, strength, and quality among other traits (Koller et al., 2003; Beamer et al., 2001; Li et al., 2002). QTL analyses have been responsible for identifying several chromosomal regions influencing skeletal phenotypes of the femur and tibia in several populations of mice. Over 60 QTL have been statistically associated with bone-related phenotypes in humans (Liu et al., 2006).

Linkage analysis conducted on intercrosses between B6 and D2 strains, and on recombinant inbred strains generated from the B6 and D2 cross, revealed a number of QTLs affecting bone quality such as material and structural properties. Lang et al. (2005) conducted a QTL analysis to identify several chromosomal regions influencing skeletal phenotypes of the femur and tibia in BXD F2 and BXD RI populations of mice. QTLs for body size, body weight, body length, and adipose mass often mapped to the same

chromosomal regions as those identified for skeletal traits, suggesting that several QTLs identified as influencing bone could be mediated through body size. QTLs, were also identified for structural and material properties as well as morphological measures of the mouse femur and tibia. These findings reaffirm the genetic contribution to skeletal phenotype and provide a basis for examining the role of gene expression in the development of bone.

A study from the same group identified QTLs that contain genes influencing trabecular architecture as measured by micro-computed tomography (μCT) (Bower et al., 2006). Micro-computed tomography acquires accurate measures of trabecular bone architecture providing phenotypic data related to bone volume and trabecular morphology. The study used crosses between B6 and D2 as progenitor strains of a second filial (F2) generation and BXD recombinant inbred strains. The proximal tibial metaphyses of the 200-day-old mice were analyzed by μCT to assess phenotypic traits characterizing trabecular bone, including bone volume fraction, trabecular connectivity, and quantitative measures of trabecular orientation and anisotropy. Heritabilities were calculated and QTLs were identified using composite interval mapping. A number of phenotypes such as degree of anisotropy and connectivity density were found to be highly heritable. These findings support the heritability of bone quality parameters and provide a basis for examining the role of gene expression in the development of bone. Identification of the genes underlying these QTLs may lead to improvements in recognizing individuals most at risk for developing osteoporosis and in the design of new therapeutic interventions.

Genetics and Exercise Performance

Strain-related skeletal phenotypes have been shown to result from genetically induced differences in natural activity levels as well as differential skeletal response to environmental factors. Although a wide range of environmental and behavioral factors have been known to directly impact physical activity, several studies in humans and animals have also presented evidence that there is a genetic contribution to physical activity levels (Perusse et al., 1989; Lauderdale et al., 1997; Swallow et al., 1998; Lerman et al., 2002). In particular, intrinsic exercise capacity and the adaptive response of prolonged exercise stimulus appear to be heritable. The interactions of the genes that affect these traits are thought to influence the skeletal differences observed in D2 and B6 mouse strains. However, the extent to which the background strain contributes to exercise-related phenotypic differences in transgenic mice remains a question. Relatively little is known about strain-dependent differences in exercise training performance.

The ability to perform endurance exercise is suggested to contribute to the differences in skeletal modeling observed between inbred strains of mice. Twin studies in humans have demonstrated a large genetic component to aerobic exercise (Sundet et al., 1994; Bouchard et al., 1986). Lightfoot et al. (2001) further examined the interstrain variation of maximal aerobic performance in rodents to provide basic heritability estimates for intrinsic exercise capacity. A total of 10 inbred strains were run on a treadmill until exhaustion. The protocol began at a speed of 22 m/min and increased approximately 6 m/min every 4 minutes. After 4 minutes at a speed of 42.4 m/min, the grade was increased 2% every 4 minutes until the mouse could not run off of the shock grid. B6 female mice performed better than D2 female mice in exercise duration,

suggesting that there were significant differences in aerobic capacity between the strains. Heritability estimates suggest that 58 to 73% of the variance in aerobic capacity was attributable to genetic background (Lightfoot et al., 2001).

Maximal endurance exercise is not analogous to daily physical activity level, but appears to be a distinct phenotype. Therefore, forced and voluntary exercise models are commonly used to evaluate exercise performance. Both models rely on many common variables such as cardiovascular, respiratory, and musculoskeletal functions, but there are also other factors that are potentially unique to each paradigm such as psychological desire to run, fear of handling, shock avoidance, and pain perception (Swallow et al., 1998; Lerman et al., 2002). A study by Lerman et al. (2002) examined the genetic contribution to both forced and voluntary exercise performance in several inbred strains, including B6 and D2 mice. The mice were exercised on an eight-lane treadmill with shock bars at the rear of the belt to stimulate each mouse to run. Two forced exercise tests were performed, an endurance exercise tolerance and an exercise stress test. The endurance exercise test consisted of a treadmill run at 20 m/min with a 7° incline for a total of 30 minutes. A double-beam infrared photon detector located above the shock grid quantified the number of shock stimuli received by each mouse. This test was used as an indicator of endurance performance with a prolonged, constant exercise stimulus. After completion of the endurance exercise tolerance, the mice were subjected to a graded exercise test, which consisted of an incremental protocol with increasing workload. The exercise stress test began at 20 m/min with a 7° incline and increased by 1.5 m/min every 2 min until reaching the target of 45 m/min. Failure was defined as the inability to continue regular treadmill exercise, despite the extra stimulus of pressurized nitrogen

from an air gun. In contrast, the voluntary exercise was measured using a wheel housed in the cage. The running duration and distance were recorded daily for each animal. There were significant strain differences in endurance exercise performance for both forced treadmill and voluntary wheel models, with D2 mice performing better than B6 mice in the treadmill exercise. Unlike forced treadmill activity, B6 mice performed the best for voluntary distance run in comparison to all examined strains. Despite strain differences in endurance exercise for both models, there was no correlation between voluntary exercise performance and forced treadmill exercise performance within each strain. The lack of correlation was greatest in B6 animals, which showed the poorest performance on the treadmill, yet ran the farthest with the highest average speed on the voluntary wheel. This suggests that B6 are more naturally active in comparison to the other studied strains. Both strains responded to *in vivo* mechanical loading with periosteal apposition, but the relative bone formation rate was significantly greater in D2 mice opposite to our findings. Since B6 are naturally more active, their skeletons are suggested to have already adapted to increased loading with greater cortical expansion relative to D2 mice.

The response to exercise training and intrinsic activity levels was compared and examined in inbred and hybrid mice strains. Male mice from three inbred and hybrid strains completed an exercise performance test before and after a 4-wk treadmill running program (Masset and Berk, 2005). Distance was used as the primary estimate of endurance exercise performance. Training responses varied considerably across strains, indicating strain-dependent differences in the adaptation response to exercise, which supported previous studies. Broad sense heritability estimates supported the genotypic

influence on the responses to training. Conversely, intrinsic exercise capacity and physiometric variables, such as heart mass and muscle mass, did not significantly contribute to the training response. The data indicates that the genetic factors determining intrinsic endurance exercise performance are different from those underlying the response to training. Furthermore, B6 mice exhibited relatively small changes in increase in distance, run time, and work. However, since the duration of the training protocol in this study is shorter than protocols used for other species, it is suggested that mice adapt rapidly to exercise training.

It is reasonable to assume that bone modeling and remodeling is dictated by both physical activity and genetics, but the extent to which genetic background contributes to exercise-related phenotypic changes in humans and mice remains inconclusive. Therefore, the main goal of this project is to measure the bone response of C57BL/6J (B6) and DBA/2J (D2) inbred strains of female mice to treadmill and tower climbing exercise. Understanding the interactions between the intrinsic and extrinsic determinants of bone adaptation is important in gaining a better understanding of basic bone biology in order to achieve optimal skeletal health in humans. Most importantly, the basis for overall variation will facilitate the development of interventions for osteoporosis and enhance the ability to predict individuals at risk.

CHAPTER 3

MATERIALS AND METHODS

Animals and Experimental Design

All procedures and animal usage were approved and complied with the Pennsylvania State University Institutional Animal Care and Use Committee. The study used female C57BL/6J (B6) and DBA/2J (D2) inbred strains of mice. The animals were bred in the barrier facility maintained by the Center for Developmental and Health Genetics. The environment was maintained under positive air pressure with controlled temperature and humidity. The animals were then moved to Noll Laboratory at The Pennsylvania State University.

When the animals were 180 days old, they were randomly assigned to experimental and control groups (Figure 3.1). B6 mice (n = 45) were divided into the following exercise treatment groups: treadmill exercise (n = 15); tower climbing (n = 15); non-exercised controls (n = 15). D2 mice (n = 45) were divided into the same treatment groups: treadmill exercise (n = 15); tower climbing (n = 15); non-exercised controls (n = 15). The animals were individually housed in a reversed 12 hour light/dark cycle. Cages were changed once a week.

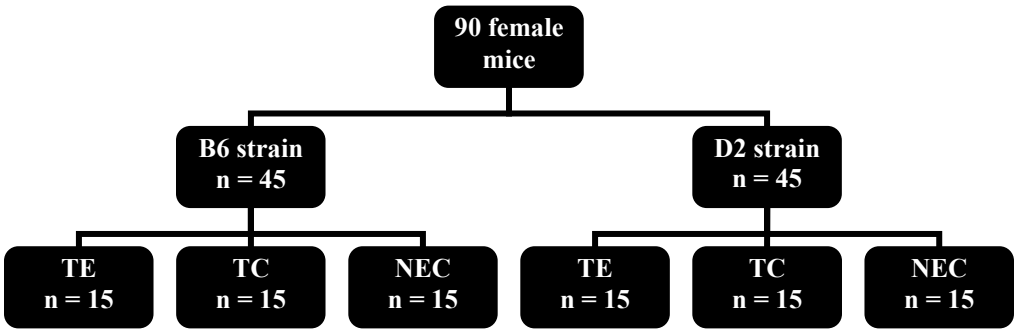

Figure 3.1 Schematic of experimental design
The study group consisted of 90 female mice from B6 and D2 strains, which were divided into the following treatment groups: treadmill exercise (TE), tower climbing (TC), and non-exercised control (NEC).

Treadmill Exercise

The B6 and D2 treadmill exercised mice (n = 15/strain) were trained simultaneously on a 6-lane rodent treadmill during the dark phase of the light cycle. The exercise regimen was performed 5 consecutive days per week for a total of 5 weeks with a gradual increase in incline, speed, and duration (Table 3.1). For the first four days, a 5 degree incline and a speed of 10 m/min were maintained to train the mice to run on the treadmill. The following week, the incline was increased by 5 degrees and the speed was increased by 1 m/min every three days. After every change in speed or incline, the duration was decreased to 20 minutes and then increased to 30 minutes on the next day. The goal of the training protocol was a 25 degree incline at 15 m/min for 30 minutes. Prior to each exercise session, each mouse was placed undisturbed on the treadmill in its respective lane with the belt unmoving, the shock grids off, and the belt motor on for five minutes. In the beginning of each session, the animals were warmed up at 10 m/min with the

shock grids on. The rate was slowly increased at 1 m/min until the target speed was reached.

Three different stimuli were used to encourage the mice to run, including gentle hand prodding, puffs of air from a hand held air pump, and an electrical stimulus at the rear of the belt. Hand prods were used at the beginning of each exercise session under the condition that the animal refused to move onto the treadmill or the animal had received four consecutive electric shocks. Puffs of air were administered throughout the exercise session whenever the mouse dropped back within 5 to 6 inches of the end of the treadmill lane. The electrical stimulus was administered whenever the mouse made contact with the electric grid in the rear of the treadmill lane. The stimulus consisted of 0.74 mA pulses for 200 ms at a rate of 2 pulses per second. The criteria for discontinuing shock exposure for the remainder of the exercise session were 2 seconds or more of shocking, sustaining a total of 20 shocks within any 5 minute period, or a total of 50 shocks during the 30 minute exercise period.

Week	Day	Incline (degrees)	Speed (m/min)	Duration (min)
1	1	5	10	10
1	2	5	10	20
1	3	5	10	20
1	4	5	10	30
1	5	10	10	20
2	8	10	10	30
2	9	10	12	30
2	10	15	12	20
2	11	15	12	30
2	12	15	13	30
3	15	20	13	20
3	16	20	13	30
3	17	20	14	30
3	18	25	14	20
3	19	25	14	30
4	22	25	14	30
4	23	25	15	30
4	24	25	15	30
4	25	25	15	30
4	26	25	15	30
5	29	25	15	30
5	30	25	15	30
5	31	25	15	30
5	32	25	15	30
5	33	25	15	30

Table 3.1 Exercise Program
The B6 and D2 treadmill exercise mice followed an exercise regimen on a 6-lane rodent treadmill. The exercise program was performed for 5 consecutive days per week for a total of 5 weeks with a gradual increase in incline, speed, and duration. The goal of the training protocol was a 25 degree incline at 15 m/min for 30 minutes.

Tower Climbing

The B6 and D2 mice (n = 15/strain) were subjected to a tower climbing exercise regimen for 7 consecutive days per week for a total of 5 weeks. Six towers were

constructed from mesh-wire cylinders, 120 cm tall with a diameter of 17 cm (See Figure 3.2). Two pieces of rectangular plexiglass were used to stabilize each tower. The base of the tower was supported by a piece of plexiglass (14" x 20" ¼) with a cutout circle surrounding the cylinder and a cutout rectangle for the food hanger. The bottom of the tower was attached to a standard mouse cage. Another piece of plexiglass (14" x 20" ¼) with a cutout circle was used to support the middle of the tower. Two pieces of foam panels (20" x 40") were placed at each side of the tower. Infrared sensors were placed along one panel and used to monitor the animal's movement in the tower. Motion is detected when an infrared source with one temperature passes in front of an infrared source with another temperature. This information is then converted into an electric signal and analyzed using a custom written MATLAB program. A holder with two water bottles was placed within the tower and adjusted to various heights ranging from 20 to 100 cm from the base of the tower. To drink from the water container, the mouse had to voluntarily climb to the water bottle. For the first five days, the water bottle was raised 20 cm each day to train the animal to climb to the top of the tower. Another sensor was attached to the water bottle tip to monitor how often the mice drank.

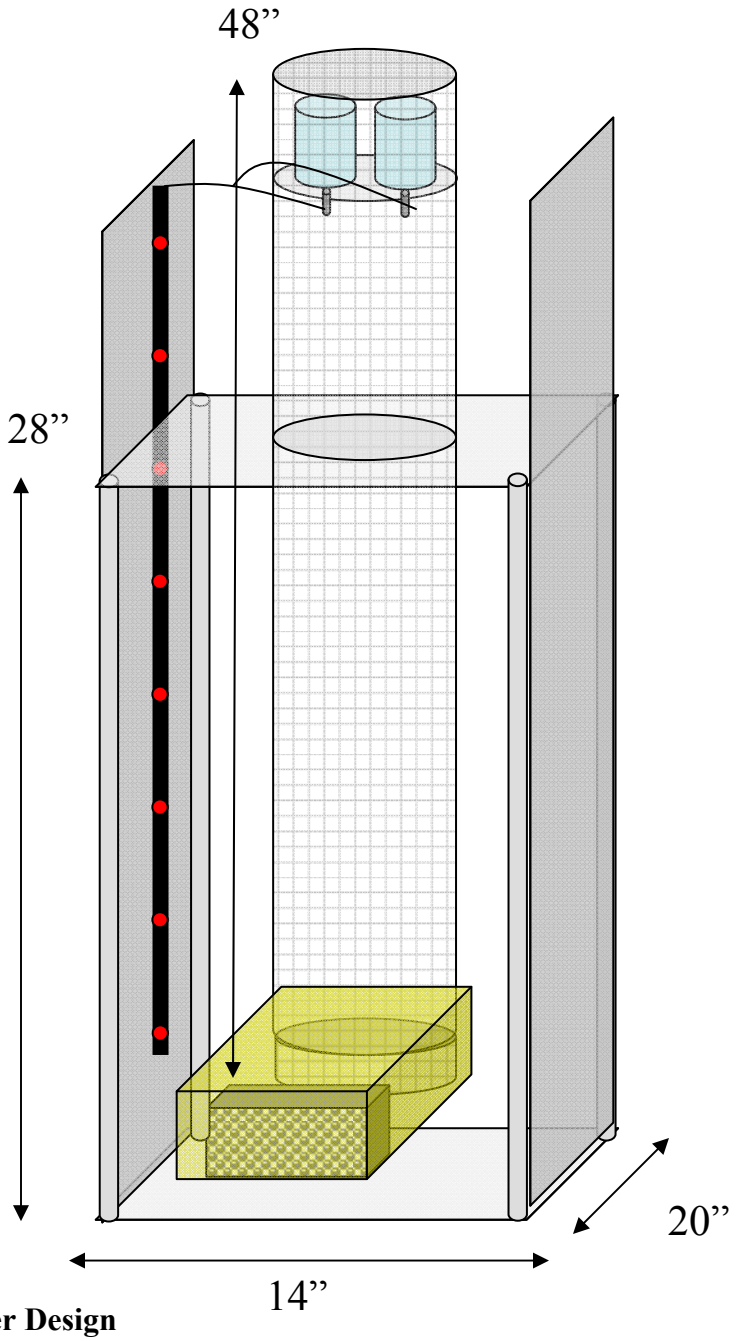

Figure 3.2 Tower Design
Each tower was constructed from mesh wire cylinders, stabilized by two pieces of rectangular plexiglass. The base of the tower was attached to a standard mouse cage with a food holder. A holder with two water bottles was placed within the tower and adjusted to various heights ranging from 20-100 cm from the base to train the animal to climb to the top. Sensors were located on the water bottle as well as the side of the tower to monitor movement and drink sessions.

Gross Morphometric Measurements

After the 5 week exercise program, all animals were euthanized by cervical dislocation. All mice were 211±20 days of age at the time of euthanasia. Immediately after death, animal weight and body length were obtained. Gastrocnemius, soleus, tibialis anterior, and extensor digitorum longus muscles were removed and weighed. The brain was extracted and frozen at -20°C for future studies. The tibias and femurs from the right and left sides were dissected, cleaned, wrapped in saline soaked gauze, and placed in appropriately labeled test tubes. All bones were stored at –20°C until subjected to micro-computed tomography (μCT). On the day of scanning, the right tibias were thawed at room temperature. A digital caliper, accurate to 0.01 mm, was used to measure the tibial length from the articular surface of the proximal condyle to the articular surface of medial malleolus. The diaphyseal width was measured below the apex of the tibial crest in both the coronal and saggittal planes. The epiphyseal width of the proximal tibia was also measured at the widest point in the coronal plane.

Microcomputed Tomography

To obtain quantitative data regarding trabecular architecture, the right tibia was scanned using Scanco Medical μCT-40 computed tomography equipment (Scanco Medical, Zürich, Switzerland). Approximately 1290 slices were obtained using scanner settings of 55Kvp, 145μA, and 200 ms integration times. Images were reconstructed in 2048 x 2048 pixel matrices and stored in 3D arrays with an isotropic voxel size of 15.4 μm.

The software included with the μCT-40 used a Gaussian smoothing operator to filter the images. The shape of the filter was dictated by two parameters: sigma (σ), which represents the standard distribution of the Gaussian curve, and support, which determines the boundaries of the curve. Repeated preliminary analyses found settings of σ = 1.2 and support = 2 to yield an accurate representation of tissue distribution for all contours. A threshold value was also selected to differentiate bone tissue from the background. However, the threshold value differed with the volume of interest (VOI).

Image Thresholding

Image thresholding refers to the process of distinguishing bone from background. One gray-scale value was used as the threshold. Values above this threshold were identified as bone while the values below were considered background.

The threshold value was determined for each volume of interest and applied during the evaluation process. Repeated preliminary analyses found the following values appropriate for accurate representation of bone distribution: threshold = 250 for whole bone contour, threshold = 350 for cortical bone contour, and threshold = 190 for metaphysis contour.

Morphometric Parameters

Instrument software calculated trabecular characteristics using three different models:

1. The VOX model was based on counting the number of voxels above and below the threshold value. This model was used to calculate parameters

including total volume (TV), bone volume (BV), relative bone volume (BV/TV), and connectivity density (Conn.D). These measurements are obtained by placing a grid of points over the two-dimensional image and counting the number of points which lie within bone versus those which lie within soft tissue or void space to create the ratio of void area to total area (AV/AT). This relationship can be extrapolated to determine the three-dimensional bone composition of void volume (VV) to total volume (TV) by:

$$\frac{AV}{AT} = \frac{VV}{TV}$$

Equation 3.2

This method is also used to determine BV, which can be combined with the previous equation to determine BV/TV.

$$BV = TV - VV$$

Equation 3.3

Conn.D is an estimate of the number of trabecular connections. This measurement depends on the Euler number (χ) (Feldkamp et al., 1989; Odgaard and Gunderson, 1993), which is defined as

$$\chi = \beta_0 - \beta_1 - \beta_2$$

Equation 3.4

where β_0 is the number of disconnected struts, β_1 is the connectivity, and β_2 is the number of isolated marrow cavities. In the Euler-Poincaré

equation, β_0 is considered to be equal to 1 because all trabeculae are connected through at least one path and β_2 is equal to 0 because all the marrow spaces are connected. This reduces the Euler-Poincaré equation to

$$\chi = 1 - \beta_1$$

Equation 3.5

Artificial boundaries of the bone are created by the contoured edges of the VOI, thus requiring a correction factor. After boundary suppression is implemented, the connectivity density is calculated as

$$\chi = \frac{1 - \beta_1}{\text{VOI}}$$

Equation 3.6

The structural parameters calculated by the VOX model are summarized in Table 3.2.

Model	Parameter	Abbreviation	Units	Definition
VOX	Total Volume	TV	mm^3	Total area of analysis
	Bone Volume	BV	mm^3	Bone tissue in TV
	Volume Fraction	BV/TV	%	Ratio of bone volume to total area
	Connectivity Density	Conn. D	$1/mm^3$	An estimate of the number of trabecular connections/ mm^3
	Structural Model Index	SMI	none	Measure of rod-like or plate-like distribution of trabeculae

Table 3.2 Parameters calculated using the VOX model
The threshold value was selected to differentiate bone tissue from background. The VOX model was based on counting the number of voxels above and below this value. This model was used to calculate parameters including total volume (TV), bone volume (BV), relative bone volume (BV/TV), and connectivity density (Conn.D).

2. The distance transformation (DT) model was based on an algorithm that superimposes virtual spheres onto the volume of interest in order to calculate the area of the spheres. The DT model was used to calculate trabecular number (Tb.N), trabecular thickness (Tb.Th), and trabecular separation (Tb.Sp). Tb.N quantifies the number of trabeculae by calculating the inverse of the average of all spheres positioned between trabecular mid-axes (Hildebrand et al., 1999). Tb.Th represents the measure of the average strut thickness while Tb.Sp is a measure of the distance between traebculae. Both parameters involve an algorithm that positions hundreds of spheres of maximum diameter either within or

between the trabeculae to calculate the average diameter of all spheres (Hildebrand et al., 1999; Hildebrand and Rüegsegger, 1997). The fraction of sampling points that fall within bone (P_P) relative to all sampling points within the volume of interest is equal to BV/TV (Feldkamp et al., 1989). Test lines are drawn over the image and the intersection between soft tissue and bone are counted and divided by the total test line length to calculate P_L. The bone surface to bone volume ratio (BS/BV) is computed using P_P and P_L:

$$\frac{BS}{BV} = \frac{2P_L}{P_P}$$

Equation 3.7

The previous equation is also used to calculate trabecular architecture parameters. The plate model calculation of trabecular thickness is represented as:

$$Tb.Th = \frac{2}{BS/BV} = \frac{P_P}{P_L}$$

Equation 3.8

The plate model calculation of Tb.N is calculated as:

$$Tb.N = \frac{BV/TV}{Tb.Th} = \frac{P_P}{P_P / P_L} = P_L$$

Equation 3.9

The previous equations are used to calculate the plate model calculation of Tb.Sp:

$$Tb.Sp = \frac{1}{Tb.N} - Tb.Th = \frac{1}{P_L} - \frac{P_P}{P_L} = \frac{1 - P_P}{P_L}$$

Equation 3.10

With the DT model, a local thickness/separation for every voxel within the bone is calculated as well as a standard deviation, resulting in Tb.N Standard Deviation (DT – Tb.1/N.SD), Tb.Th Standard Deviation (DT – Tb.Th.SD), and Tb.Sp Standard Deviation (DT – Tb.Sp.SD).

The structural parameters calculated by the DT model are summarized in Table 3.3.

Model	Parameter	Abbreviation	Units	Definition
DT	Trabecular Number	Tb.N	1/mm	The number of trabeculae per millimeter
	Trabecular Thickness	Tb.Th	Mm	An estimate of trabecular thinning calculated from bone surface and bone volume
	Trabecular Separation	Tb.Sp	Mm	The distance between trabeculae
	Tb.N Standard Deviation	DT – Tb.1/N.SD	1/mm	Standard deviation of local inverse number
	Tb.Th Standard Deviation	DT – Tb.Th.SD	Mm	Standard deviation of local thicknesses
	Tb.Sp Standard Deviation	DT – Tb.Sp.SD	Mm	Standard deviation of local separations

Table 3.3 Parameters calculated using the DT model
The DT model was based on an algorithm that positions virtual spheres onto the volume of interest to calculate the area. The DT model was used to calculate trabecular number (Tb.N), trabecular thickness (Tb.Th), and trabecular separation (Tb.Sp).

3. The TRI model was based on the virtual triangularization of the bone surface. This model produced values for TV, BV, BV/TV, Tb.N, Tb.Th, and Tb.Sp as well as bone surface (BS), bone surface ratio (BS/TV), structural model index (SMI) and degree of anisotropy (DA).

   SMI and DA are both quantitative determinations of architecture. SMI is a descriptive parameter that indicates the extent to which the trabeculae are more rod-like or more plate-like (Hildebrand and Rüegsegger, 1997). The

bone surface is expanded in normal direction by an infinitesimal amount (dr). The new bone surface is recalculated to determine the derivative of the bone surface (dBS/dr). Once the bone volume and the derivative of the surface area are determined, the SMI can be calculated as:

$$SMI = 6 \times \frac{BV \times \frac{dBS}{dr}}{BS^2}$$

Equation 3.11

An SMI value of 0 indicates that the trabeculae exhibit plate-like structure while an SMI value of 3 indicates that the trabeculae demonstrate rod-like struts. DA is a measurement of the preferred orientation of trabecular bone. To measure the DA in a contoured volume, a modification of the mean intercept length methodology was applied in order to use the bone surface triangles to calculate the cosine-weighted directionality of the bone lattice (Laib, 2000). The surface triangles are projected onto a virtual sphere with the positions around this sphere representing the three-dimensional orientations of the triangles. This distribution is the exact inverse of the mean intercept length (MIL) (Harrigan and Mann, 1984; Whitehouse, 1974). These projected surface values are then inverted and fit to the function for an ellipsoid (Harrigan and Mann, 1984). DA is defined as the ratio of the primary axis to the tertiary axis of the mean intercept length ellipsoid (Goulet et al., 1994). A DA value of 1 indicates that the structure is isotropic, meaning that the object possesses the same properties in all directions of testing. As the number increases from 1, the object becomes

increasingly anisotropic such as trabecular bone, which exhibits individual trabeculae oriented to best resist the direction of loading. The structural parameters calculated by the TRI model are summarized in Table 3.4.

Model	Parameter	Abbreviation	Units	Definition
TRI	Total Volume	TV	mm^3	Total area of analysis
	Bone Volume	BV	mm^3	Bone tissue in TV
	Volume Fraction	BV/TV	%	Ratio of bone volume to total area
	Bone Surface	BS	mm^2	Two dimensional measurement of bone/soft tissue interface
	Bone Surface Fraction	BS/BV	1/mm	Ratio of bone surface area to bone volume
	Trabecular Number	Tb.N	1/mm	The number of trabeculae per millimeter
	Trabecular Separation	Tb.Sp	mm	The distance between trabeculae
	Trabecular Thickness	Tb.Th	mm	An estimate of trabecular thinning calculated from bone surface and bone volume
	Degree of Anisotropy	DA	None	Description of trabecular bone orientation

Table 3.4 Parameters calculated using the TRI model
The TRI model was based on the positioning of virtual triangles on the bone surface. This model produced values for TV, BV, BV/TV, Tb.N, Tb.Th, and Tb.Sp as well as bone surface (BS), bone surface ratio (BS/TV), structural model index (SMI) and degree of anisotropy (DA).

Scanning Preparation

The tibias were placed in a cylindrical polyetherimide container that consisted of

twelve wells to hold each specimen (Figure 3.3). Each well was assigned an identification letter from A to L. A notch was located at the perimeter of the holder as a marker for orientation. Each individual well was partially filled with 0.9% NaCl to maintain hydration. The proximal tibia was placed first into the well so that the epiphysis was against the bottom of the well. The diaphysis was vertically positioned against the side of the well to ensure a straight alignment. Tissue soaked in saline was placed around each bone to restrict movement in the well. The specimen holder was placed in a vacuum jar for approximately 30 minutes to remove air bubbles around the bone and the tissue. A plastic adhesive sheet was placed over the top of the holder to prevent the specimens from drying out during scanning. The specimen holder was placed into the bottom of the scanner tube holder, which was then loaded into the CT machine.

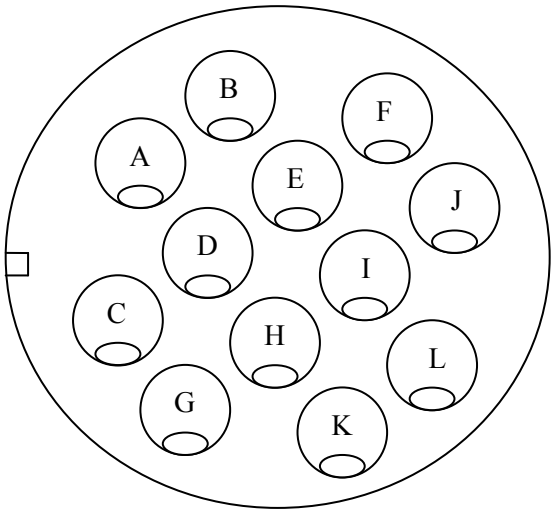

Figure 3.3 µCT Specimen Holder
A circular polyetherimide container consisted of twelve wells to hold each bone. Each well was assigned an identification letter from A to L. A notch was located at the perimeter of the holder as a marker for orientation. The proximal tibia was placed first into the well so that the epiphysis was against the bottom of the well and the diaphysis was vertically positioned against the side of the well to ensure a straight alignment. Each bone was surrounded by tissue soaked in saline to restrict movement in the well.

Whole Bone Contours

Using the notch as a reference point, each bone was located and identified in the sample holder. A circle contour was constructed and placed over the outline of the well in the sample holder (Figure 3.4A, Figure 3.4B, Figure 3.4C). The contour consisted of the slice in which the bone first appears (top slice) to the slice in which the bone disappears (bottom slice). Each bone was contoured individually and saved to its own file. The scanning software performed three-dimensional analyses of the contours. The text files produced by the evaluating software were converted into Microsoft Excel files for analysis of the data.

A. B. C.

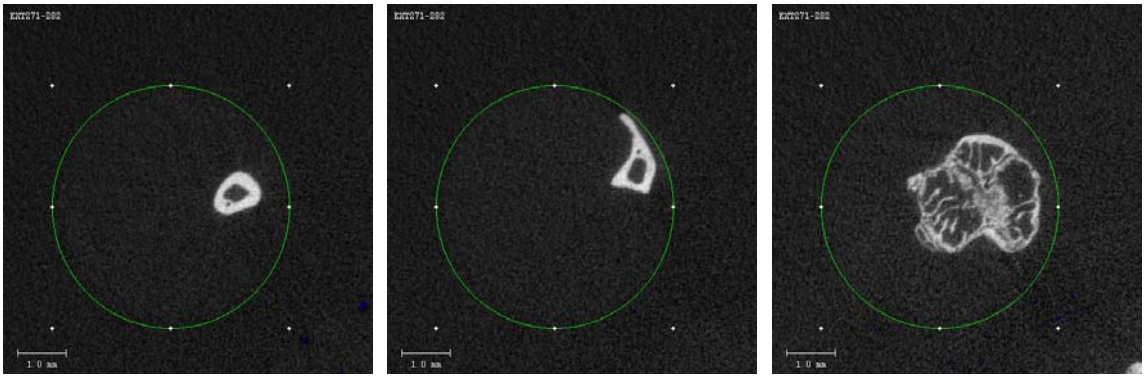

Figure 3.4 Whole Bone Contour
The whole bone was scanned using the μCT-40. A circle contour was constructed and placed over the outline of the well in the sample holder. The contour consisted of the slice in which the bone first appears to the slice in which the bone disappears. Figures A, B, C illustrate examples of whole bone contours from distal to proximal directions

---

Cross Section of Mid-Shaft

Each bone was located and identified in reference to the notch in the sample holder. The mid-shaft was selected using the slices from the whole bone contours. The

difference of the bottom and top slices was divided by two and then added to the top slice, resulting in the mid-shaft slice (Figure 3.5A, Figure 3.5B). The image was captured and used to determine cross-sectional geometry with a custom made MATLAB program.

A. B.

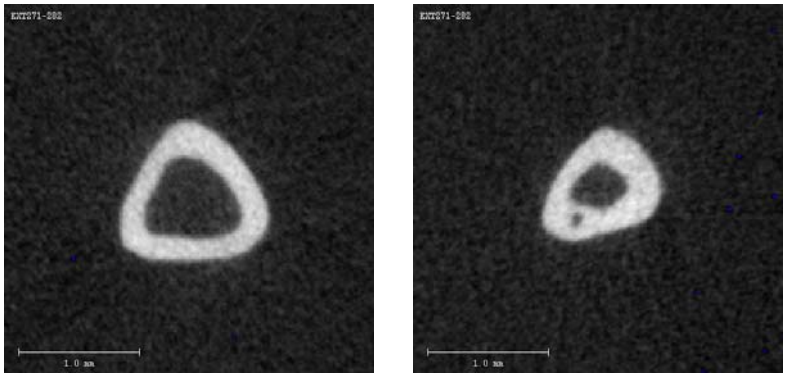

Figure 3.5 Captured Image of Mid-Shaft Cross Section
Images of the mid-shaft cross section were captured using the μCT-40. The mid-shaft was selected using the slices from the whole bone contours. The difference of the bottom and top slices was divided by two and then added to the top slice in order to obtain the mid-shaft cross section slice.
A. Mid-Shaft Cross Section of B6 mouse B. Mid-Shaft Cross Section of D2 mouse

---

Cortical Contour

Using the notch as a reference point, each bone was located and identified in the sample holder. The mid-shaft slice was used to determine the range of the cortical contours. A total of 40 slices were contoured including 20 slices before and after the mid-shaft slice. Contouring was completed around the perimeter of the cortical shell (Figure 3.6A, 3.6B). The process was repeated for each bone and saved to its own file. The scanning software performed three-dimensional analyses of the contours. The text files produced by the evaluating software were converted into Microsoft Excel files for

analysis of the data.

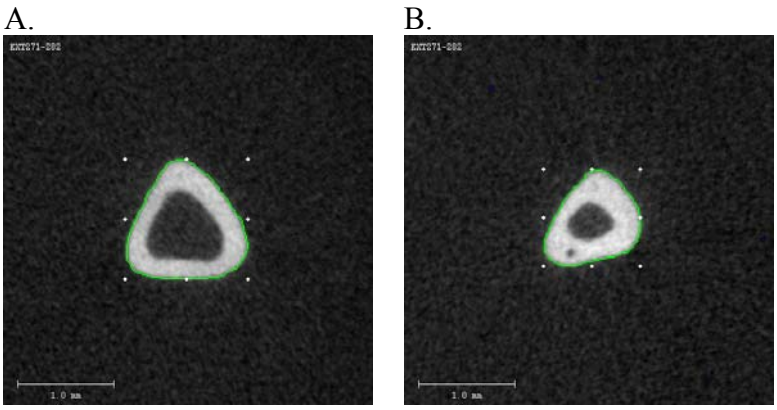

Figure 3.6 Cortical Contour
The range of the cortical contours was determined by the captured mid-shaft slice. Cortical contours included a total of 40 slices, including 20 slices before and 20 slices after the mid-shaft slice. Contouring was completed around the perimeter of the cortical shell. A. Cortical Contour of B6 mouse B. Cortical Contour of D2 mouse

Metaphysis Contour

Each individual bone was located and identified in reference to the notch in the sample holder. The growth plate was located in the proximal aspect of the tibia (Figure 3.7A). The analysis began at the slice where the growth plate was no longer visible (Figure 3.7B). Contouring ended 50 slices away from the growth plate in the distal direction (Figure 3.7C). Contouring was completed as close to the inner surface of the cortical bone as possible. The scanning software performed three-dimensional analyses of the contours. The text files produced by the evaluating software were converted into Microsoft Excel files for analysis of the data.

A. B. C.

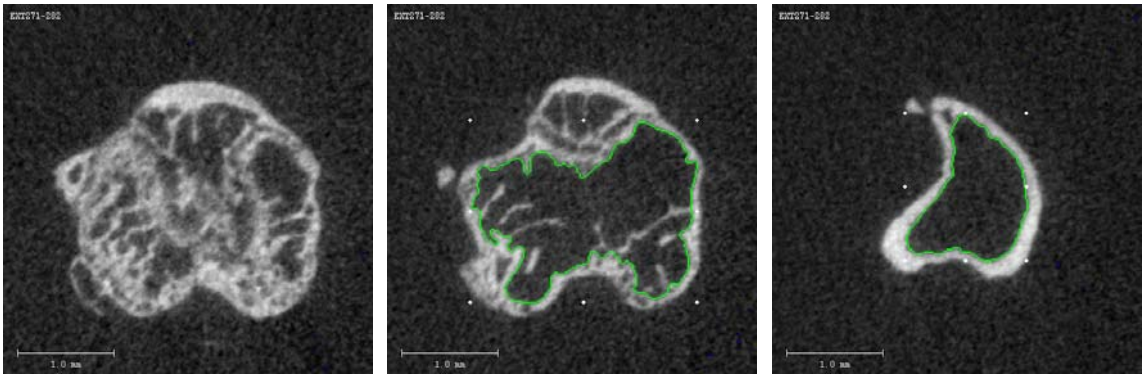

Figure 3.7 Metaphysis Contour
A. The growth plate was located in the proximal aspect of the tibia. B. The analysis began at the slice where the growth plate was no longer visible and C. included 50 slices in the distal direction from the growth plate. Contouring was completed as close to the inner surface of the cortical bone as possible.

Mechanical Testing

The midshaft of the tibia was tested to failure in three-point bending using a semi-hydraulic Materials Testing System (MTS) 858 MiniBionix apparatus. The loading nose was attached to an 8-inch extension aluminum rod connected to the actuator of the MTS machine. The loading nose had a radius of curvature of 0.30 mm and a length of 10 mm. The actuator was warmed and conditioned for approximately 15 minutes prior to experimentation. Appendix A contains the specific settings of the MTS machine during the actuator warm up. After the hydraulics were properly conditioned, the support span fixture was attached to a 50lb load cell, which was attached to the support mounting plate. A 10 mm support span was used to test the tibia. The plate was adjusted so that the center of the support span was in line with the center of the loading nose for the three-point bending test. A small section of the anterior flare of the proximal tibia was carefully removed before testing so that the tibia would lie flat on the support span and remains

motionless during loading. The bone was loaded posterior side up with the nosepiece on the MTS actuator placed at the center of the tibial shaft. Specimens were loaded onto the supports with the proximal aspect of the tibia to the right support and the distal aspect of the tibia was placed on the left support. The operator held onto the tibia in the correct position until the nosepiece contacted the center of the shaft. The MTS equipment was set to apply a continuous load to the specimen at a rate of 1 mm/min until failure, while the software simultaneously recorded load, displacement and time data at 20 Hz. Throughout testing, the tibia was kept hydrated with saline. Data was subsequently imported into a custom written MATLAB program that determined yield load, yield displacement, energy absorbed at yield, failure load, failure displacement, energy absorbed at failure, ultimate load, ultimate displacement, ultimate energy absorption, and stiffness.

After mechanical testing, the proximal fragment of the tibia was fixed in 70% ethanol for histomorphometry while the distal fragment was used for compositional analysis.

Material Properties

The structural parameters obtained from mechanical testing are dependent on the shape and size of each bone as well as the material properties of the tissue itself. Estimates of material properties, yield stress, yield strain, failure stress, failure strain, and tissue modulus of the mid-diaphysis were calculated based upon cross-sectional geometry obtained from the mid-shaft CT analysis. These cross-section images were consistently oriented and analyzed in a MATLAB program that calculated cross-sectional moment of inertia and average thickness as well as thicknesses at the anterior, posterior, medial, and lateral positions. These data, together with data from the three-point bending flexural

tests, were used to calculate stress (σ), strain (ε), and elastic modulus (E) for the diaphysis using beam theory equations. Stress was calculated using Equation 3.12, where σ is the bending stress, F is the yield/failure load, L is the unsupported span length, c is the distance from the cross-section centroid to the tensile periosteal surface and I is the cross-sectional moment of inertia. Strain was calculated using Equation 3.13, where c is the distance from the cross-section centroid to the tensile periosteal surface, d is the actuator displacement, and L is the unsupported span length. Elastic modulus was calculated using Equation 3.14, where F, L, d, and I are previously described.

$$\sigma = FLc/4I$$

Equation 3.12

$$\varepsilon = 12cd/L^2$$

Equation 3.13

$$E = FL^3/d48I$$

Equation 3.14

Tissue Processing and Dynamic Histomorphometry

During the treadmill exercise regimen, all animals received sequential IP injections of calcein and alizarin, dyes that integrate into new bone as it mineralizes. The dyes were administered 7 days and 3 days prior to the conclusion of the exercise intervention.

Following mechanical testing, the proximal end of the tibia was stored in 70% ethanol at 4ºC. During the dehydration process, the bones were immersed in increasing concentrations of ethanol (95%, and 100%) for a total of an hour. The bones were then infiltrated with three different solutions of methyl methacrylate, dibutyl phthalate, and benzoyl peroxide (Table 3.6). Solution III was placed in a 20mL glass container (27 x 63

mm) to form a prelayer for each specimen. The jars were placed in a dessicator and then stored in a water bath at 35ºC for two days. After the prelayer became tacky, the proximal end of the tibia was placed anterior side facing upward so that the shaft was parallel to the top surface of the prelayer. Solution III was prepared using the previous steps and poured into the glass container to cover the bone. After the layer hardened, the bone was sectioned to a thickness of 100µm diaphyseal cross sections using a Buehler Isomet 1000 precision saw. Digital images of each cross section was captured and analyzed under epifluorescence filters using an Axioplan 2 microscope (Carl Zeiss, Thornwood, NY) interfaced with an Axioplan HR digital camera and Axiovision 3.0 software to examine bone formation based on the uptake of the calcein and alizarin labels given during exercise.

For this pilot work, one representative cross-section from each experimental group was qualitatively assessed to ascertain the degree of periosteal and endosteal modeling.

	Ingredients		Infiltration Time
Solution I	Methyl Methacrylate Dibutyl phthalate	95.0cc 5.0cc	20 minutes
Solution II	Methyl Methacrylate Dibutyl phthalate Benzoyl peroxide	95.0cc 5.0cc 1.0g	30 minutes
Solution III	Methyl Methacrylate Dibutyl phthalate Benzoyl peroxide	95.0cc 5.0cc 2.5g	45 minutes

Table 3.5 Methyl Methacrylate Preparation Three different solutions were used for the infiltration and embedding processes. Each tibia was placed in a glass bottle and stored in each solution for the appropriate amount of time.

Compositional Analysis

After mechanical testing, the distal segment of the tibia was used to determine bone composition. A series of measurements was taken using a Mettler H51 balance accurate to 0.01 mg. To avoid contamination, the crucible and the tibia were handled using forceps. An empty ceramic crucible was weighed and used to hold the specimen. The specimen was blotted to remove excess moisture and then weighed with the crucible. The difference between the mass of the crucible plus the wet specimen and the mass of the empty crucible was calculated as the wet mass of the tibia (m_w). Then, each specimen and its respective crucible were placed in a vacuum oven at 100°C for 24 hours. The crucible and the specimen were weighed on the previous balance. The difference between the mass of the crucible plus the dry specimen and the mass of the empty crucible was recorded as the dry mass (m_d). Lastly, the distal tibia and the crucible were placed in a muffled 800°C furnace for 24 hours. The specimen was allowed to cool for at least two hours prior to measurement. The difference between the mass of the crucible plus the ashed specimen and the mass of the empty crucible was recorded as the ash mass (m_a). Using these values, the percent hydration, percent ash, percent organic, and tissue mineralization were calculated as follow (Turner and Burr, 1993):

Percent Hydration (t_{wat})

$$(m_w - m_d) / m_w * 100 = t_{wat}$$

Equation 3.15

Percent Organic (t_{org})

$$(m_d - m_a) / m_w * 100 = t_{org}$$

Equation 3.16

Percent Ash (t_{ash})

$$m_a / m_w * 100 = t_{ash}$$

Equation 3.17

Percent Mineralization (t_{min})

$$m_a / m_d * 100 = t_{min}$$

Equation 3.18

Statistical Analysis

The data was evaluated in JMP 7.0 to determine statistical outliers beyond four standard deviations of the mean. These outliers were removed and corrections for skewness were applied as necessary using SPSS 13.0. The corrections utilized were a natural log transformation and a square root transformation. The complete set of data was then re-run in JMP 7.0 for a 2-way ANOVA. This evaluation examined the effects of genetic strain, treatment, and strain by treatment interactions. Level of significance was set at the 95% confidence level. When treatment was found to have a significant overall effect, the difference between the treadmill running, tower climbing, and non-exercised control was assessed by Tukey-Kramer post hoc test.

CHAPTER 4

RESULTS

This study investigates the skeletal response of female C57BL/6J (B6) and DBA/2J (D2) inbred mouse strains to different types of exercise interventions. A summary of the most significant results is provided in this chapter. Differences due to strain, treatment, and treatment by strain interactions were prevalent throughout the results. Significant ($p \leq 0.05$) or almost significant ($p \leq 0.1$) dependency on the animal's genetic strain was observed for a majority of the evaluated parameters. Of primary interest were those skeletal phenotypes that displayed an exercise intervention main effect or an interaction effect with exercise. A complete list of the evaluated parameters along with their p-values is included in Appendix B.

Strain Differences for Bone Strength and Architecture

Several skeletal measurements were found to differ between the inbred mouse strains as shown in Table 4.1. B6 animals exhibited greater values in all of the mechanical properties with the exception of yield and ultimate displacement. Similarly, the cross-sectional moments of inertia in B6 mice were significantly greater than in D2 mice. However, B6 mice displayed lower percent ash and percent mineralization than D2 mice. The bar graphs in Figure 4.1 illustrate these trends with respect to mechanical, architectural, and compositional properties. Table 4.2 further examines the differences between strains across the three treatment groups.

Strain Differences in Bone Strength, Architecture, and Composition (n=45/strain)				
Category	**Measurement (Units)**	**B6**	**D2**	**p-value**
Mechanical Properties	**Yield Load (N)**			
	Mean	**8.37**	**6.29**	*<0.0001
	Standard Deviation	(0.865)	(0.757)	
	Yield Displacement (mm)			
	Mean	**0.182**	**0.211**	*<0.0001
	Standard Deviation	(0.0255)	(0.0215)	
	Yield Work (N*mm)			
	Mean	**0.816**	**0.710**	*0.0004
	Standard Deviation	(0.146)	(0.126)	
	Ultimate Load (N)			
	Mean	**10.00**	**7.48**	*<0.0001
	Standard Deviation	(0.912)	(0.753)	
	Ultimate Displacement (mm)			
	Mean	**0.278**	**0.299**	*0.0023
	Standard Deviation	(0.0362)	(0.0251)	
	Ultimate Work (N*mm)			
	Mean	**1.70**	**1.32**	*<0.0001
	Standard Deviation	(0.269)	(0.185)	
	Stiffness (N/mm)			
	Mean	**49.7**	**31.5**	*<0.0001
	Standard Deviation	(8.41)	(4.31)	
Architectural Properties	**Total Area (mm^2)**			
	Mean	**0.985**	**0.676**	*<0.0001
	Standard Deviation	(0.0439)	(0.0402)	
	Cross Sectional Moment of Inertia u-direction (mm^4)			
	Mean	**0.0720**	**0.0322**	*<0.0001
	Standard Deviation	(0.0068)	(0.0055)	
	Cross Sectional Moment of Inertia v-direction (mm^4)			
	Mean	**0.0663**	**0.0432**	*<0.0001
	Standard Deviation	(0.0070)	(0.0047)	
	Whole Bone Volume Fraction-VOX (%)			
	Mean	**0.0508**	**0.0479**	*0.0211
	Standard Deviation	(0.0030)	(0.0028)	
	Trabecular Bone Volume-TRI (mm^3)			
	Mean	**0.152**	**0.109**	*<0.0001
	Standard Deviation	(0.0535)	(0.0436)	
Compositional Properties	**Percent Ash (%)**			
	Mean	**48.14**	**52.78**	*<0.0001
	Standard Deviation	(4.24)	(4.76)	
	Percent Mineralization (%)			
	Mean	**63.48**	**65.23**	*0.0372
	Standard Deviation	(3.50)	(4.44)	

Table 4.1 Table Displaying Skeletal Measurement Differences between Strains
* = significant at $p \leq 0.05$

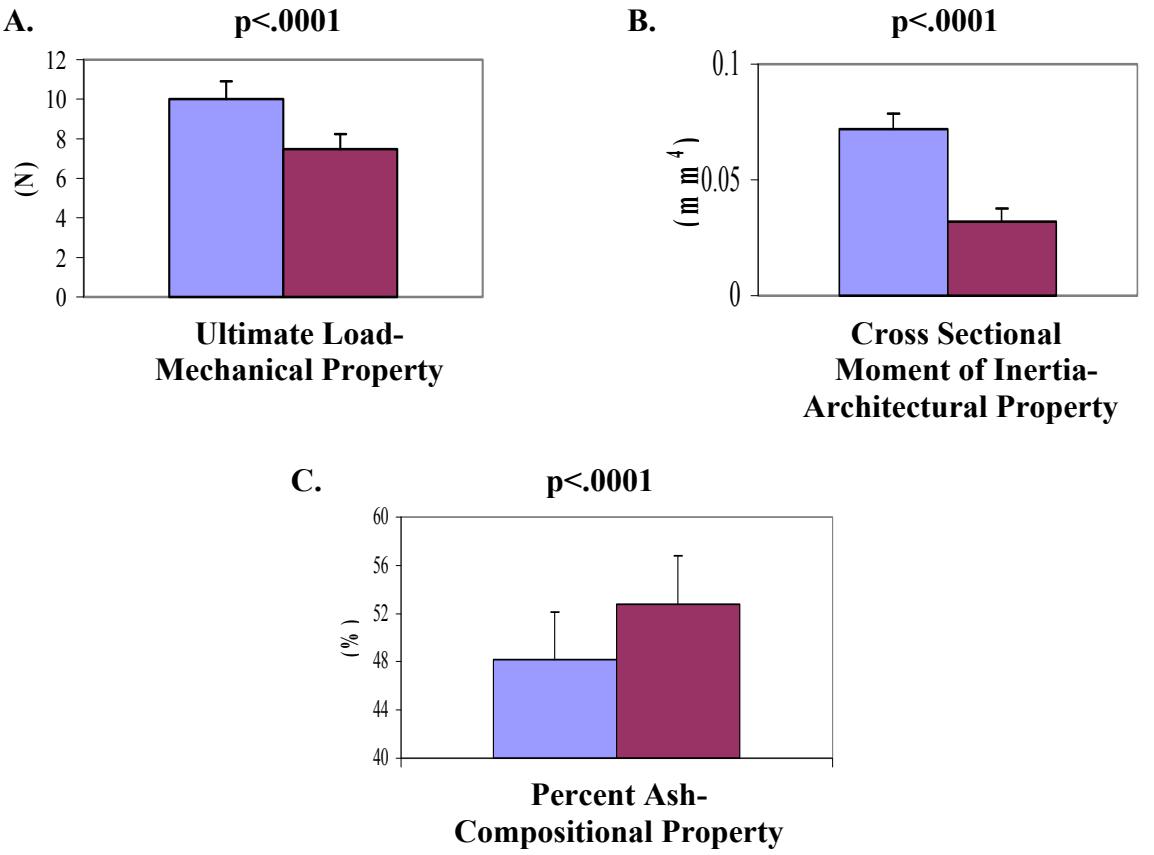

Figure 4.1 Graphs Displaying Skeletal Differences between B6 and D2 mouse strains
Error bars represent 1 standard deviation, n = 45.
A. Ultimate Load- Mechanical Property ($p \leq 0.05$)
B. Cross Sectional Moment of Inertia (x-direction)- Architectural Property ($p \leq 0.05$)
C. Percent Ash- Compositional Property ($p \leq 0.05$)

Strain and Treatment Differences in Bone Strength, Architecture, and Composition (n=15/group)							
Category	**Measurement (Units)**	**TR**		**TC**		**NEC**	
		B6	**D2**	**B6**	**D2**	**B6**	**D2**
Mechanical Properties	**Yield Load (N)**						
	Mean	**8.36**	**6.20**	**8.42**	**6.42**	**8.33**	**6.22**
	Standard Deviation	(0.916)	(0.902)	(0.941)	(0.735)	(0.789)	(0.662)
	Yield Displacement (mm)						
	Mean	0.182	0.204	**0.175**	**0.220**	0.188	0.209
	Standard Deviation	(0.0270)	(0.0228)	(0.0275)	(0.0174)	(0.0219)	(0.0229)
	Yield Work (N*mm)						
	Mean	0.814	0.678	0.786	0.750	**0.850**	**0.696**
	Standard Deviation	(0.148)	(0.150)	(0.158)	(0.103)	(0.132)	(0.121)
	Ultimate Load (N)						
	Mean	**10.1**	**7.55**	**10.1**	**7.49**	**9.82**	**7.41**
	Standard Deviation	(1.09)	(0.919)	(1.03)	(0.692)	(0.555)	(0.695)
	Ultimate Displacement (mm)						
	Mean	0.278	0.296	0.273	0.304	0.282	0.297
	Standard Deviation	(0.0360)	(0.0199)	(0.0398)	(0.0251)	(0.0345)	(0.0300)
	Ultimate Work (N*mm)						
	Mean	**1.72**	**1.32**	**1.70**	**1.34**	**1.67**	**1.30**
	Standard Deviation	(0.290)	(0.141)	(0.264)	(0.202)	(0.269)	(0.210)
	Stiffness (N/mm)						
	Mean	**49.3**	**31.9**	**52.8**	**31.1**	**46.9**	**31.6**
	Standard Deviation	(6.89)	(4.06)	(11.0)	(4.59)	(5.84)	(4.49)
Architectural Properties	**Total Area (mm^2)**						
	Mean	**0.990**	**0.679**	**0.992**	**0.678**	**0.973**	**0.671**
	Standard Deviation	(0.0492)	(0.0454)	(0.0390)	(0.0435)	(0.0434)	(0.0331)
	Cross Sectional Moment of Inertia u-direction (mm^4)						
	Mean	**0.0726**	**0.0326**	**0.0739**	**0.0329**	**0.0696**	**0.0312**
	Standard Deviation	(0.0069)	(0.0065)	(0.0069)	(0.0059)	(0.0064)	(0.0045)
	Cross Sectional Moment of Inertia v-direction (mm^4)						
	Mean	**0.0680**	**0.0436**	**0.0668**	**0.0426**	**0.0642**	**0.0434**
	Standard Deviation	(0.0077)	(0.0056)	(0.0062)	(0.0043)	(0.0068)	(0.0045)
	Whole Bone Volume Fraction-VOX (%)						
	Mean	18.42	17.45	**18.23**	**16.98**	17.77	16.87
	Standard Deviation	(1.09)	(1.08)	(1.16)	(1.03)	(1.04)	(0.823)
	Metaphysis Bone Volume-TRI (mm^3)						
	Mean	**0.176**	**0.126**	**0.159**	**0.0984**	0.121	0.101
	Standard Deviation	(0.0560)	(0.0520)	(0.0523)	(0.0460)	(0.0374)	(0.0253)
Compositional Properties	**Percent Ash (%)**						
	Mean	48.95	53.27	49.09	53.78	**46.38**	**51.35**
	Standard Deviation	(3.01)	(2.87)	(2.76)	(2.75)	(5.91)	(7.13)
	Percent Mineralization (%)						
	Mean	64.04	65.40	64.87	65.84	61.53	64.50
	Standard Deviation	(1.79)	(3.26)	(1.34)	(2.53)	(5.20)	(6.56)

Table 4.2 Table Displaying Skeletal Measurement Differences between Strains and Treatment Groups

TR=Treadmill Running, TC=Tower Climbing, NEC=Non-Exercised Control

Within each treatment, strain pairs that are significantly different are bolded ($\alpha = 0.05$).

Treatment Effect on Cortical Bone Morphology

Several cortical bone measurements were dependent upon the type of intervention received. Phenotypes that were found to be significantly different at either the 95% or almost significant at the 90% confidence level as a function of the exercise intervention are listed in Table 4.3.

Average cortical thickness was found to be significantly different across treatment groups in the global analysis incorporating both strains, where treadmill running mice exhibited an increase in average cortical thickness in comparison with the non-exercised controls ($p=0.0227$). Tower climbing animals were found to be intermediate and did not differ significantly between the treadmill or non-exercised control animals. There were no significant differences when examining treatment effects separately within each strain ($p=0.7719$); however, B6 tower climbing mice trended toward greater changes in cortical thickness as a function of tower climbing relative to treadmill exercise. Contrarily, D2 animals trended toward greater changes in average cortical thickness as a function of treadmill running relative to tower climbing. The bar graphs in Figure 4.2 illustrate these trends.

Treatment Differences in Cortical Bone Morphology (n=15/group)							
Strain	**B6**			**D2**			**Treatment p-value**
Treatment	**TR**	**TC**	**NEC**	**TR**	**TC**	**NEC**	
Measurement (Units)							
Cortical Area (mm^2)							
Mean	**0.629**	**0.631**	**0.608**	**0.572**	**0.569**	**0.561**	0.0712
Standard Deviation	(0.0274)	(0.0283)	(0.0305)	(0.0342)	(0.0314)	(0.0267)	
Medullary Area (mm^2)							
Mean	**0.361**	**0.361**	**0.365**	**0.107**	**0.109**	**0.110**	0.0851
Standard Deviation	(0.0281)	(0.0294)	(0.0320)	(0.0166)	(0.0156)	(0.0135)	
Average Cortical Thickness (mm)							
Mean	**0.182**	**0.183**	**0.177**	**0.229**	**0.227**	**0.224**	*0.0227
Standard Deviation	(0.0052)	(0.0087)	(0.0093)	(0.0081)	(0.0067)	(0.0085)	
Medial Cortical Thickness (mm)							
Mean	**0.198**	**0.187**	**0.186**	**0.278**	**0.267**	**0.264**	0.0924
Standard Deviation	(0.0150)	(0.0235)	(0.0135)	(0.0228)	(0.0308)	(0.0364)	

Table 4.3. Table Displaying Treatment Differences for Cortical Mid-Shaft Morphology

TR=Treadmill Running, TC=Tower Climbing, NEC=Non-Exercised Control
Treatment p-value represents the overall treatment effect in the global analysis incorporating data from both strains (n=30/treatment group).
There were no significant effects of treatment when each strain was examined seperately.

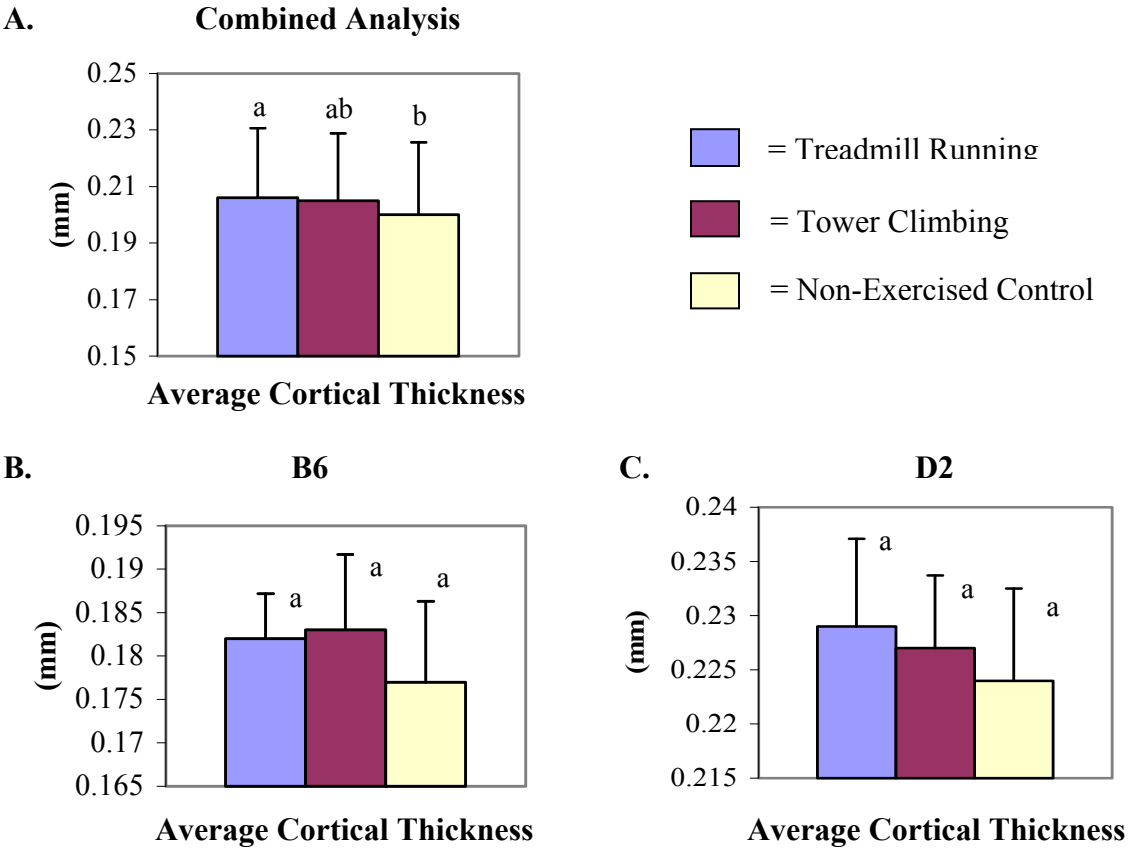

Figure 4.2 Graphs Displaying Treatment Differences for Cortical Mid-Shaft Morphology
Error bars represent 1 standard deviation.
Within each strain, treatments with no letter assignments in common are significantly different ($\alpha = 0.05$) as determined by follow-up Tukey individual comparisons.
A. Average Cortical Thickness for B6 and D2 Strains (n=30/group)
B. Average Cortical Thickness for B6 Strain (n=15/group)
C. Average Cortical Thickness for D2 Strain (n=15/group)

Treatment Effect on Whole Bone Architecture

Several whole bone measurements were dependent upon the type of intervention received. Table 4.4 presents the phenotypes that were found to be significantly different ($p \leq 0.05$) or nearly so as a function of the exercise intervention in the global analysis incorporating both strains.

Connectivity density was found to be significantly different across treatment groups at p=0.0001. In the combined analysis on both strains, treadmill running induced significant decreases in connectivity in comparison to either tower climbing or absence of exercise (p=0.0001). Looking within the B6 strain, non-exercised control animals exhibited significantly greater connectivity than treadmill exercised animals. Connectivity in the tower climbing group was not significantly different than either treadmill exercised or non-exercised controls. D2 animals exhibited a similar pattern, with the non-exercised mice being the highest, followed by tower climbing and treadmill running animals; however, their values were not significantly different across treatment groups.

Degree of anisotropy was also found to be significantly affected by treatment ($p \leq 0.0001$). The bar graphs in Figure 4.3 illustrate these trends. In the global analysis for both strains, treadmill mice were significantly higher than both tower climbing and non-exercised animals. Within B6 animals, treadmill mice exhibited the highest value followed by B6 tower climbing and non-exercised animals, respectively. D2 mice displayed the same pattern. Similar to connectivity density, differences due to treatment were significant in B6 mice whereas the D2 mice did not show a significant effect.

Treatment Differences in Whole Bone Architecture (n=15/group)							
Strain	**B6**			**D2**			**Treatment p-value**
Treatment	**TR**	**TC**	**NEC**	**TR**	**TC**	**NEC**	
Measurement (Units)							
Whole BV-VOX (mm^3)							
Mean	**18.42**	**18.23**	**17.77**	**17.45**	**16.98**	**16.87**	
Standard Deviation	(1.09)	(1.16)	(1.04)	(1.08)	(1.03)	(0.823)	0.0941
Tukey Value	a	ab	b	a	ab	b	
Whole Conn.D-VOX ($1/mm^3$)							
Mean	**0.401**	**0.510**	**0.542**	**0.327**	**0.379**	**0.407**	
Standard Deviation	(0.0955)	(0.118)	(0.0983)	(0.0756)	(0.0848)	(0.0937)	*0.0001
Tukey Value	a	ab	b	a	a	a	
Whole BS/BV-TRI (1/mm)							
Mean	**9.10**	**9.29**	**9.32**	**8.08**	**8.25**	**8.30**	
Standard Deviation	(0.348)	(0.590)	(0.424)	(0.399)	(0.266)	(0.284)	0.0706
Tukey Value	a	a	a	b	b	b	
Whole DA-TRI (none)							
Mean	**1.97**	**1.89**	**1.88**	**1.82**	**1.75**	**1.75**	
Standard Deviation	(0.0739)	(0.0512)	(0.0557)	(0.0645)	(0.0657)	(0.0431)	*<0.0001
Tukey Value	a	b	b	a	a	a	

Table 4.4 Table Displaying Treatment Differences for Whole Bone Architecture of VOX and TRI models

TR=Treadmill Running, TC=Tower Climbing, NEC=Non-Exercised Control
Treatment p-value represents the overall treatment effect in the global analysis incorporating data from both strains (n=30/treatment group).
Within each strain, treatments with no letter assignments in common are significantly different ($\alpha = 0.05$) as determined by follow-up Tukey individual comparisons.

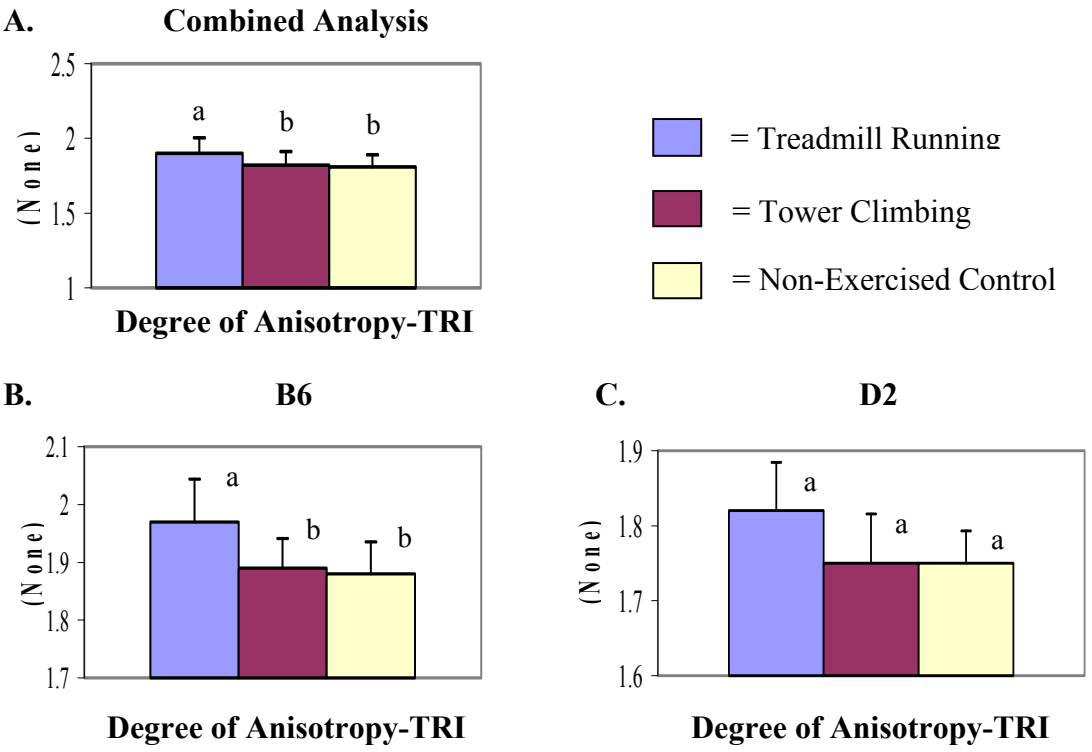

Figure 4.3 Graphs Displaying Treatment Differences for Whole Bone Architecture
Error bars represent 1 standard deviation.
Within each strain, treatments with no letter assignments in common are significantly different ($\alpha = 0.05$) as determined by follow-up Tukey individual comparisons.
A. Degree of Anisotropy-TRI for B6 Strain and D2 Strains (n=30/group)
B. Degree of Anisotropy-TRI for B6 Strain (n=15/group)
C. Degree of Anisotropy-TRI for D2 Strain (n=15/group)

Treatment Effect on Metaphyseal Architecture

The majority of trabecular parameters in the metaphysis were dependent upon the type of intervention received. Phenotypes that were found to be significantly ($p \leq 0.05$) or marginally ($p \leq 0.1$) affected by the exercise intervention are listed in Table 4.5.

In most cases, treadmill exercised animals displayed the greatest changes in architecture irrespective of strain. Elevated parameters include bone volume, bone

volume fraction, and connectivity density from the VOX model. The same trend was found with trabecular number and thickness from the TRI model. These results suggest that for both strains, treadmill exercise induced a greater anabolic response resulting in more trabecular bone with thicker struts. The bar graphs in Figure 4.4 illustrate these trends.

In several cases displaying significant treatment effects, follow up analyses revealed that phenotypes in B6 animals responded significantly to exercise while D2 mice displayed similar, but less dramatic non-significant trends. In particular, B6 treadmill mice exhibited significantly greater values than the B6 control animals while the B6 tower climbing animals were found to be intermediate. These phenotypes include bone volume, bone volume fraction, structural model index of the VOX model as well as bone volume, bone volume fraction, bone surface fraction, and trabecular thickness of the TRI model. The bar graphs in Figure 4.5 illustrate these trends.

Treatment Differences in Metaphyseal Architecture (n=15/group)							
Strain	**B6**			**D2**			**Treatment p-value**
Treatment	**TR**	**TC**	**NEC**	**TR**	**TC**	**NEC**	
Measurement (Units)							
Metaphysis BV-VOX (mm^3)							
Mean	**0.190**	**0.172**	**0.133**	**0.142**	**0.112**	**0.115**	
Standard Deviation	(0.0573)	(0.0544)	(0.0393)	(0.0541)	(0.0491)	(0.0265)	*0.0048
Tukey Value	a	ab	b	a	a	a	
Metaphysis BV/TV-VOX (%)							
Mean	**0.154**	**0.138**	**0.108**	**0.139**	**0.114**	**0.111**	
Standard Deviation	(0.0531)	(0.0375)	(0.0251)	(0.0421)	(0.0445)	(0.0217)	*0.0016
Tukey Value	a	ab	b	a	a	a	
Metaphysis Conn.D-VOX ($1/mm^3$)							
Mean	**13.38**	**13.30**	**9.23**	**20.05**	**14.31**	**14.14**	
Standard Deviation	(9.55)	(7.69)	(4.79)	(9.27)	(10.26)	(8.12)	0.0756
Tukey Value	a	ab	b	a	a	a	
Metaphysis SMI-VOX (none)							
Mean	**2.57**	**2.67**	**3.07**	**2.71**	**2.92**	**2.76**	
Standard Deviation	(0.402)	(0.365)	(0.448)	(0.501)	(0.436)	(0.450)	*0.0183
Tukey Value	a	ab	b	a	a	a	
Metaphysis Mean1 (mm^3)							
Mean	**1.61**	**1.53**	**1.38**	**1.59**	**1.44**	**1.45**	
Standard Deviation	(2.26)	(1.77)	(1.48)	(1.66)	(2.01)	(8.46)	*0.0004
Tukey Value	a	ab	b	a	a	a	
Metaphysis BS-TRI (mm^3)							
Mean	**4.72**	**4.39**	**3.66**	**3.81**	**3.13**	**3.21**	
Standard Deviation	(1.08)	(1.27)	(0.985)	(1.35)	(1.29)	(0.777)	*0.0209
Tukey Value	a	ab	b	a	b	b	
Metaphysis BS/BV-TRI (1/ mm)							
Mean	**27.35**	**27.92**	**30.78**	**30.87**	**32.34**	**32.12**	
Standard Deviation	(3.07)	(1.87)	(2.59)	(2.70)	(1.94)	(4.39)	*0.0092
Tukey Value	a	ab	b	a	a	a	
Metaphysis Tb.N-TRI (1/ mm)							
Mean	**1.97**	**1.82**	**1.54**	**1.95**	**1.65**	**1.60**	
Standard Deviation	(0.545)	(0.465)	(0.315)	(0.527)	(0.638)	(0.336)	*0.0092
Tukey Value	a	a	a	a	a	a	
Metaphysis Tb.Th-TRI (mm)							
Mean	**0.0740**	**0.0719**	**0.0654**	**0.0653**	**0.0621**	**0.0633**	
Standard Deviation	(0.0080)	(0.0049)	(0.0052)	(0.0057)	(0.0039)	(0.0079)	*0.0053
Tukey Value	a	a	b	b	b	b	
Metaphysis Tb.Sp-TRI (mm)							
Mean	**0.458**	**0.511**	**0.614**	**0.480**	**0.600**	**0.587**	
Standard Deviation	(0.108)	(0.143)	(0.150)	(0.132)	(0.268)	(0.134)	*0.0086
Tukey Value	a	a	a	a	a	a	

Table 4.5 Table Displaying Treatment Differences for Metaphyseal Architecture
TR=Treadmill Running, TC=Tower Climbing, NEC=Non-Exercised Control
Treatment p-value represents the overall treatment effect in the global analysis incorporating data from both strains (n=30/treatment group).
Within each strain, treatments with no letter assignments in common are significantly different ($\alpha = 0.05$) as determined by follow-up Tukey individual comparisons.

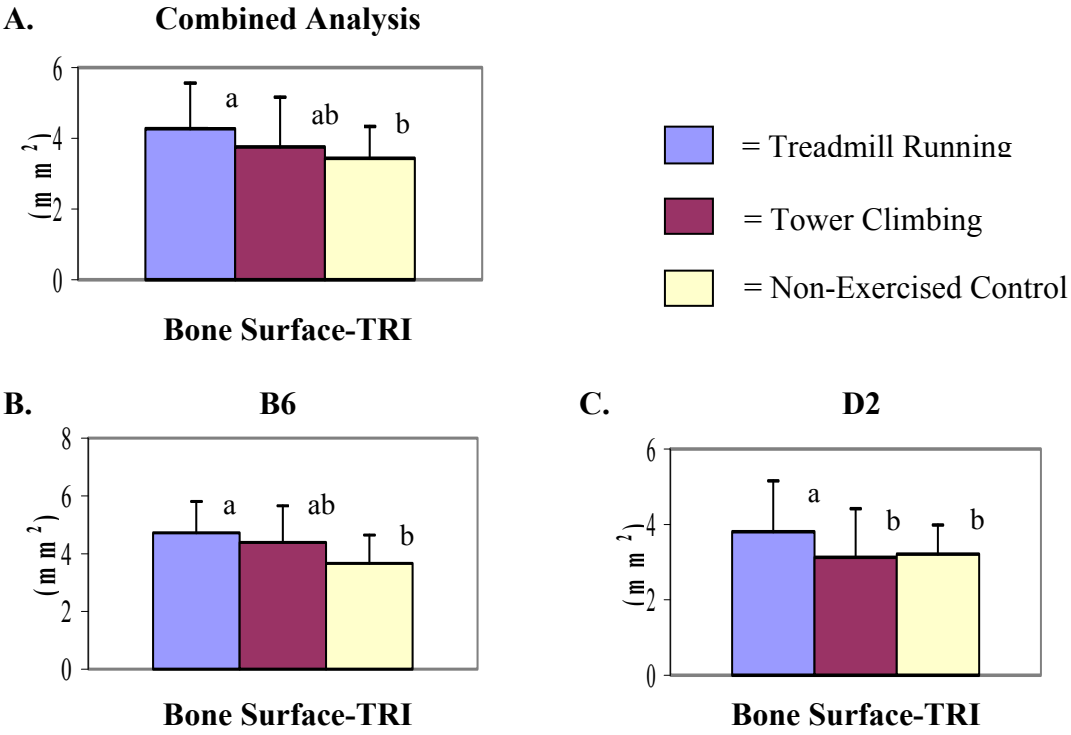

Figure 4.4 Graphs Displaying Treatment Differences for Metaphyseal Architecture
Error bar represent 1 standard deviation.
Within each strain, treatments with no letter assignments in common are significantly different ($\alpha = 0.05$) as determined by follow-up Tukey individual comparisons.
A. Bone Surface-TRI for B6 Strain and D2 Strains (n=30/group)
B. Bone Surface-TRI for B6 Strain (n=15/group)
C. Bone Surface-TRI for D2 Strain (n=15/group)

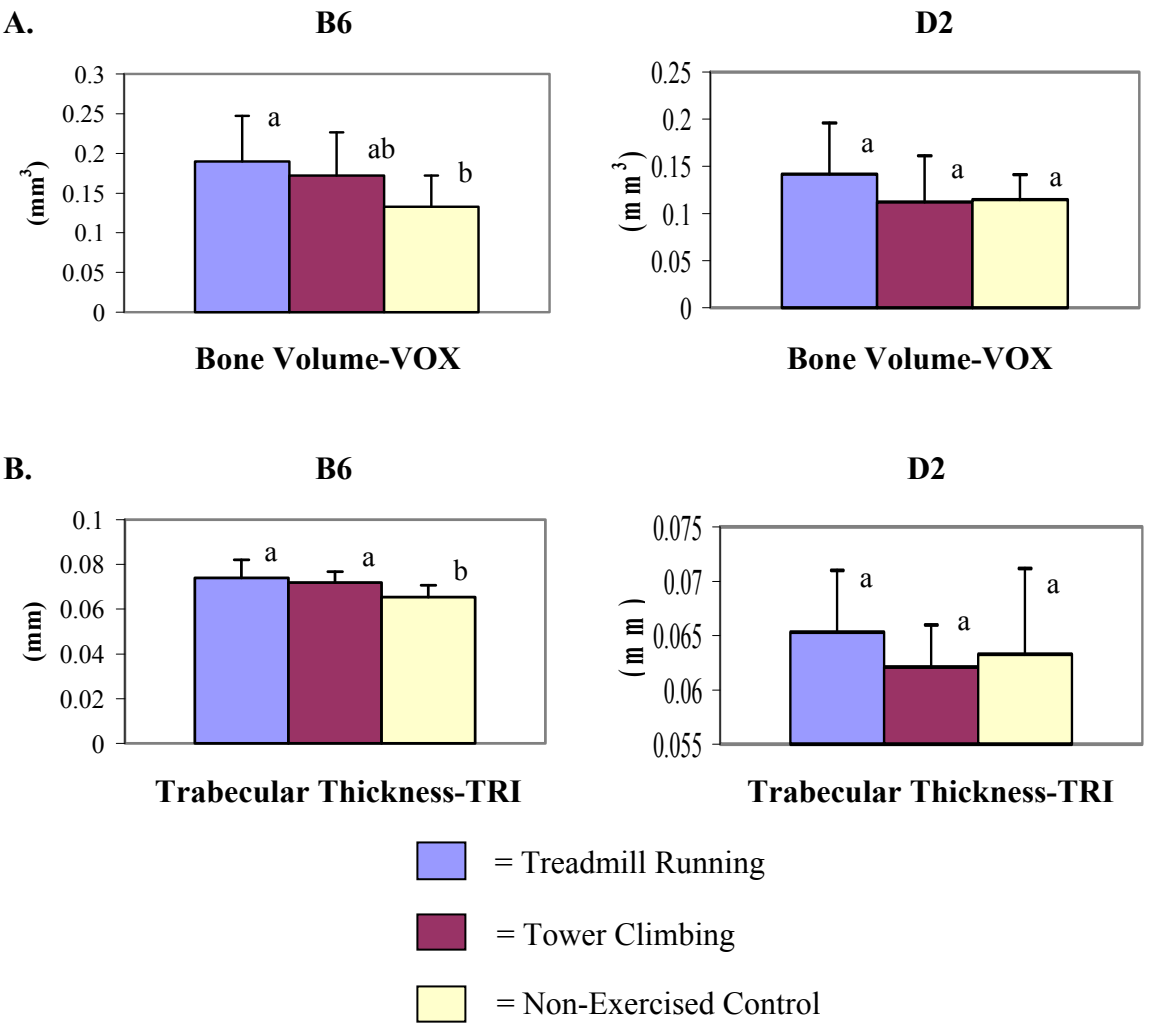

Figure 4.5 Graphs Displaying Significant Exercise by Strain Interactions in the Metaphysis

B6 mice responded positively to exercise while D2 mice displayed no such effect.
Error bar represent 1 standard deviation.
Within each strain, treatments with no letter assignments in common are significantly different ($\alpha = 0.05$) as determined by follow-up Tukey individual comparisons.
A. Bone Volume-VOX for B6, D2 Strains (n=15/group)
B. Trabecular Thickness-TRI for B6, D2 Strains (n=15/group)

Tissue Processing and Dynamic Histomorphometry

Both labels appear in both strains and for all treatment groups, indicating the presence of bone formation based on the uptake of the calcein and alizarin injections given during exercise, as shown in Figure 4.6 and Figure 4.7.

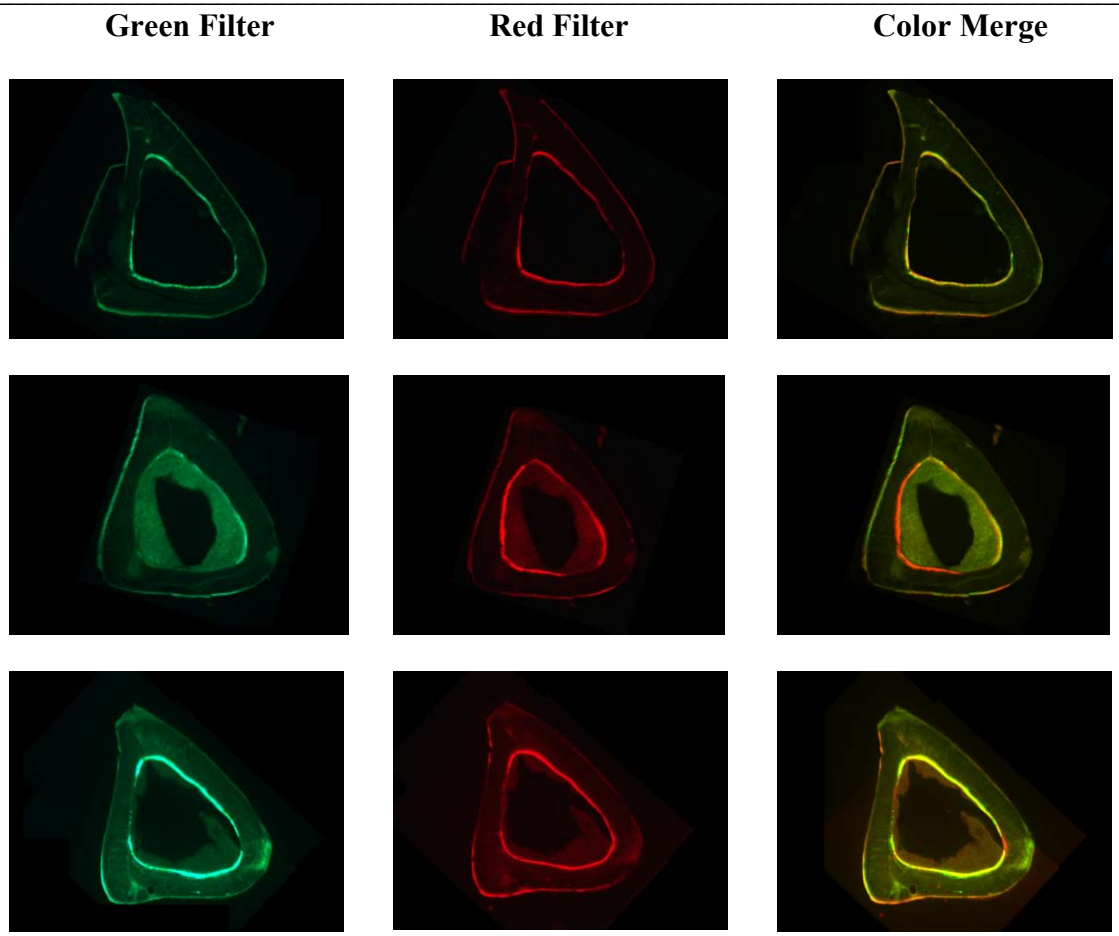

Figure 4.6 Fluorescent Cross-Sectional Images of B6 mice
The green filter was used to excite the calcein label while the red filter was used to excite the alizarin label.
The digital images from both filters were combined to determine the presence of bone formation during the exercise intervention.
TR= Treadmill, TC= Tower Climbing, NEC= Non-Exercised Control

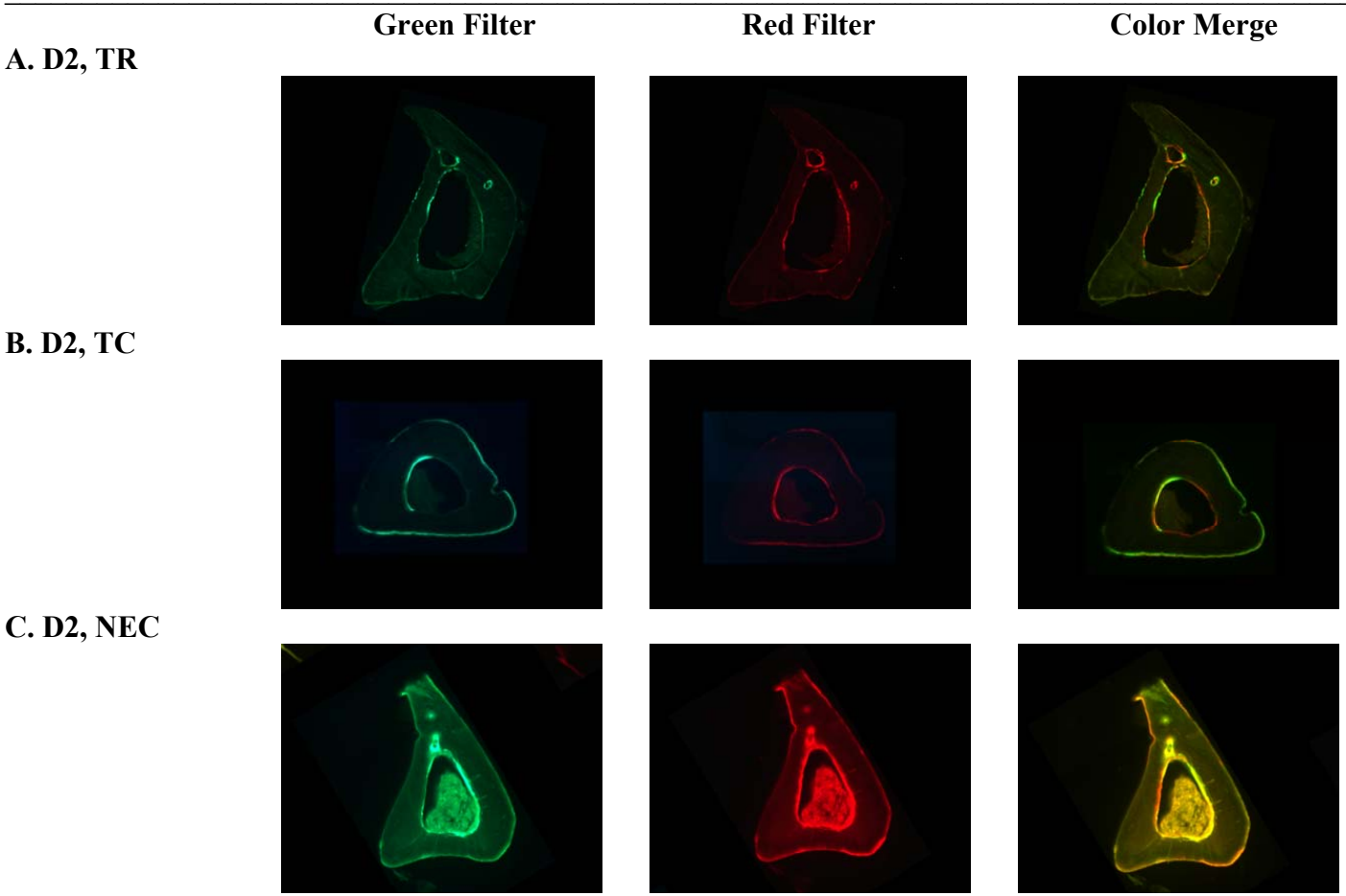

Figure 4.7 Fluorescent Cross-Sectional Images of D2 mice
The green filter was used to excite the calcein label while the red filter was used to excite the alizarin label.
The digital images from both filters were combined to determine the presence of bone formation during the exercise intervention.
TR= Treadmill, TC= Tower Climbing, NEC= Non-Exercised Control

CHAPTER 5

DISCUSSION

Observations and Comparisons to Previous Work

Research leading to improved bone health is a critical need for today's aging, female population. Osteoporosis is a prevalent condition of major concern to this particular group due to the increased morbidity and mortality following osteoporotic fractures. Because loss of bone occurs gradually throughout adulthood, younger populations are often the target for preventative interventions designed to slow progression of this debilitating disease. One such strategy is increased physical activity. The variable outcomes as a consequence of exercise may be due in large part to genetics. Physical activity and genetics have been shown to independently influence bone quality across the lifespan; however, little research has explored the interactive effect of these factors. As a first step toward examining the impact of these interactions, this study measured the skeletal responses to different types of exercise in female B6 and D2 inbred mouse strains; two extensively studied strains with distinctly different skeletal morphology. A more complete understanding of the underlying factors involved in bone regulation may lead to advancements and improvements in recognizing individuals most at risk for developing osteoporosis as well as in the design of new therapeutic patient-specific interventions.

From consultation with previous studies, it was expected that the B6 and D2 inbred strains would exhibit measurable differences in bone strength and architecture. Indeed, significant mechanical and structural distinctions were found between B6 and D2 animals. B6 mice displayed significantly greater mechanical strength (yield load, yield

work, ultimate load, and ultimate work) and stiffness compared to those in D2 mice ($p<0.0001$). As with mechanical properties, bone architecture was also significantly different between the two strains ($p<0.0001$). The mid-tibial diaphyses of B6 mice possessed larger total area and cross sectional moments of inertia (x- and y- directions) than those in D2 mice. The higher moments of inertia in B6 mice confers greater structural strength to the long bones of this mouse strain, since bone material makes a greater contribution to structural bending strength as its distance from the neutral axis of bending increases (Wallace et al., 2007). Contrary to previous phenotypes, D2 mice exhibited greater percentages of mineral within their bones. In particular, D2 mice exhibited significantly higher percent ash ($p<0.0001$) and percent mineralization ($p=0.0372$) than B6 animals. A study by Akhter et al. 2004 suggested that B6 mice exhibit greater cross-sectional area to compensate for the poor intrinsic material properties by distributing bone over a larger-cross sectional area. Clearly, there are alternative but equally effective strategies for producing strong bones. Furthermore, these results further support the notion that mechanical, architectural, and compositional properties are under considerable genetic control. Identifying genes that exert influence on such things as bone architecture, composition, and mechanosensitivity has the potential to reveal target molecules and signaling pathways that may prove useful for pharmacological intervention.

In addition to strain differences, it was also expected that data would support the concept that bone mounts an anabolic response to exercise. We specifically hypothesized that aerobic and resistance exercise will induce different changes in bone architecture. Cortical bone in both strains exhibited an osteogenic response to treadmill exercise.

Exercise produced a significant increase in average cortical thickness at the diaphysis of the tibia ($p=0.0227$). Increases in cortical thickness with exercise have been reaffirmed in several studies in pigs and humans (Woo et al., 1981; Vainionpaa et al., 2007). In the global analysis, treadmill running mice exhibited an increase in average cortical thickness in comparison with non-exercised controls. However, the tower climbing animals were found to be intermediate and did not differ significantly between the treadmill or non-exercised control animals. This does not support previous findings in growing Sprague Dawley-rats and B6 mice. In comparison to sedentary animals, voluntary climbing exercise has been found to accelerate the radial cortical growth of the midfemur by stimulating periosteal bone formation to strengthen the structure of the mid-diaphysis (Notomi et al., 2000; Notomi et al., 2001; Mori et al., 2003). These studies further suggest that an increase in cortical thickness associated with tower climbing exercise supports cortical drift by mechanical stimulation, resulting in improved mechanical characteristics. This discrepancy could be attributed to the tower climbing protocol. It was observed that the D2 animals did not climb the tower as frequently, thus limiting the mechanical stimulation to cause an osteogenic response in bone architecture and strength. In addition, the forelimbs of the tower climbing animals should be examined in future studies. Because of increased demand placed upon the upper body during climbing, greater strength and endurance in the arms would be advantageous (Giles et al., 2006). In particular, a study by Sylvester et al., 2006 examined the osteological changes in the hands of rock climbers. The results suggest that climbers exhibit greater bone thickness, cross-sectional area as well as second moment of inertia. There could have been less osteogenic response in the hindlimbs compared to the forelimbs of the tower climbing

mice. It may be scientifically valuable to conduct studies on the forelimbs to examine site-specific changes during tower climbing.

Similar to cortical bone, treadmill exercise also produced a positive osteogenic response in trabecular bone of the proximal tibial metaphysis. The majority of trabecular parameters were dependent upon the type of intervention received. Treadmill exercised mice exhibited a significant increase in bone volume ($p=0.0048$), trabecular number ($p=0.0092$), and thickness (0.0053). The data indicate that treadmill exercise produced an increase in trabecular bone volume due to the creation of thicker trabeculae, thus decreasing trabecular spacing. These properties, in turn, may assist in the ability to withstand loading (Joo et al., 2003). Tower climbing also tended to produce an osteogenic response in the metaphysis, but bones from these animals did not differ significantly from treadmill running or non-exercised control groups. Again, there findings do not agree with previous studies comparing tower climbing and non-exercised Sprague-Dawley rats and B6 mice (Notomi et al., 2001 and Mori et al., 2003). These studies have found that tower climbing exhibited significant increase in trabecular bone formation rate, trabecular mass, and trabecular thickness in the tibia. The increase in trabecular bone mass of the tibia was caused by increased bone formation and reduced bone resorption in growing rats (Notomi et al., 2001). There may have been less response in our study because the ages of our animals during the exercise program were around 220 days old while the ages of animals in previous studies are about 40 days. The skeleton is sensitive to mechanical stimuli at all ages, but the adaptability of bone is greater before skeletal maturity. As a result, there may have been less of a response because our animals were considerably older.

The results from this study do not agree with previous studies that have compared resistance and aerobic exercise (Notomi et al., 2000b). Thirty Sprague Dawley rats were assigned to one of three experimental groups: sedentary, treadmill running, or jumping. In comparison to the other treatment groups, the resistance exercise jumping rats exhibited increases in the mass and strength of the lumbar vertebrae and mid-diaphysis of the femur. The study suggests that resistance exercise increases bone mass and strength more efficiently than aerobic exercise. This may seem contradictory to the results of our study, as treadmill exercise mice exhibited greater osteogenic response than the tower climbing animals. Although jumping is another form of resistance exercise, tower climbing exercise produces different strains on bone, resulting in unique adaptations specific to the exercise intervention. These results support the notion that mechanical loading affects bone development and that different types of exercise exert distinct effects. In addition, these studies explored the osteogenic responses in rats and the results may not be applicable to inbred strains of mice with distinctly different skeletal phenotypes. These conflicting results further support the need for studies that compare treadmill exercise and tower climbing in mice.

It was also expected that skeletal changes as a consequence of exercise would be dependent upon genetic strain. Exercise intervention studies in humans and rodents have demonstrated that there is an intrinsic component to bone adaption due to the variation of anabolic responses among individuals when subjected to the same degree of mechanical loading. Several phenotypes in B6 animals responded significantly to exercise while D2 mice displayed similar, but less dramatic trends. Lerman et al. (2002) examined the genetic contribution to both forced and voluntary exercise performance in B6 and D2

inbred mouse stains. According to this study, both strains responded to mechanical loading with periosteal apposition, but the relative bone formation rate was significantly greater in D2 mice. Since B6 mice are naturally more active, their skeletons were suggested to have already adapted to increased loading with greater cortical expansion relative to D2 mice. Our results did not agree with this study. Our data suggests that exercised B6 mice show a greater increase in ability to withstand mechanical loading with exercise as compared to other groups. It has been suggested that bones with greater cross sectional area are more sensitive to mechanical loading signals (Beamer et al., 1996; Akhter et al., 2000; Robling and Turner, 2002; Turner, 2002). Therefore, B6 mouse strain possesses a propensity to better respond to mechanical loading. In contrast, D2 mice exhibited a less dramatic effect. It is possible that the response to bending loads is less intense in the high bone density mouse strain (D2) than the low bone density mouse strain (B6) because D2 animals lack the machinery needed to induce high levels of periosteal modeling to increase high cross-sectional moments of inertia (Akhter et al., 2000). As a result, D2 mice maintain normal bone mass distributed over a relatively small region, causing higher bone density. Our histology supports the presence of periosteal bone formation in the cortical bone for both strains, but it does not provide quantitative measurements of the bone formation rate. In future studies, these slides should be analyzed to compare the apposition rate between the treatment groups. For the tower climbing animals, strain differences could be attributed to the observation that D2 mice did not climb the towers as frequently as the B6 mice.

While this study provides a novel examination of the intrinsic and extrinsic factors influencing tibial bone properties, several limitations of this particular approach

should be noted. Although significant results were obtained, numerous improvements can be made in the experimental design. One possible improvement can be attributed to the exercise intervention protocols. Treadmill exercise was forced, and thus the observed results may have been influenced by stress, fear of handling, and pain perception. In contrast, tower climbing was not forced, but was motivated by the need to drink so this exercise program was not as rigorous as the treadmill exercise. Furthermore, forced and voluntary exercise models appear to produce distinct phenotypes for each paradigm. A study by Lerman et al. 2002 has shown that there was no correlation between forced treadmill exercise performance and voluntary wheel exercise performance within each strain. In particular, B6 mice showed the poorest performance on the treadmill, yet ran the farthest with the highest average speed on the voluntary wheel. Furthermore, data indicates that the genetic factors determining intrinsic endurance exercise performance are different from those underlying the response to forced training. Therefore, voluntary wheel running may be substituted for forced treadmill running in order to validate the comparison between aerobic and resistance exercise programs.

In addition to possible limitations of the different exercise protocols, the described analysis does not incorporate in-cage activity, but will be incorporated into this study in the near future. In particular, it was observed that some tower climbing mice did not climb the towers as much as other animals; therefore, some tower climbing animals may not have exhibited a significant response in bone architecture and strength. It is also reasonable to suggest that some experimental subjects in the non-exercised control group may have engaged in substantial physical activity within the confines of their habitat, thus affecting the criteria for “exercise” and “control” groups. This activity data was

collected and will be incorporated into studies in order to explain possible discrepancies among the treatment groups.

In subsequent analyses of the interactive effects of genotype and exercise on bone properties, increasing the number of animals in the experiment will lend more statistical power to the study and possibly elucidate further trends that were obscured by the limited sample size. Additional data can also be garnered by incorporating data from other skeletal sites such as the vertebrae and the femur with the tibia results. Different bones experience specific types of strain, resulting in unique anabolic responses. Iwamoto et al. (1999) examined trabecular bone changes induced by treadmill exercise on the lumbar vertebra, the proximal, and distal tibia in young growing rats. This study demonstrated increased trabecular bone volume/tissue volume (BV/TV) in the proximal and distal tibia, but not in the lumbar vertebrae. The results suggest that osteogenic responses differ with skeletal site, suggesting a need for comparison between skeletal sites. Future studies should also attempt to link differences in gene expression across strains to any detected differences in mechanical responsiveness. Identification of differential gene expression across strains may lead to improvements in recognizing individuals most at risk for osteoporosis and in the design of new therapeutic interventions.

Hypothesis Acceptance or Rejection

Central Hypothesis: Aerobic versus resistance exercise will induce distinctly different changes in bone strength and architecture. Furthermore, these changes noted as a consequence of exercise will be dependent upon genetic strain.

Significant distinctions were found between the bones of B6 and D2 animals, supporting the notion that mechanical, architectural, and compositional properties are under considerable genetic control. In addition, it was also found that bone mounts an anabolic response to exercise. Our data partially supports the hypothesis that aerobic and resistance exercise induced distinctly different changes in bone architecture. Tower climbing animals were found to be intermediate and did not differ significantly between the treadmill or non-exercised control animals. This inconsistency can possibly be attributed to the length and experimental design of the tower climbing intervention as well as the trip frequency of each animal to climb the tower for water. It was also found that skeletal changes as a consequence of exercise are dependent upon genetic strain. Several phenotypes in B6 animals responded significantly to exercise while D2 mice displayed similar, but less dramatic trends. These findings support the hypothesis that bone formation responses vary among individuals and are strongly regulated by genetic factors.

Conclusions

These findings indicate that anabolic responses in bone are dependent on genetics as well as intervention type. The data serve to partially explain the wide discrepancy in

findings across clinical and experimental models as well as emphasize the need for carefully controlled studies that consider not only the type of intervention, but the genotype of the individual undergoing treatment. These results can help provide better prevention as well as earlier detection, intervention, and treatment of bone density loss. Additionally, there will be many other advances in the treatments of other bone diseases. A more thorough understanding of genetic and environmental factors will enhance the abilities to decipher the molecular and physiological mechanisms affecting skeletal health and could lead to new treatment options that effectively target patient-specific details, thus decreasing expenses to health care systems and enhancing quality of life.

REFERENCES

Akhter, M.P., Iwaniec, U.T., Covey, M.A., Cullen, D.M., Kimmel, D.B., Recker, R.R. (2000). Genetic variations in bone density, histomorphometry, and strength in mice. *Calcif Tissue Int*, 67(4):337-344.

Akhter, M.P., Fan, Z., Rho, J.Y. (2004). Bone intrinsic material properties in three inbred mouse strains. *Calcif Tissue Int,* 75(5):416-420.

Barengolts, E.I., Curry, D.J., Bapna, M.S., Kukreja, S.C. (1993). Effects of endurance exercise on bone mass and mechanical properties in intact and ovariectomized rats. *J Bone Miner Res,* 8(8):937-942.

Bassey, E.J., Ramsdale, S.J. (1994). Increase in femoral bone density in young women following high-impact exercise. *Osteoporos Int,* 4(2):72-75.

Beamer, W.G., Donahue, L.R., Rosen, C.J., Baylink, D.J. (1996). Genetic Variability in Adult Bone Density Among Inbred Strains of Mice. *Bone,* 18(5):397-403.

Beamer, W.G., Shultz, K.L., Donahue, L.R., Churchill, G.A., Sen, S., Wergedal, J.R., Baylink, D.J., Rosen, C.J. (2001). Quantitative trait loci for femoral and lumbar vertebral bone mineral density in C57BL/6J and C3h/HeJ inbred mouse strains. *J Bone Miner Res,* 16(7):1195-1206.

Bikle, D.D., Halloran, B.P. (1999). The response of bone to unloading. *J Bone Miner Metab,* 17(4):233-244.

Bouchard, C., Lesage, R., Lortie, G., Simoneau, J.A., Hamel, P., Boulay, M.R., Pérusse, L. Thériault, G. LeBlanc, C. (2000). Aerobic performance in brothers, dizygotic and monozygotic twins. *Med Sci Sports Exerc,* 18(6):639-46.

Bower, A.L., Lang, D.H., Volger, G.P., Vandenbergh, D.J., Blizard, D.A., Stout, J.T., McClearn, G.E., Sharkey, N.A. (2006). QTL analysis of trabecular bone in BXD F_2 and RI mice. *J Bone Miner Res,* 21(8):1267-1275.

Dalsky, G.P., Stocke, K.S., Ehsani, A.A., Slatopolsky, E., Lee, W.C., Birge, S.J. Jr. (1988). Weight-bearing exercise training and lumbar bone mineral content in postmenopausal women. *Ann Intern Med,* 108(6):824-828.

Dequeker, J., Nijs, J., Verstraeton, A., Geusens, P., Gevers, G. (1987). Genetic determinants of bone mineral content at the spine and radius: a twin study. *Bone,* 8(4):207-209.

Feldkamp, L. A., Goldstein, S. A., Parfitt, A. M., Jesion, G., & Kleerekoper, M. (1989). The direct examination of three-dimensional bone architecture in vitro by computed tomography. *J Bone Miner Res, 4*(1):3-11.

Festing, M.F. (1979). Properties of inbred strains and outbred stocks, with special reference to toxicity testing. *J Toxicol Environ Health*, 5(1):53-68.

Fluckey, J.D., Dupont-Versteegden, E.E., Montague, D.C., Knox, M., Tesch, P., Peterson, C.A., Gaddy-Kurten, D. (2002). A rat resistance exercise regimen attenuates losses of musculoskeletal mass during hindlimb suspension. *Acta Physiol Scand*, 176(4):293-300.

Friedlander, A.L., Genant, H.K., Sadowsky, S., Byl, N.N., Gluer, C.C. (1993). A two-year program of aerobics and weight training enhances bone mineral density of young women. *J Bone Miner Res,* 10(4):574-585.

Frost, H.M. (1999). On the estrogen-bone relationship and postmenopausal bone loss: A new model. *J Bone Miner Res,* 14(9):1473-1477.

Fyhrie, D. P., Kimura, J. H. (1999). NACOB presentation Keynote lecture. Cancellous bone biomechanics. North American Congress on Biomechanics. *J Biomech,* 32(11):1139-1148.

Giles, L.V., Rhodes, E.C., Taunton, J.E. (2006). The physiology of rock climbing. *Sports Med*, 36(6):529-545.

Gleeson, P.B., Protas, E.J., LeBlanc, A.D., Schnedier, V.S., and Evans, H.J. (1990). Effects of weight lifting on bone mineral density in premenopausal women. *J Bone Miner Res,* 5(2):153-158.

Goulet, R.W., Goldstein, S.A., Ciarelli, M.J., Kuhn, J.L., Brown, M.B., and Feldkamp, L.A. (1994). The relationship between the structural and orthogonal compressive properties of trabecular bone. *J Biomech,* 27(4):375–389.

Gutin, B. and Kasper, M.J. (1992). Can vigorous exercise play a role in osteoporosis prevention? A review. *Osteoporosis Int*, 2(2):55-69.

Haapasalo, H., Kontulainen, S., Sievänen H., Kannus, P., Järvinen, M., Vuori, I. (2000). Exercise-induced bone gain is due to enlargement in bone size without a change in volumetric bone density: a peripheral quantitative computed tomography study of the upper arms of male tennis players. *Bone*, 27(3):351-357.

Harrigan, T.P., Mann, R.W. (1984). Characterization of microstructural anisotropy in orthotropic materials using a second rank tensor. *J Mater Sci*, 19(3):761–767.

Hildebrand, T., Rüegsegger, P. (1997a). Quantification of Bone Microarchitecture with the Structure Model Index. *Comput Methods Biomech Biomed Engin,* 1(1):15-23.

Hildebrand, T., Rüegsegger, P. (1997b). A New Method for the Model-Independent

Assessment of Thickness in Three-Dimensional Images. *Journal of Microscopy,* 185(1):67-75.

Hildebrand, T., Laib, A., Müller, R., Dequeker, J., Rüegsegger, P. (1999). Direct three-dimensional morphometric analysis of human cancellous bone: microstructural data from spine, femur, iliac crest, and calcaneus. *J Bone Miner Res*, 14(7):1167-1174.

Iwamoto, J., Shimamura, C., Takeda, T., Abe, H., Ichimura, S., Sato, Y., Toyama, Y. (2004). Effects of treadmill exercise on bone mass, bone metabolism, and calciotropic hormones in young growing rats. *J Bone Miner Metab*, 22(1):26-31.

Iwamoto, J., Takeda, T., Sato, Y. (2005). Effect of treadmill exercise on bone mass in female rats. *Exp Animal*, 54(1):1-6.

Iwamoto, J., Yeh, J.K., Aloia, J.F. (1999). Differential effect of treadmill exercise on three cancellous bone sites in the young growing rat. *Bone*, 24(3):163-169.

Iwamoto, J., Yeh, J.K., Aloia, J.F. (2000). Effect of deconditioning on cortical and cancellous bone growth in the exercise trained young rats. *J Bone Miner Res,* 15(9):1842-1849.

Joo, Y.I., Sone, T., Fukunaga, M., Lim, S.G., Onodera, S. (2003). Effects of endurance exercise on three-dimensional trabecular bone microarchitecture in young growing rats. *Bone,* 33(4):485-493.

Kannus, P., Sievänen, H., Vuori, I. (1996). Physical loading, exercise, and bone. *Bone*, 8(1 Suppl):1S-3S.

Kesavan, C., Mohan, S., Oberholtzer, S., Wergedal, J.E., Baylink, D.J. (2005). Mechanical loading-induced gene expression and BMD changes are different in two inbred mouse strains. *J Appl Physiol,* 99(5): 1951-1957.

Klein, R.F., Mitchell, S.R., Phillips, T.J., Belknap, J.K., Orwoll, E.S. (1998). Quantitative trait loci affecting peak bone mineral density in mice. *J Bone Miner Res,* 13(11):1648-1656.

Klein, R.F. (2002). Genetic regulation of bone mineral density in mice. *J Musculoskel Neuron Interact*, 2(3):232-236.

Kodama, Y., Umemura, Y., Nagasawa, S., Beamer, W.G., Donahue, L.R., Rosen, C.R., Baylink, D.J., Farley, J.R. (2000). Exercise and mechanical loading increase periosteal bone formation and whole bone strength in C57BL/6J mice but not in C3H/Hej mice. *Calcif Tissue Int,* 66(4): 298-306.

Kohrt, W.M., Ehsani, A.A., Birge, S.J., Jr. (1997). Effects of exercise involving predominantly either joint-reaction or ground-reaction forces on bone mineral density in older women. *J Bone Miner Res,* 12(8):1253-1261.

Koller, D.L., Schriefer, J., Sun, Q., Shultz, K.L., Donahue, L.R., Rosen, C.J., Foroud, T., Beamer, W.H., Turner, C.H. (2003). Genetic effects for femoral biomechanics, structure, and density in C57BL/6J and C3h/HeJ inbred strains of mice. *J Bone Miner Res,* 18(10):1758-1765.

Laib, A., Barou, O., Vico, L., Lafage-Proust, M.H., Alexandre, C., Rügsegger, P. (2000). 3D micro-computed tomography of trabecular and cortical bone architecture with application to a rat model of immobilisation osteoporosis. *Med Biol Eng Comput*, 38(3):326-332.

Lang, D.H., Sharkey, N.A., Mack, H.A., Vogler, G.P., Vandenbergh, D.J., Blizard, D.A., Stout, J.T., McClearn, G.E. (2005). Quantitative trait loci analysis of structural and material skeletal phenotypes in C57BL/6J and DBA/2 second-generation and recombinant inbred mice. *J Bone Miner Res,* 20(1):88-99.

Lang, T.F., LeBlanc, A.D., Evans, H.J., Lu, Y. (2006). Adaptation of the proximal femur to skeletal reloading after long-duration spaceflight. *J Bone Miner Res,* 21(8):1224-1230.

Lanyon, L.E. (1987). Functional strain in bone tissue as an objective, and controlling stimulus for adaptive bone remodelling. *J Biomech,* 20(11-12):1083-1093.

Lauderdale, D.S., Fabsitz, R., Meyer, J.M., Sholinsky, P., Ramakrishnan, V., Goldberg, J. (1997). Familial determinants of moderate and intense physical activity: a twin study. *Med Sci Sports Exerc*, 29(8):1062-1068.

Lerman, I., Harrison, B.C., Freeman, K., Hewett, T.E., Allen, D.L., Robbins, J., Leinwand, L.A. (2002). Genetic variability in forced and voluntary endurance exercise performance in seven inbred mouse strains. *J Appl Physiol,* 92(6): 2245-2255.

Li, X., Masinde, G., Gu, W., Wergedal, J., Mohan, S. Baylink, D.J. (2002). Genetic dissection of femur breaking strength in a large population (MRL/MpJxSJL/J) of F2 mice: single QTL effects, epistasis, and pleiotropy. *Genomics,* 79(5):734-740.

Lightfoot, J.T., Turner, M.J., Debate, K.A., Kleeberger, S.R. (2001). Interstrain variation in murine aerobic capacity. *Med Sci Sports Exerc,* 33(12):2053-2057.

Liu, Y.J., Shen, H., Xiao, P., Xiong, D.H., Li, L.H., Recker, R.R., Deng, H.W. (2006). Molecular genetic studies of gene identification for osteoporosis: a 2004 update. *J Bone Miner Res,* 21(10):1511-1535.

Martin, R. B., Sharkey, N. A., & Burr, D. B. (1998). *Skeletal Tissue Mechanics.* New York, NY: Springer-Verlag.

Massett, M.P., Berk, B.C. (2005). Strain-dependent differences in responses to exercise training in inbred and hybrid mice. *Am J Physiol Regul Integr Comp Physiol,* 288(4):R1006-1013.

Menkes, A., Mazel, S., Redmond, R.A., Koffler, K., Libanati, C.R., Gundberg, C.M., Zizic, T.M., Hagberg, J.M., Pratley, R.E., Hurley B.F. (1993). Strength training increases regional bone mineral density and bone remodeling in middle-aged and older men. *J Appl Physiol,* 74(5):2478-2484.

Morey, E.R. (1979). Spaceflight and bone turnover: Correlation with a new rat model of weightlessness. *BioSci*, 29:168-172.

Morey-Holton, E.R., Globus, R.K. (1998). Hindlimb unloading of growing rats: a model for predicting skeletal changes during space flight. *Bone*, 22(5 Suppl):83S-88S.

Mori, T., Okimoto, N., Sakai, A., Okazaki, Y., Nakura, N., Notomi, T., Nakamura, T. (2003). Climbing exercise increases bone mass and trabecular bone turnover through transient regulation of marrow osteogenic and osteoclastogenic potentials in mice. *J Bone Miner Res,* 18(11):2002-2009.

Mosley, J.R., March, B.M., Lynch J., Lanyon, L.E. (1997). Strain magnitude related changes in whole bone architecture in growing rats. *Bone,* 20(3):191-198.

National Osteoporosis Foundation. (2008) Osteoporosis Facts [Web Page] URL http://www.nof.org/osteoporosis/diseasefacts.htm (accessed May 2008)

Notomi, T., Lee, S.J., Okimoto, N., Okazaki, Y., Takamoto, T., Nakamura, T., Suzuki, M. (2000a). Effects of resistance exercise training on mass, strength, and turnover of bone in growing rats. *Eur J Appl Physiol,* 82(4):268-274.

Notomi, T., Okazaki, Y., Okimoto, N., Saitoh, S., Nakamura, T., Suzuki, M. (2000b). A comparison of resistance and aerobic training for mass, strength and turnover of bone in growing rats. *Eur J Appl Physiol*, 83(6):469-474.

Notomi, T., Okimoto, N., Okazaki, Y., Tanaka, Y., Nakamura, T., Suzuki, M. (2001). Effects of tower climbing exercise on bone mass, strength, and turnover in growing rats. *J Bone Miner Res,* 16(1):166-74

Notomi, T., Okazaki, Y., Okimoto, N., Tanaka, Y., Nakamura, T., Suzuki, M. (2002). Effects of tower climbing exercise on bone mass, strength, and turnover in orchidectomized growing rats. *J Appl Physiol,* 93(3):1152-1158.

Notomi, T., Okimoto, N., Okazaki, Y., Nakamura, T., Suzuki, M. (2003). Tower climbing exercise started 3 months after ovariectomy recovers bone strength of the femur and lumbar vertebrae in aged osteopenic rats. *J Bone Miner Res*, 18(1):140-9.

Odgaard, A. Gundersen, H.J. (1993). Quantification of connectivity in cancellous bone, with special emphasis on 3-D reconstructions. *Bone,* 14(2):173–182.

Pérusse, L., Tremblay, A., LeBlanc, C., and Bouchard, C. (1989). Genetic and environmental influences on level of habitual physical activity and exercise participation. *Am J Epidemiol*, 129(5):1012-1022.

Pocock, N.A., Eisman, J.A., Hopper, J.L., Yeates, M.G., Sambrook, P.N., Eberl, S. (1987). Genetic Determinants of Bone Mass in Adults. A Twin Study. *J Clin Invest*, 80(3):706-710.

Pouilles, J.M., Bernard J., Tremollières, F., Louvet, J.P., Ribot, C. (1989). Femoral bone density in young male adults with stress fractures. *Bone*, 10(2):105-108.

Ridler, T.W., Calvard, S. (1978). Picture thresholding using an iterative selection method. *IEEE Trans Syst Manage and Cybern,* 8(8):630-632.

Robling, A.G., Turner, C.H. (2002). Mechanotransduction in bone: genetic effects on mechanosensitivity in mice. *Bone*, 31(5):562-569.

Ryan, A.S. Treuth, M.S., Hunter, G.R., Elahi, D. (1998). Resistive training maintains bone mineral density in postmenopausal women. *Calcif Tissue Int,* 62(4):295-299.

Shackelford, L.C., LeBlanc, A.D., Driscoll, T.B., Evans, H.J., Rianon, N.J., Smith, S.M., Spector, E., Feeback, D.L., Lai, D. (2004). Resistance exercise as a countermeasure to disuse-induced bone loss. *J Appl Physiol,* 97(1):119-129.

Slemenda, C.W., Christian, J.C., Williams, C.J., Norton, J.A., Johnston, C.C. Jr. (1991). Genetic determinants of bone mass in adult women: a re-evaluation of the twin model and the potential importance of gene interaction on heritability estimates. *J Bone Miner Res,* 6(6):561-567.

Smith, D.M., Nance, W.E., Kang K.W., Christian, J.C., Johnston, C.C. Jr. (1973). Genetic Factors in Determining Bone Mass. *J Clin Invest,* 52(11):2800-2808.

Snow-Harter, C., Bouxsein, M.L., Lewis, B.T., Carter, D.R., Marcus, R. (1992). Effects of resistance and endurance exercise on bone mineral status of young women: a randomized exercise intervention trial. *J Bone Miner Res,* 7(7):761-769.

Sundet, J.M. Magnus, P., Tambs, K. (1994). The heritability of maximal aerobic power: a study of Norwegian twins. *Scand J Med Sci Sports,* 4:181-185.

Swallow, J.G., Garland, T. Jr., Carter, P.A., Zhan, W.Z., Sieck, G.C. (1998). Effects of voluntary activity and genetic selection on aerobic capacity in house mice (*Mus domesticus*). *J Appl Physiol*, 84(1):69-76.

Sylvester, A.D., Christensen, A.M., Kramer, P.A. (2006). Factors influencing osteological changes in the hands and fingers of rock climbers. *J Anat*, 209(5):597-609.

Trussell, H.J. (1979). Comments on "Picture thresholding using an iterative selection method." *IEEE Trans Syst Manage and Cybern,* 9(5):311-311.

Turner, C.H., Burr, D.B. (1993). Basic biomechanical measurements of bone: a tutorial. *Bone*, 14(4):595-608.

Vainionpää, A., Korpelainen, R., Sievänen, H., Vihriälä, E., Leppäluoto, J., Jämsä, T. (2007). Effect of impact exercise and its intensity on bone geometry at weight-bearing tibia and femur. *Bone* 40(3):604-611.

Wallace, J.M., Rajachar, R.M., Allen, M.R., Bloomfield, S.A., Robey, P.G., Young, M.F., Kohn, D.H. (2007). Exercise-induced changes in the cortical bone of growing mice are bone- and gender-specific. *Bone*, 40(4):1120-1127.

Warner, S.E., Shea, J.E., Miller, S.C., Shaw, J.M. (2006). Adaptations in cortical and trabecular bone in response to mechanical loading with and without weight bearing. *Calcif Tissue Int*, 79(6):395-403.

Whitehouse, W. J. (1974). The quantitative morphology of anisotropic trabecular bone. *J Microsc*, 101(Pt 2):153–168.

Woitge, H.W., Friedmann, B., Suttner, S., Farahmand, I., Müller, M., Schmidt-Gayk, H., Baertsch, P. Ziegler, R., Seibel, M.J. (1998). Changes in bone turnover induced by aerobic and anaerobic exercise in young males. *J Bone Miner Res,* 13(12): 1797-1804.

Wolff, J. (1892). *The Law of Bone Remodeling.* Translation of Wolff's Das Gesetz der Transformation der Knochen by P. Marquet and R. Furlong. Berlin: Springer-Verlag.

Woo, S.L., Kuei, S.C., Amiel, D., Gomez, M.A., Hayes, W.C., White, F.C., Akeson, W.H. (1981). The effect of prolonged physical training on the properties of long bone: a study of Wolff's Law. *J Bone Joint Surg Am*, 63(5):780-787.

Yeh, J.K., Aloia, J.F. (1990). Deconditioning increases bone resorption and decreases bone formation in the rat. *Metabolism,* 39(6):659-663.

Yeh, J. K., Aloia, J.F., Chen, M.M, Tierney, J.M., Sprintz, S. (1993a). Influence of exercise on cancellous bone of the aged female rat. *J Bone Miner Res,* 8(9):1117-1125.

Yeh, J.K., Liu, C.C., Aloia, J.F. (1993b). Effects of exercise and immobilization on bone formation and resorption in young rats. *Am J Physiol*, 264(2 Pt 1):E182-189.

Zernicke, R., MacKay, C., Lorincz, C. (2006). Mechanisms of bone remodeling during weight-bearing exercise. *Appl Physiol Nutr Metab,* 31(6):655-660.

Zerwekh, J.E., Ruml, L.A., Gottschalk, F., Pak, C.Y. (1998). The effects of twelve weeks of bed rest on bone histology, biochemical markers of bone turnover, and calcium homeostasis in eleven normal subjects. *J Bone Miner Res,* 13(10):1594-1601

APPENDIX A

Channel	Axial
Control Mode	Displacement
Active Mode	Displacement
Command Type	Cyclic
Target Setpoint	0.00 mm
Amplitude	$\pm$ 40 mm
Frequency	2.0 Hz
Segment Generator Options	Check – Soft start/stop
Wave Shape	Square
Compensator	None

Settings for warming up MTS device

The midshaft of the tibia was tested to failure in three-point bending using a semi-hydraulic Materials Testing System (MTS) 858 MiniBionix apparatus. The actuator was warmed up for approximately 15 minutes prior to experimentation under these settings.

APPENDIX B

RESULTS

Effect of strain, treatment, strain by treatment differences on bone strength, composition, and architecture. The following tables show means, standard deviations, observed effects, and p-values

Measurement	Units	Mean (SD)	Strain		Treatment			Strain*Treatment						Obs. effect	p-value
			B6	D2	TR	TC	NEC	B6, TR	B6, TC	B6, NEC	D2, TR	D2, TC	D2, NEC		
Body Weight	g	Mean (SD)	**22.6** (1.50)	**23.3** (1.40)	**22.6** (1.37)	**23.2** (1.34)	**23.1** (1.68)	**22.4** (1.47)	**23.0** (1.30)	**22.5** (1.73)	**22.7** (1.28)	**23.4** (1.37)	**23.6** (1.49)	a	0.0458
Tibia Length	mm	Mean (SD)	**17.8** (0.281)	**17.7** (0.259)	**17.8** (0.281)	**17.7** (0.295)	**17.7** (0.261)	**17.8** (0.294)	**17.8** (0.292)	**17.8** (0.272)	**17.7** (0.247)	**17.6** (0.292)	**17.7** (0.250)	a	0.0312
Tibia Sagittal Width	mm	Mean (SD)	**1.13** (0.050)	**0.941** (0.077)	**1.04** (0.122)	**1.04** (0.109)	**1.03** (0.118)	**1.14** (0.050)	**1.13** (0.047)	**1.12** (0.054)	**0.927** (0.054)	**0.951** (0.077)	**0.945** (0.096)	a	<0.0001
Tibia Coronal Width	mm	Mean (SD)	**1.10** (0.041)	**0.873** (0.053)	**0.988** (0.127)	**0.975** (0.122)	**0.990** (0.119)	**1.10** (0.045)	**1.09** (0.034)	**1.09** (0.045)	**0.871** (0.046)	**0.861** (0.046)	**0.887** (0.065)	a	<0.0001
Tibia Epiphysial Width	mm	Mean (SD)	**2.84** (0.140)	**2.75** (0.118)	**2.81** (0.117)	**2.79** (0.162)	**2.79** (0.130)	**2.86** (0.125)	**2.82** (0.166)	**2.84** (0.133)	**2.77** (0.089)	**2.76** (0.158)	**2.73** (0.100)	a	0.0021
Yield Load (TYL)	N	Mean (SD)	**8.37** (0.865)	**6.29** (0.757)	**7.36** (1.41)	**7.42** (1.31)	**7.31** (1.29)	**8.36** (0.916)	**8.42** (0.941)	**8.33** (0.789)	**6.20** (0.902)	**6.42** (0.735)	**6.22** (0.662)	a	<0.0001
Yield Displacement (TYD)	mm	Mean (SD)	**0.182** (0.026)	**0.211** (0.022)	**0.192** (0.027)	**0.197** (0.032)	**0.198** (0.025)	**0.182** (0.027)	**0.175** (0.028)	**0.188** (0.022)	**0.204** (0.023)	**0.220** (0.017)	**0.209** (0.023)	a	<0.0001
Ultimate Energy Absorption (TYW)	N*mm	Mean (SD)	**0.816** (0.146)	**0.710** (0.126)	**0.751** (0.162)	**0.768** (0.133)	**0.773** (0.147)	**0.814** (0.148)	**0.786** (0.158)	**0.850** (0.132)	**0.678** (0.150)	**0.750** (0.103)	**0.696** (0.121)	a	0.0004
Ultimate Load (TUL)	N	Mean (SD)	**10.0** (0.912)	**7.48** (0.753)	**8.91** (1.62)	**8.81** (1.60)	**8.66** (1.37)	**10.1** (1.09)	**10.1** (1.03)	**9.82** (0.555)	**7.55** (0.919)	**7.49** (0.692)	**7.41** (0.695)	a	<0.0001
Ultimate Displacement (TUD)	mm	Mean (SD)	**0.278** (0.036)	**0.299** (0.025)	**0.287** (0.031)	**0.288** (0.036)	**0.289** (0.033)	**0.278** (0.036)	**0.273** (0.040)	**0.282** (0.035)	**0.296** (0.020)	**0.304** (0.025)	**0.297** (0.030)	a	0.0023
Ultimate Work (TUW)	N*mm	Mean (SD)	**1.70** (0.269)	**1.32** (0.185)	**1.53** (0.307)	**1.52** (0.295)	**1.49** (0.304)	**1.72** (0.290)	**1.70** (0.264)	**1.67** (0.269)	**1.32** (0.141)	**1.34** (0.202)	**1.30** (0.210)	a	<0.0001
Stiffness (TST)	N/mm	Mean (SD)	**49.7** (8.41)	**31.5** (4.31)	**41.2** (10.5)	**42.0** (13.8)	**39.5** (9.32)	**49.3** (6.89)	**52.8** (11.0)	**46.9** (5.84)	**31.9** (4.06)	**31.1** (4.59)	**31.6** (4.49)	a	<0.0001
Failure Load (TFL)	N	Mean (SD)	**0.200** (0.430)	**0.079** (0.105)	**0.144** (0.214)	**0.213** (0.499)	**0.065** (0.060)	**0.183** (0.244)	**0.371** (0.679)	**0.045** (0.050)	**0.099** (0.172)	**0.0556** (0.044)	**0.0859** (0.065)		
Failure Displacement (TFD)	mm	Mean (SD)	**0.598** (0.326)	**0.721** (0.163)	**0.713** (0.296)	**0.665** (0.285)	**0.566** (0.204)	**0.686** (0.385)	**0.587** (0.366)	**0.520** (0.198)	**0.743** (0.151)	**0.737** (0.162)	**0.683** (0.180)	a	0.0310
Energy Absorption at Failure (TFW)	N*mm	Mean (SD)	**4.05** (1.97)	**3.59** (0.818)	**4.07** (1.58)	**3.94** (1.82)	**3.45** (1.02)	**4.29** (2.06)	**4.22** (2.47)	**3.60** (1.15)	**3.81** (0.754)	**3.66** (0.761)	**3.30** (0.902)		

Note: TR=Treadmill Running, TC=Tower Climbing, NEC=Non-Exercised Control, a = strain effect, b = treatment effect, c = strain by treatment

Measurement	Units	Mean (SD)	Strain		Treatment			Strain*Treatment						Obs. effect	p-value
			B6	D2	TR	TC	NEC	B6, TR	B6, TC	B6, NEC	D2, TR	D2, TC	D2, NEC		
Cortical Area (TCA)	mm^2	Mean (SD)	**0.623** (0.030)	**0.567** (0.031)	**0.600** (0.042)	**0.600** (0.043)	**0.585** (0.037)	**0.629** (0.027)	**0.631** (0.028)	**0.608** (0.031)	**0.572** (0.034)	**0.569** (0.031)	**0.561** (0.027)	a	<0.0001
Medullary Area (TMA)	mm^2	Mean (SD)	**0.362** (0.029)	**0.108** (0.015)	**0.234** (0.132)	**0.235** (0.130)	**0.237** (0.132)	**0.361** (0.281)	**0.361** (0.029)	**0.365** (0.032)	**0.107** (0.017)	**0.109** (0.016)	**0.110** (0.014)	a	<0.0001
Total Area (TTA)	mm^2	Mean (SD)	**0.985** (0.044)	**0.676** (0.040)	**0.834** (0.165)	**0.835** (0.165)	**0.822** (0.158)	**0.990** (0.049)	**0.992** (0.039)	**0.973** (0.043)	**0.679** (0.045)	**0.678** (0.044)	**0.671** (0.033)	a	<0.0001
Cross Sectional Moment of Inertia- u-direction (Tiuu)	mm^4	Mean (SD)	**0.072** (0.0068)	**0.032** (0.0055)	**0.053** (0.021)	**0.053** (0.022)	**0.050** (0.020)	**0.073** (0.0069)	**0.074** (0.0069)	**0.070** (0.0064)	**0.033** (0.0065)	**0.033** (0.0059)	**0.031** (0.0045)	a	<0.0001
Cross Sectional Moment of Inertia- v-direction (Tivv)	mm^4	Mean (SD)	**0.066** (0.0070)	**0.043** (0.0047)	**0.056** (0.0140)	**0.055** (0.0134)	**0.054** (0.0120)	**0.068** (0.0077)	**0.067** (0.0062)	**0.064** (0.0068)	**0.044** (0.0056)	**0.043** (0.0043)	**0.043** (0.0045)	a	<0.0001
Average Cortical Thickness (TAT)	mm	Mean (SD)	**0.181** (0.0083)	**0.227** (0.0079)	**0.206** (0.025)	**0.205** (0.024)	**0.200** (0.026)	**0.182** (0.0052)	**0.183** (0.0087)	**0.177** (0.0093)	**0.229** (0.0081)	**0.227** (0.0067)	**0.224** (0.0085)	a b	<0.0001 0.0227
Cortical Thickness at medial- 3 o'clock position (T3T)	mm	Mean (SD)	**0.190** (0.018)	**0.270** (0.030)	**0.238** (0.045)	**0.227** (0.049)	**0.225** (0.048)	**0.198** (0.015)	**0.187** (0.024)	**0.186** (0.014)	**0.278** (0.023)	**0.267** (0.031)	**0.264** (0.036)	a	<0.0001
Tibia inner radius at medial-3 o'clock position (TIR3)	mm	Mean (SD)	**0.356** (0.027)	**0.235** (0.024)	**0.289** (0.064)	**0.298** (0.072)	**0.300** (0.063)	**0.349** (0.020)	**0.360** (0.038)	**0.358** (0.017)	**0.228** (0.020)	**0.235** (0.031)	**0.241** (0.021)	a	<0.0001
Tibia outer radius at medial-3 o'clock position (TOR3)	mm	Mean (SD)	**0.546** (0.023)	**0.505** (0.024)	**0.527** (0.031)	**0.525** (0.033)	**0.525** (0.0294	**0.547** (0.022)	**0.547** (0.027)	**0.544** (0.020)	**0.507** (0.026)	**0.503** (0.022)	**0.505** (0.024)	a	<0.0001
Cortical Thickness at anterior- 6 o'clock position (T6T)	mm	Mean (SD)	**0.308** (0.019)	**0.305** (0.032)	**0.308** (0.028)	**0.311** (0.029)	**0.301** (0.203)	**0.310** (0.018)	**0.314** (0.019)	**0.299** (0.016)	**0.306** (0.036)	**0.307** (0.038)	**0.303** (0.024)		

Note: TR=Treadmill Running, TC=Tower Climbing, NEC=Non-Exercised Control, a = strain effect, b = treatment effect, c = strain by treatment

Measurement	Units	Mean (SD)	Strain		Treatment			Strain*Treatment						Obs. effect	p-value
			B6	D2	TR	TC	NEC	B6, TR	B6, TC	B6, NEC	D2, TR	D2, TC	D2, NEC		
Tibia inner radius at anterior- 6 o'clock position (TIR6)	mm	Mean (SD)	**0.341** (0.023)	**0.178** (0.021)	**0.256** (0.085)	**0.263** (0.086)	**0.260** (0.087)	**0.337** (0.016)	**0.344** (0.028)	**0.343** (0.026)	**0.175** (0.062)	**0.182** (0.021)	**0.177** (0.017)	a	<0.0001
Tibia outer radius at anterior- 6 o'clock position (TOR6)	mm	Mean (SD)	**0.650** (0.024)	**0.484** (0.032)	**0.564** (0.088)	**0.574** (0.091)	**0.562** (0.087)	**0.647** (0.020)	**0.659** (0.024)	**0.643** (0.025)	**0.482** (0.032)	**0.489** (0.036)	**0.481** (0.028)	a	<0.0001
Cortical Thickness at lateral- 9 o'clock position (T9T)	mm	Mean (SD)	**0.208** (0.021)	**0.289** (0.018)	**0.252** (0.043)	**0.247** (0.048)	**0.246** (0.046)	**0.214** (0.018)	**0.204** (0.0222)	**0.205** (0.022)	**0.290** (0.021)	**0.290** (0.018)	**0.288** (0.016)	a	<0.0001
Tibia inner radius at lateral- 9 o'clock position (TIR9)	mm	Mean (SD)	**0.337** (0.025)	**0.193** (0.020)	**0.262** (0.076)	**0.266** (0.080)	**0.268** (0.074)	**0.333** (0.021)	**0.341** (0.029)	**0.337** (0.016)	**0.192** (0.026)	**0.191** (0.017)	**0.198** (0.017)	a	<0.0001
Tibia outer radius at lateral- 9 o'clock position (TOR9)	mm	Mean (SD)	**0.545** (0.021)	**0.483** (0.013)	**0.515** (0.038)	**0.514** (0.036)	**0.514** (0.034)	**0.548** (0.023)	**0.545** (0.018)	**0.543** (0.021)	**0.483** (0.014)	**0.482** (0.012)	**0.486** (0.013)	a	<0.0001
Cortical Thickness at posterior- 12 o'clock position (T12T)	mm	Mean (SD)	**0.204** (0.025)	**0.234** (0.024)	**0.216** (0.030)	**0.225** (0.027)	**0.215** (0.030)	**0.198** (0.022)	**0.215** (0.029)	**0.198** (0.022)	**0.235** (0.025)	**0.235** (0.020)	**0.231** (0.028)	a	<0.0001
Tibia inner radius at posterior- 12 o'clock position (TIR12)	mm	Mean (SD)	**0.299** (0.031)	**0.144** (0.022)	**0.221** (0.084)	**0.218** (0.078)	**0.224** (0.087)	**0.301** (0.028)	**0.290** (0.034)	0.305 (0.030)	**0.142** (0.019)	**0.146** (0.023)	**0.143** (0.024)	a	<0.0001
Tibia outer radius at posterior- 12 o'clock position (TOR12)	mm	Mean (SD)	**0.503** (0.022)	**0.378** (0.024)	**0.438** (0.065)	**0.443** (0.067)	**0.439** (0.070)	**0.499** (0.016)	**0.504** (0.027)	**0.504** (0.023)	**0.377** (0.022)	**0.382** (0.024)	**0.374** (0.027)	a	<0.0001

Note: TR=Treadmill Running, TC=Tower Climbing, NEC=Non-Exercised Control, a = strain effect, b = treatment effect, c = strain by treatment

Measurement	Units	Mean (SD)	Strain		Treatment			Strain*Treatment						Obs. effect	p-value
			B6	D2	TR	TC	NEC	B6, TR	B6, TC	B6, NEC	D2, TR	D2, TC	D2, NEC		
Yield Stress (TYS)	N/mm^2	Mean (SD)	**1.89** (1.85)	**2.38** (2.04)	**2.08** (3.17)	**2.14** (3.11)	**2.16** (3.15)	**1.87** (1.76)	**1.88** (1.68)	**1.93** (2.13)	**2.33** (2.56)	**2.40** (1.59)	**2.40** (2.01)	a	<0.0001
Yield Strain (TYN)	N/mm^2	Mean (SD)	**0.014** (0.0019)	**0.012** (0.0016)	**0.013** (0.0022)	**0.013** (0.0017)	**0.013** (0.0021)	**0.014** (0.0021)	**0.014** (0.0021)	**0.015** (0.0017)	**0.012** (0.0014)	**0.013** (0.0013)	**0.012** (0.0018)	a	<0.0001
Modulus of Elasticity (TYE)	N/mm^2	Mean (SD)	**1.36** (1.75)	**1.96** (2.25)	**1.65** (3.78)	**1.63** (3.23)	**1.66** (4.01)	**1.34** (1.47)	**1.39** (2.09)	**1.35** (1.73)	**2.00** (1.82)	**1.88** (2.03)	**2.00** (2.70)	a	<0.0001
Ultimate Stress (TUS)	N/mm^2	Mean (SD)	**2.26** (1.75)	**2.84** (2.18)	**2.52** (3.67)	**2.54** (3.40)	**2.56** (3.53)	**2.25** (1.51)	**2.26** (2.12)	**2.28** (1.67)	**2.84** (2.65)	**2.81** (1.91)	**2.87** (2.09)	a	<0.0001
Ultimate Strain(TUN)	N/mm^2	Mean (SD)	**0.022** (0.0030)	**0.017** (0.0018)	**0.019** (0.0033)	**0.020** (0.0030)	**0.020** (0.0036)	**0.022** (0.0031)	**0.022** (0.0030)	**0.022** (0.0031)	**0.017** (0.0011)	**0.018** (0.0016)	**0.017** (0.0024)	a	<0.0001
Percent hydration (Twat)	%	Mean (SD)	**24.25** (4.08)	**19.19** (3.56)	**21.06** (4.02)	**21.41** (4.82)	**22.76** (4.83)	**23.60** (3.35)	**24.30** (4.53)	**24.85** (4.43)	**18.51** (2.90)	**18.32** (2.84)	**20.68** (4.41)	a	<0.0001
Percent Organic (Torg)	%	Mean (SD)	**27.61** (2.33)	**28.03** (3.11)	**27.83** (2.36)	**27.23** (2.29)	**28.37** (3.38)	**27.44** (1.30)	**26.61** (2.17)	**28.77** (2.86)	**28.22** (3.09)	**27.90** (2.31)	**27.97** (3.89)		
Percent Ash (Tash)	%	Mean (SD)	**48.14** (4.24)	**52.78** (4.76)	**51.11** (3.63)	**51.35** (3.61)	**48.87** (6.91)	**48.95** (3.01)	**49.09** (2.76)	**46.38** (5.91)	**53.27** (2.87)	**53.78** (2.75)	**51.35** (7.13)	a	<.0001
Percent Mineralization (Tmin)	%	Mean (SD)	**63.48** (3.50)	**65.23** (4.44)	**64.72** (2.67)	**65.34** (2.03)	**63.02** (6.01)	**64.04** (1.79)	**64.87** (1.34)	**61.53** (5.20)	**65.40** (3.26)	**65.84** (2.53)	**64.50** (6.56)	a	0.0372

Note: TR=Treadmill Running, TC=Tower Climbing, NEC=Non-Exercised Control, a = strain effect, b = treatment effect, c = strain by treatment

Measurement	Units	Mean (SD)	Strain		Treatment			Strain*Treatment						Obs. effect	p-value
			B6	D2	TR	TC	NEC	B6, TR	B6, TC	B6, NEC	D2, TR	D2, TC	D2, NEC		
Whole Total Volume-VOX (WVOXTV)	mm^3	Mean (SD)	**357.36** (14.98)	**356.63** (11.70)	**360.02** (14.78)	**355.18** (13.79)	**355.97** (11.52)	**365.68** (14.30)	**353.54** (15.05)	**352.84** (12.76)	**353.50** (12.90)	**356.83** (12.70)	**359.31** (9.33)	c	0.0190
Whole Bone Volume-VOX (WVOXBV)	mm^3	Mean (SD)	**18.14** (1.11)	**17.09** (0.989)	**17.97** (1.18)	**17.61** (1.25)	**17.34** (1.03)	**18.42** (1.09)	**18.23** (1.16)	**17.77** (1.04)	**17.45** (1.08)	**16.98** (1.03)	**16.87** (0.823)	a	<0.0001
Whole Bone Volume Fraction-VOX (WVOXBVTV)	%	Mean (SD)	**0.0508** (0.0030)	**0.0479** (0.0028)	**0.0499** (0.0028)	**0.0496** (0.0033)	**0.0488** (0.0035)	**0.0504** (0.0028)	**0.0516** (0.0023)	**0.0505** (0.0038)	**0.0494** (0.0029)	**0.0476** (0.0030)	**0.0471** (0.0019)	a	<0.0001
Whole Connectivity Density-VOX (WConnDens)	$1/mm^3$	Mean (SD)	**0.484** (0.119)	**0.372** (0.089)	**0.367** (0.093)	**0.445** (0.121)	**0.477** (0.117)	**0.401** (0.096)	**0.510** (0.118)	**0.542** (0.098)	**0.327** (0.076)	**0.379** (0.085)	**0.407** (0.094)	a b	<0.0001 0.0001
Whole Structural Model Index-VOX (WVOXSMI)	None	Mean (SD)	**-0.649** (0.162)	**-0.954** (0.244)	**-0.780** (0.275)	**-0.821** (0.247)	**-0.787** (0.251)	**-0.664** (0.172)	**-0.675** (0.134)	**-0.609** (0.181)	**-0.914** (0.316)	**-0.967** (0.250)	**-0.978** (0.159)	a	<0.0001
Whole Trabecular Number-DT (WDTTbN)	1/mm	Mean (SD)	**0.713** (0.361)	**0.769** (0.579)	**0.762** (0.496)	**0.739** (0.434)	**0.720** (0.514)	**0.735** (0.462)	**0.769** (0.342)	**0.636** (0.264)	**0.794** (0.550)	**0.709** (0.521)	**0.809** (0.691)		
Whole Trabecular Thickness-DT (WDTTbTh)	mm	Mean (SD)	**0.247** (0.011)	**0.286** (0.0098)	**0.268** (0.023)	**0.266** (0.023)	**0.265** (0.021)	**0.249** (0.0081)	**0.246** (0.014)	**0.247** (0.0062)	**0.289** (0.012)	**0.285** (0.0092)	**0.285** (0.0082)	a	<0.0001
Whole Trabecular Separation-DT (WDTTbSp)	mm	Mean (SD)	**1.77** (0.561)	**1.93** (0.785)	**1.82** (0.664)	**1.81** (0.665)	**1.92** (0.726)	**1.85** (0.602)	**1.59** (0.493)	**1.87** (0.575)	**1.78** (0.753)	**2.02** (0.756)	**1.96** (0.880)		

Note: TR=Treadmill Running, TC=Tower Climbing, NEC=Non-Exercised Control, a = strain effect, b = treatment effect, c = strain by treatment

Measurement	Units	Mean (SD)	Strain		Treatment			Strain*Treatment						Obs. effect	p-value
			B6	D2	TR	TC	NEC	B6, TR	B6, TC	B6, NEC	D2, TR	D2, TC	D2, NEC		
Whole Mean1 (TWMean1)	mm^3	Mean (SD)	**4.55** (3.86)	**4.60** (3.37)	**5.39** (3.06)	**3.78** (3.77)	**4.62** (3.88)	**5.31** (2.99)	**3.46** (4.52)	**4.88** (3.94)	**5.46** (3.25)	**4.11** (2.96)	**4.34** (3.94)		
Whole Mean1 (WMean2)	mm^3	Mean (SD)	**1.01** (1.27)	**1.07** (1.36)	**1.04** (3.21)	**1.04** (3.07)	**1.04** (3.01)	**1.01** (1.46)	**1.02** (1.31)	**1.02** (1.06)	**1.07** (1.55)	**1.07** (1.37)	**1.07** (1.23)	a	<0.0001
Whole Standard Deviation of Trabecular Number (WDTTb1NSD)	mm	Mean (SD)	**0.849** (0.219)	**0.853** (0.300)	**0.860** (0.281)	**0.866** (0.264)	**0.828** (0.241)	**0.879** (0.266)	**0.826** (0.211)	**0.843** (0.182)	**0.838** (0.307)	**0.905** (0.310)	**0.813** (0.299)		
Whole Standard Deviation of Trabecular Thickness (WDTTbThSD)	mm	Mean (SD)	**0.076** (0.0027)	**0.094** (0.0046)	**0.083** (0.0090)	**0.085** (0.0098)	**0.086** (0.010)	**0.076** (0.0020)	**0.076** (0.0035)	**0.077** (0.0025)	**0.092** (0.0056)	**0.094** (0.0036)	**0.095** (0.0040)	a	<0.0001
Whole Standard Deviation of Trabecular Separation (WDTTbSpSD)	mm	Mean (SD)	**0.749** (0.179)	**0.694** (0.226)	**0.741** (0.235)	**0.736** (0.197)	**0.691** (0.180)	**0.789** (0.202)	**0.734** (0.187)	**0.723** (0.147)	**0.685** (0.265)	**0.738** (0.213)	**0.657** (0.210)		
Whole Total Volume-TRI (WTRITV)	mm^3	Mean (SD)	**355.43** (14.94)	**354.70** (11.67)	**358.09** (14.73)	**353.27** (13.74)	**354.05** (11.48)	**363.73** (14.26)	**351.62** (15.00)	**350.93** (12.73)	**351.58** (12.87)	**354.91** (12.66)	**357.38** (9.29)	c	0.0188
Whole Bone Volume-TRI (WTRIBV)	mm^3	Mean (SD)	**18.35** (1.11)	**17.27** (0.995)	**18.16** (1.19)	**17.80** (1.26)	**17.53** (1.04)	**18.63** (1.10)	**18.45** (1.16)	**17.98** (1.04)	**17.62** (1.09)	**17.16** (1.03)	**17.05** (0.828)	a	<0.0001
Whole Bone Volume Fraction-TRI (WTRIBVTV)	%	Mean (SD)	**0.052** (0.0031)	**0.049** (0.0028)	**0.051** (0.0028)	**0.050** (0.0034)	**0.050** (0.0036)	**0.051** (0.0028)	**0.053** (0.0023)	**0.051** (0.0039)	**0.050** (0.0029)	**0.048** (0.0031)	**0.048** (0.0019)	a	<0.0001

Note: TR=Treadmill Running, TC=Tower Climbing, NEC=Non-Exercised Control, a = strain effect, b = treatment effect, c = strain by treatment

Measurement	Units	Mean (SD)	Strain		Treatment			Strain*Treatment						Obs. effect	p-value
			B6	D2	TR	TC	NEC	B6, TR	B6, TC	B6, NEC	D2, TR	D2, TC	D2, NEC		
Whole Bone Surface-TRI (WTRIBS)	mm^3	Mean (SD)	**169.05** (5.77)	**141.68** (6.77)	**156.65** (15.57)	**156.15** (16.12)	**154.74** (13.98)	**169.14** (5.79	**170.87** (6.67	**167.15** (4.37	**142.23** (9.25)	**141.43** (5.46)	**141.45** (5.72)	a	<0.0001
Whole Bone Surface Fraction-TRI (WTRIBSBV)	1/mm	Mean (SD)	**9.23** (0.465)	**8.22** (0.325)	**8.62** (0.634)	**8.77** (0.693)	**8.83** (0.627)	**9.10** (0.348)	**9.29** (0.590)	**9.32** (0.424)	**8.08** (0.399)	**8.25** (0.266)	**8.30** (0.284)	a	<0.0001
Whole Trabecular Number-TRI (WTRITbN)	1/mm	Mean (SD)	**0.238** (0.011)	**0.200** (0.011)	**0.219** (0.20)	**0.221** (0.025)	**0.219** (0.023)	**0.233** (0.011)	**0.243** (0.011)	**0.238** (0.011)	**0.202** (0.014)	**0.199** (0.010)	**0.198** (0.0082)	a	<0.0001
Whole Trabecular Thickness-TRI (WTRITbTh)	mm	Mean (SD)	**0.217** (0.011)	**0.244** (0.0096)	**0.233** (0.017)	**0.229** (0.017)	**0.228** (0.016)	**0.220** (0.0084)	**0.216** (0.013)	**0.215** (0.0099)	**0.248** (0.012)	**0.243** (0.0078)	**0.241** (0.0080)	a	<0.0001
Whole Trabecular Separation-TRI (WTRITbSp)	mm	Mean (SD)	**3.99** (0.199)	**4.77** (0.262)	**4.38** (0.413)	**4.34** (0.495)	**4.39** (0.466)	**4.08** (0.199)	**3.90** (0.169)	**3.99** (0.195)	**4.71** (0.329)	**4.78** (0.253)	**4.82** (0.206)	a	<0.0001
Whole Degree of Anisotropy-TRI (WTRIDA)	none	Mean (SD)	**1.91** (0.071)	**1.77** (0.064)	**1.90** (0.103)	**1.82** (0.091)	**1.82** (0.082)	**1.97** (0.074)	**1.89** (0.051)	**1.88** (0.056)	**1.82** (0.065)	**1.75** (0.066)	**1.75** (0.043)	a b	<0.0001 <0.0001

Note: TR=Treadmill Running, TC=Tower Climbing, NEC=Non-Exercised Control, a = strain effect, b = treatment effect, c = strain by treatment

Measurement	Units	Mean (SD)	Strain		Treatment			Strain*Treatment						Obs. effect	p-value
			B6	D2	TR	TC	NEC	B6, TR	B6, TC	B6, NEC	D2, TR	D2, TC	D2, NEC		
Metaphysis Total Volume-VOX (MVOXTV)	mm^3	Mean (SD)	**1.23** (0.123)	**1.01** (0.106)	**1.12** (0.170)	**1.11** (0.177)	**1.13** (0.139)	**1.25** (0.114)	**1.24** (0.139)	**1.21** (0.122)	**1.00** (0.118)	**0.985** (0.105)	**1.04** (0.0931)	a	<0.0001
Metaphysis Bone Volume-VOX (MVOXBV)	mm^3	Mean (SD)	**0.165** (0.055)	**0.123** (0.046)	**0.166** (0.060)	**0.142** (0.059)	**0.124** (0.034)	**0.190** (0.057)	**0.172** (0.054)	**0.133** (0.039)	**0.142** (0.054)	**0.112** (0.049)	**0.115** (0.027)	a b	<0.0001 0.0048
Metaphysis Bone Volume Fraction-VOX (MVOXBVTV)	%	Mean (SD)	**0.133** (0.044)	**0.121** (0.039)	**0.147** (0.048)	**0.126** (0.042)	**0.109** (0.023)	**0.154** (0.053)	**0.138** (0.038)	**0.108** (0.025)	**0.139** (0.042)	**0.114** (0.045)	**0.111** (0.022)	b	0.0016
Metaphysis Connectivity Density-VOX (MConnDens)	$1/mm^3$	Mean (SD)	**11.97** (7.68)	**16.17** (9.46)	**16.71** (9.85)	**13.80** (8.92)	**11.69** (7.01)	**13.38** (9.55)	**13.30** (7.69)	**9.23** (4.79)	**20.05** (9.27)	**14.31** (10.26)	**14.14** (8.12)	a	0.0211
Metaphysis Structural Model Index-VOX (MVOXSMI)	none	Mean (SD)	**2.77** (0.452)	**2.80** (0.461)	**2.64** (0.452)	**2.80** (0.415)	**2.92** (0.467)	**2.57** (0.402)	**2.67** (0.365)	**3.07** (0.448)	2.71 (0.501)	**2.92** (0.436)	**2.76** (0.450)	c	0.0410
Metaphysis Trabecular Number-DT (MDTTbN)	1/mm	Mean (SD)	**3.29** (0.406)	**3.15** (0.354)	**3.28** (0.452)	**3.24** (0.398)	**3.15** (0.288)	**3.36** (0.545)	**3.32** (0.364)	**3.19** (0.266)	**9.20** (0.334)	**3.15** (0.423)	**3.11** (0.313)		
Metaphysis Trabecular Thickness-DT (MDTTbTh)	mm	Mean (SD)	**0.089** (0.0075)	**0.075** (0.0068)	**0.085** (0.0095)	**0.082** (0.011)	**0.080** (0.0083)	**0.091** (0.0076)	**0.090** (0.0077)	**0.085** (0.0059)	**0.078** (0.0062)	**0.073** (0.0062)	**0.075** (0.0073)	a b	<0.0001 0.0183
Metaphysis Trabecular Separation-DT (MDTTbSp)	mm	Mean (SD)	**0.315** (0.042)	**0.333** (0.042)	**0.320** (0.043)	**0.318** (0.049)	**0.334** (0.037)	**0.314** (0.047)	**0.300** (0.042)	**0.331** (0.032)	**0.327** (0.038)	**0.336** (0.049)	**0.337** (0.042)	a	0.0390

Note: TR=Treadmill Running, TC=Tower Climbing, NEC=Non-Exercised Control, a = strain effect, b = treatment effect, c = strain by treatment

Measurement	Units	Mean (SD)	Strain		Treatment			Strain*Treatment						Obs. effect	p-value
			B6	D2	TR	TC	NEC	B6, TR	B6, TC	B6, NEC	D2, TR	D2, TC	D2, NEC		
Metaphysis Mean1 (MMean1)	mm^3	Mean (SD)	**1.51** (2.06)	**1.49** (1.69)	**1.60** (1.95)	**1.48** (1.92)	**1.41** (1.24)	**1.61** (2.26)	**1.53** (1.77)	**1.38** (1.48)	**1.59** (1.66)	**1.44** (2.01)	**1.45** (8.46)	b	0.0004
Metaphysis Mean1 (MMean2)	mm^3	Mean (SD)	**6.27** (2.37)	**5.91** (3.06)	**6.08** (2.77)	**6.12** (3.68)	**6.06** (3.33)	**6.21** (2.07)	**6.34** (2.48)	**6.24** (2.50)	**5.95** (2.82)	**5.90** (3.38)	**5.88** (3.15)	a	<.0001
Metaphysis Standard Deviation of Trabecular Number (MDTTb1NSD)	mm	Mean (SD)	**0.114** (0.019)	**0.119** (0.017)	**0.119** (0.020)	**0.113** (0.018)	**0.118** (0.018)	**0.115** (0.020)	**0.113** (0.021)	**0.115** (0.018)	**0.122** (0.019)	**0.113** (0.014)	**0.121** (0.019)		
Metaphysis Standard Deviation of Trabecular Thickness (MDTTbThSD)	mm	Mean (SD)	**0.030** (0.0041)	**0.028** (0.0043)	**0.029** (0.0040)	**0.029** (0.0046)	**0.029** (0.0042)	**0.029** (0.0042)	**0.029** (0.0044)	**0.031** (0.0037)	**0.029** (0.0039)	**0.028** (0.0048)	**0.028** (0.0041)		
Metaphysis Standard Deviation of Trabecular Separation (MDTTbSpSD)	mm	Mean (SD)	**0.124** (0.027)	**0.115** (0.021)	**0.124** (0.025)	**0.113** (0.024)	**0.122** (0.023)	**0.128** (0.027)	**0.116** (0.031)	**0.129** (0.023)	**0.121** (0.024)	**0.111** (0.017)	**0.114** (0.021)		
Metaphysis Total Volume-TRI (MTRITV)	mm^3	Mean (SD)	**1.20** (0.122)	**0.971** (0.103)	**1.09** (0.168)	**1.08** (0.174)	**1.09** (0.139)	**1.21** (0.112)	**1.20** (0.136)	**1.18** (0.124)	**0.963** (0.114)	**0.949** (0.102)	**1.00** (0.090)	a	<0.0001
Metaphysis Bone Volume-TRI (MTRIBV)	mm^3	Mean (SD)	**0.152** (0.054)	**0.109** (0.044)	**0.151** (0.059)	**0.129** (0.057)	**0.111** (0.033)	**0.176** (0.056)	**0.159** (0.052)	**0.121** (0.037)	**0.126** (0.052)	**0.984** (0.046)	**0.101** (0.025)	a b	<0.0001 0.0046

Note: TR=Treadmill Running, TC=Tower Climbing, NEC=Non-Exercised Control, a = strain effect, b = treatment effect, c = strain by treatment

Measurement	Units	Mean (SD)	Strain		Treatment			Strain*Treatment						Obs. effect	p-value
			B6	D2	TR	TC	NEC	B6, TR	B6, TC	B6, NEC	D2, TR	D2, TC	D2, NEC		
Metaphysis Bone Volume Fraction-TRI (MTRIBVTV)	%	Mean (SD)	**0.127** (0.044)	**0.111** (0.039)	**0.138** (0.049)	**0.117** (0.042)	**0.101** (0.023)	**0.148** (0.054)	**0.131** (0.037)	**0.101** (0.025)	**0.129** (0.043)	**0.103** (0.043)	**0.101** (0.022)	b	0.0017
Metaphysis Bone Surface-TRI (MTRIBS)	mm^3	Mean (SD)	**4.25** (1.18)	**3.38** (1.18)	**4.27** (1.29)	**3.76** (1.41)	**3.43** (0.901)	**4.72** (1.08)	**4.39** (1.27)	**3.66** (0.985)	**3.81** (1.35)	**3.13** (1.29)	**3.21** (0.777)	a b	0.0005 0.0209
Metaphysis Bone Surface Fraction-TRI (MTRIBSBV)	1/mm	Mean (SD)	**28.68** (2.92)	**31.78** (3.17)	**29.11** (3.36)	**30.13** (2.92)	**31.45** (3.61)	**27.35** (3.07)	**27.92** (1.87)	**30.78** (2.59)	**30.87** (2.70)	**32.34** (1.94)	**32.12** (4.39)	a b	<0.0001 0.0092
Metaphysis Trabecular Number-TRI (MTRITbN)	1/mm	Mean (SD)	**1.78** (0.478)	**1.73** (0.527)	**1.96** (0.527)	**1.73** (0.555)	**1.57** (0.322)	**1.97** (0.545)	**1.82** (0.465)	**1.54** (0.315)	**1.95** (0.527)	**1.65** (0.638)	**1.60** (0.336)	b	0.0092
Metaphysis Trabecular Thickness-TRI (MTRITbTh)	mm	Mean (SD)	**0.070** (0.0071)	**0.064** (0.0060)	**0.070** (0.0081)	**0.070** (0.0066)	**0.064** (0.0066)	**0.074** (0.0080)	**0.072** (0.00492)	**0.065** (0.0052)	**0.065** (0.0057)	**0.062** (0.0039)	**0.063** (0.0079)	a b	<0.0001 0.0053
Metaphysis Trabecular Separation-TRI (MTRITbSp)	mm	Mean (SD)	**0.528** (0.147)	**0.555** (0.191)	**0.469** (0.119)	**0.554** (0.214)	**0.601** (0.141)	**0.458** (0.108)	**0.511** (0.143)	**0.614** (0.150)	**0.480** (0.132)	**0.600** (0.268)	**0.587** (0.134)	b	0.0086
Metaphysis Degree of Anisotropy-TRI (MTRIDA)	none	Mean (SD)	**1.62** (0.144)	**1.31** (0.121)	**1.46** (0.243)	**1.48** (0.167)	**1.45** (0.210)	**1.68** (0.142)	**1.61** (0.0770)	**1.58** (0.186)	**1.25** (0.0830)	**1.35** (0.123)	**1.32** (0.139)	a c	<0.0001 0.0306

Note: TR=Treadmill Running, TC=Tower Climbing, NEC=Non-Exercised Control, a = strain effect, b = treatment effect, c = strain by treatment

Measurement	Units	Mean (SD)	Strain		Treatment			Strain*Treatment						Obs. effect	p-value
			B6	D2	TR	TC	NEC	B6, TR	B6, TC	B6, NEC	D2, TR	D2, TC	D2, NEC		
Cortical Total Volume-VOX (CVOXTV)	mm^3	Mean (SD)	**0.568** (0.025)	**0.398** (0.023)	**0.485** (0.091)	**0.485** (0.091)	**0.479** (0.087)	**0.571** (0.029)	**0.572** (0.022)	**0.562** (0.024)	**0.399** (0.027)	**0.399** (0.025)	**0.396** (0.018)	a	<0.0001
Cortical Bone Volume-VOX (CVOXBV)	mm^3	Mean (SD)	**0.344** (0.018)	**0.322** (0.018)	**0.336** (0.023)	**0.335** (0.022)	**0.328** (0.018)	**0.346** (0.019)	**0.348** (0.017)	**0.337** (0.017)	**0.325** (0.022)	**0.322** (0.018)	**0.318** (0.014)	a	<0.0001
Cortical Bone Volume Fraction-VOX (CVOXBVTV)	%	Mean (SD)	**0.606** (0.019)	**0.809** (0.016)	**0.710** (0.106)	**0.709** (0.102)	**0.0702** (0.105)	**0.607** (0.016)	**0.610** (0.020)	**0.600** (0.022)	**0.814** (0.017)	**0.808** (0.014)	**0.804** (0.016)	a	<0.0001
Cortical Connectivity Density-VOX (CConnDens)	$1/mm^3$	Mean (SD)	**1.80** (0.590)	**2.48** (0.899)	**2.10** (1.01)	**2.26** (0.760)	**2.03** (0.680)	**1.701** (0.435)	**2.03** (0.840)	**1.167** (0.335)	**2.50** (1.26)	**2.50** (0.609)	**2.42** (0.747)	a	0.0006
Cortical Structural Model Index-VOX (CVOXSMI)	none	Mean (SD)	**-2.85** (0.870)	**-13.91** (3.96)	**-8.70** (7.14)	**-8.20** (5.78)	**2.915** (0.467)	**-2.53** (0.269)	**-2.95** (0.638)	**-3.06** (0.844)	**-14.87** (4.80)	**-13.46** (3.08)	**-13.41** (3.91)	a	<0.0001
Cortical Trabecular Number-DT (CDTTbN)	1/mm	Mean (SD)	**16.09** (8.394)	**8.23** (5.576)	**11.21** (8.38)	**12.41** (7.35)	**12.85** (8.74)	**16.28** (8.43)	**13.70** (8.75)	**18.29** (7.90)	**6.15** (4.39)	**11.12** (5.63)	**7.42** (5.69)	a c	<0.0001 0.0445
Cortical Trabecular Thickness-DT (CDTTbTh)	mm	Mean (SD)	**0.211** (0.010)	**0.277** (0.0116)	**0.246** (0.0365)	**0.246** (0.0330)	**0.240** (0.0350)	**0.212** (0.0100)	**0.216** (0.0103)	**0.207** (0.00861)	**0.280** (0.0125)	**0.277** (0.0124)	**0.214** (0.00949)	a	<0.0001
Cortical Trabecular Separation-DT (CDTTbSp)	mm	Mean (SD)	**0.240** (0.191)	**0.27** (0.032)	**0.26** (0.133)	**0.27** (0.128)	**0.24** (0.150)	**0.25** (0.189)	**0.27** (0.181)	**0.20** (0.206)	**0.26** (0.033)	**0.27** (0.033)	**0.27** (0.030)		

Note: TR=Treadmill Running, TC=Tower Climbing, NEC=Non-Exercised Control, a = strain effect, b = treatment effect, c = strain by treatment

Measurement	Units	Mean (SD)	Strain		Treatment			Strain*Treatment						Obs. effect	p-value
			B6	D2	TR	TC	NEC	B6, TR	B6, TC	B6, NEC	D2, TR	D2, TC	D2, NEC		
Cortical Mean1 (CMean1)	mm^3	Mean (SD)	**7.65** (2.65)	**1.04** (2.13)	**9.05** (1.43)	**9.06** (1.38)	**8.94** (1.42)	**7.65** (2.25)	**7.73** (2.7)	**7.57** (2.87)	**1.04** (2.07)	**1.04** (1.90)	**1.03** (2.33)	a	<0.0001
Cortical Mean1 (CMean2)	mm^3	Mean (SD)	**1.19** (1.89)	**1.29** (1.59)	**1.24** (5.63)	**1.24** (5.22)	**1.24** (5.56)	**1.18** (1.18)	**1.19** (1.84)	**1.19** (2.03)	**1.29** (2.073)	**1.29** (1.32)	**1.29** (2.33)	a	<0.0001
Cortical Standard Deviation of Trabecular Number (CDTTb1NSD)	1/mm	Mean (SD)	**0.046** (0.0490)	**0.089** (0.0518)	**0.075** (0.0568)	**0.060** (0.0483)	**0.067** (0.0590)	**0.045** (0.0493)	**0.060** (0.0539)	**0.32** (0.0420)	**0.115** (0.0483)	**0.598** (0.0438)	**0.101** (0.0532)	a c	<0.0001 0.0131
Cortical Standard Deviation of Trabecular Thickness (CDTTbThSD)	mm	Mean (SD)	**0.036** (0.0049)	**0.044** (0.0062)	**0.041** (0.0086)	**0.40** (0.0046)	**0.039** (0.0069)	**0.036** (0.0057)	**0.038** (0.0043)	**0.034** (0.0040)	**0.046** (0.0081)	**0.042** (0.0041)	**0.044** (0.0056)	a c	<0.0001 0.0468
Cortical Standard Deviation of Trabecular Separation (CDTTbSpSD)	mm	Mean (SD)	**0.02** (0.028)	**0.03** (0.015)	**0.0309** (0.024)	**0.03** (0.024)	**0.02** (0.020)	**0.02** (0.031)	**0.03** (0.032)	**0.02** (0.021)	**0.03** (0.015)	**0.03** (0.013)	**0.03** (0.017)		

Note: TR=Treadmill Running, TC=Tower Climbing, NEC=Non-Exercised Control, a = strain effect, b = treatment effect, c = strain by treatment

Measurement	Units	Mean (SD)	Strain		Treatment			Strain*Treatment						Obs. effect	p-value
			B6	D2	TR	TC	NEC	B6, TR	B6, TC	B6, NEC	D2, TR	D2, TC	D2, NEC		
Cortical Total Volume-TRI (CTRITV)	mm^3	Mean (SD)	**0.554** (0.025)	**0.386** (0.023)	**0.472** (0.090)	**0.472** (0.090)	**0.466** (0.086)	**0.556** (0.029)	**0.557** (0.022)	**0.547** (0.024)	**0.388** (0.026)	**0.387** (0.025)	**0.384** (0.018)	a	<0.0001
Cortical Bone Volume-TRI (CTRIBV)	mm^3	Mean (SD)	**0.316** (0.017)	**0.297** (0.017)	**0.309** (0.021)	**0.309** (0.0039)	**0.302** (0.016)	**0.318** (0.018)	**0.321** (0.016)	**0.309** (0.016)	**0.301** (0.20)	**0.298** (0.017)	**0.294** (0.013)	a	<0.0001
Cortical Bone Volume Fraction-TRI (CTRIBVTV)	%	Mean (SD)	**0.571** (0.019)	**0.770** (0.016)	**0.674** (0.191)	**0.672** (0.100)	**0.666** (0.104)	**0.572** (0.016)	**0.575** (0.020)	**0.565** (0.021)	**0.776** (0.017)	**0.769** (0.014)	**0.766** (0.016)	a	<0.0001
Cortical Bone Surface-TRI (CTRIBS)	mm^3	Mean (SD)	**1.22** (0.054)	**0.677** (0.059)	**0.949** (0.052)	**0.947** (0.289)	**0.955** (0.276)	**1.22** (0.057)	**1.22** (0.061)	**1.22** (0.049)	**0.674** (0.062)	**0.669** (0.065)	**0.688** (0.053)	a	<0.0001
Cortical Bone Surface Fraction-TRI (CTRIBSBV)	1/mm	Mean (SD)	**3.88** (0.238)	**2.28** (0.188)	**3.051** (0.845)	**3.04** (0.833)	**3.15** (0.840)	**3.85** (0.232)	**3.83** (0.256)	**3.96** (0.221)	**2.25** (0.208)	**2.25** (0.179)	**2.34** (0.170)	a	<0.0001
Cortical Trabecular Number-TRI (CTRITbN)	1/mm	Mean (SD)	**1.11** (0.036)	**0.877** (0.062)	**0.986** (0.130)	**0.982** (0.129)	**1.01** (0.121)	**1.10** (0.041)	**1.10** (0.038)	**1.12** (0.027)	**0.870** (0.067)	**0.864** (0.059)	**0.896** (0.058)	a	<0.0001
Cortical Trabecular Thickness-TRI (CTRITbTh)	mm	Mean (SD)	**0.517** (0.031)	**0.883** (0.073)	**0.709** (0.201)	**0.709** (0.196)	**0.683** (0.185)	**0.521** (0.030)	**0.524** (0.032)	**0.507** (0.030)	**0.897** (0.084)	**0.895** (0.070)	**0.858** (0.060)	a	<0.0001
Cortical Trabecular Separation-TRI (CTRITbSp)	mm	Mean (SD)	**0.388** (0.013)	**0.262** (0.017)	**0.323** (0.068)	**0.327** (0.062)	**0.325** (0.067)	**0.388** (0.012)	**0.387** (0.013)	**0.389** (0.015)	**0.258** (0.016)	**0.267** (0.016)	**0.262** (0.020)	a	<0.0001
Cortical Degree of Anisotropy-TRI (CTRIDA)	none	Mean (SD)	**8.21** (1.03)	**9.26** (1.83)	**8.67** (1.64)	**8.68** (1.57)	**8.85** (1.54)	**8.51** (1.15)	**7.85** (1.10)	**8.28** (0.735)	**8.83** (2.05)	**9.51** (1.55)	**9.42** (1.91)	a	0.0014

Note: TR=Treadmill Running, TC=Tower Climbing, NEC=Non-Exercised Control, a = strain effect, b = treatment effect, c = strain by treatment